SYNTHESIS AND PHOTOPHYSICAL PROPERTIES OF ANTIMONY AND LEAD PHTHALOCYANINES

A thesis submitted in completion of the requirements

for the degree of

MASTERS IN SCIENCE

Of

RHODES UNIVERSITY

By

KWENA DESMOND MODIBANE

January 2009

DEDICATION

To my brother

Buti Jeffery "Lekgola" Modibane

Without him, none of this would have been possible. He is my biggest supporter, fan and financial aid, and has kept me on the path.

To my mother

Mogale "Boledi" Modibane,

To every one who taught me Chemistry

And

My grand mother

Mma Mohube "Hunadi" Modibane

ACKNOWLEDGEMENTS

Firstly I would like to thank the **Creator** of all things, true source of light and wisdom, origin of all being, the **God Almighty**, for pointing out the beginning, directing the progress and helping in completion of the task of writing this work.

I wish to express my deepest thanks to **Prof. T. Nyokong**, Professor of Medicinal Chemistry and Nanotechnology, for supervision, valuable guidance and fruitful discussions.

I would like to thank **Dr E. Antunes**, for her remarkable help throughout the duration of this project. My thanks are extended to my research colleagues in **S22** for the discussions we shared and for providing such a conducive environment and making Grahamstown enjoyable and a family away from home. I would also like to thank the Chemistry Department staff (technical and academic) and post-graduate students for their assistance.

Thanks to the Department of Science and Technology (DST) and National Research Foundation (NRF), South Africa through DST/NRF South African Research Chairs Initiative for Professor of Medicinal Chemistry and Nanotechnology and Rhodes University for support in this work. Also thanks to CSIR/ARMSCOR for a bursary.

I also wish to thank my friends and comrades, too numerous to mention, for the support and encouragement. I cherish all the moments we shared together. To Kerileng Molapo, your valuable friendship kept me sane. You are truly the best and greatest friend I could ever ask for. I would like to express my deepest gratitude and love to my family: mom, Modipadi "Mangwane" Kgetedi and everybody, too numerous to mention, for their moral support, prayers, love, understanding and patience. Lastly, thanks to Mr C. M. Manyaka for support, guidance and encouragement.

ABSTRACT

This work hereby presents the synthesis, spectroscopic and photophysical properties of newly synthesized lead (PbPc) and antimony (SbPc) phthalocyanines. The complexes are either unsubstituted or substituted at the peripheral and non-peripheral positions with phenoxy, 4-t-butylphenoxy and 4-benzyloxyphenoxy groups.

The photophysical properties of these complexes were studied in dimethylsulfoxide, dimethylformamide, toluene, tetrahydrofuran and chloroform as solvents. The fluorescence spectra for PbPc complexes were different to that of the excitation spectra due to demetallation upon excitation. On the other hand, the excitation spectra of oxidized antimony (Sb(V)Pc) derivatives were found to be similar to absorption spectra. High triplet quantum yields for PbPc and SbPc complexes ranging from 0.70 to 0.86, low triplet lifetimes (20–60 μs in DMSO, while they were <10 μs in the rest of the solvents) and low fluorescence quantum yields were observed and is attributed to the presence of heavy atoms (Pb and Sb ions). The nonlinear optical properties of PbPc complexes were studied in dimethylsulfoxide. The optical limiting threshold intensity (I_{lim}) for the PbPc derivatives were calculated and ranged from 2.1 to 6.8 W/cm^2. The photodegradation studies of the PbPc and SbPc complexes synthesized showed that then are stable.

TABLE OF CONTENTS

Dedication ii

Acknowledgements……..……iii

Abstract iv

Table of contents v

List of symbols.....ix

List of Abbreviations xxi

List of schemes……xiv

List of tables.....xvi

List of figures xvii

1. Introduction.....1

1.1. Phthalocyanine…….2

Aim 2

1.1.1. Discovery and history of phthalocyanines…….....2

1.1.2. Structure and application of phthalocyanines……4

1.1.3. Origin of phthalocyanine spectra……...7

1.1.4. Solubilization of Phthalocyanines……11

1.1.5. Aggregation of Phthalocyanines……...14

1.1.6. Synthesis of Phthalocyanines……...16

1.1.7. Review of lead (Pb) and antimony (Sb) Phthalocyanines……24

1.1.7.1. Lead (Pb) Phthalocyanines……..…….24

1.1.7.2. Antimony (Sb) Phthalocyanines……..……...26

Aim of thesis……...33

1.2. Photophysical and photochemical properties……37

1.2.1. Photophysics……..37

1.2.1.1. Jablonski diagram……..37

1.2.1.2. Fluorescence……..38

1.2.1.3. Triplet quantum yield and lifetime……41

1.2.2. Nonlinear optics……..44

1.2.2.1. Optical limiting effect……...46

1.2.2.2. Nonlinear optical parameters……50

1.2.3. Review of photophysical and nonlinear optical parameter of PbPcs and SbPcs……52

1.2.3.1. Review of photophysical properties of SbPcs……...…52

1.2.3.2. Review of photophysical and nonlinear optical parameter of PbPcs ...53

1.2.4. Photodegradation/photobleaching……....54

1.3. Summary of aims of the thesis……58

2. Experimental.....59

2.1. Materials……60

2.2. Equipments……60

2.3. Synthesis……...63

2.3.1. Phthalonitriles……63

2.3.1.1. 3-Nitrophthalonitrile……63

2.3.1.2. 4-Nitrophthalonitrile……65

2.3.1.3. 4,5-Dichlorophthalonitrile……...66

2.3.1.4. Mono-substituted phthalonitrile……..67

2.3.1.5. Disubstituted phthalonitrile……69

2.3.2. Unsubstituted metallophthalocyanines……..71

2.3.3. Aryloxy substituted Pb phthalocyanines……74

2.3.4. Aryloxy substituted Sb phthalocyanines……76

3. Results and discussion 82

3.1. Synthesis and characterization……...84

3.1.1. Unsubstituted lead and antimony phthalocyanines……...84

3.1.2. Synthesis of phthalonitriles for substituted Pcs……..……...87

3.1.2.1. 3- and 4-Nitrophthalonitriles……...87

3.1.2.2. 4,5-Dichlorophthalonitriles……..88

3.1.2.3. Substituted phthalonitriles with phenoxy derivatives…..……...89

3.1.3. Substituted lead phthalocyanines……...91

3.1.4. Substituted antimony phthalocyanines……103

3.2. Photophysical properties……115

3.2.1. Photophysical properties of PbPc complexes……..115

3.2.1.1. Fluorescence spectra and quantum yields of PbPc complexes…….115

3.2.1.2 Triplet quantum yields and lifetime of PbPc complexes…….123

3.2.1.3. Nonlinear optical parameters of PbPc complexes…….……..125

3.2.2. Photophysical properties of SbPc complexes……...128

3.2.2.1. Fluorescence spectra and quantum yields of SbPc complexes ……128

3.2.2.2 Triplet quantum yields and lifetime of SbPc complexes…….132

3.3. Photodegradation/bleaching quantum yields…..……136

4. Conclusion 141

5. References 142

LIST OF SYMBOLS

α	- fraction of light absorbed
	- non-peripheral position
β	- peripheral position
	- nonlinear absorption term
ε	- molar extinction coefficient
ε_S	- singlet state molar extinction coefficient
ε_T	- triplet state molar extinction coefficient
n	- refractive index
	- number of electrons transferred
Φ_{IC}	- internal conversion quantum yield
Φ_{ISC}	- intersystem crossing quantum yield
Φ_T	- triplet state quantum yield
Φ_F	- fluorescence quantum yield
Φ_{Pd}	- photodegradation quantum yield
τ_T	- triplet lifetime
γ	- second order susceptibility
σ_{ex}	- absorption cross section of the excited state

σ_g - absorption cross section of the ground state

ΔA - change in absorbance

A - absorbance

C - concentration

f - Lorentz local field factor

I_{abs} - amount of light absorbed by sensitizer

I - light intensity

$I_m[\chi^{(3)}]$ - third order susceptibility

k - ratio of the absorption cross section of the singlet and triplet states

N_A - Avogadro's constant

S_0 - ground singlet state

S_g - ground singlet state

S_1 - excited singlet state

T - transmittance

T_1 - first excited triplet state

T_2 - second excited triplet state

ω* - frequency

λ - wavelength

LIST OF ABBREVIATIONS

A - absorbance

A_s - area of the sample under an emission band

A_{std} - area of the standard under an emission band

C - concentration

CT - charge transfer

1-CNP - 1-chloronaphthalene

DBU - 1,8-diazabicyclo[5.4.0]undec-7-ene

DCM - dichloromethane

DMF - dimethylformamide

DMSO - dimethylsulfoxide

DMSO-d_6 - deuterated dimethylsulfoxide

F - fluorescence

H_2Pc - metal-free phthalocyanine

^{1}H-NMR - proton nuclear magnetic resonance

HOMO - highest occupied molecular orbital

HPLC - high performance liquid chromatography

IC - internal conversion

I_{lim} - limiting threshold intensity

IR - infrared

ISC - intersystem crossing

LMCT - ligand to metal charge transfer

LUMO - lowest unoccupied molecular orbital

MLCT - metal to ligand charge transfer

MPc - metallophthalocyanine

NIR - near infra red

NLO - nonlinear optics

NPcs - naphthaphalocyanines

OL - optical limiting

P - phosphorescence

PbPc - lead phthalocyanine

Pc - phthalocyanine

PDT - photodyanamic therapy

RSA - reverse saturable absorption

SA - saturable absorption

[SbPc]I_3 - antimony phthalocyanine triiodide

TBHP - tert-butylhydroperoxide

THF - tetrahydrofuran

TX - triton X-100

UV/Vis - ultraviolet/visible

VR - vibrational relaxation

LIST OF SCHEMES

Scheme 1.1: First synthesis of a metal-free phthalocyanine…….……2

Scheme 1.2: Synthesis of iron phthalocyanine……...…3

Scheme 1.3: Potential applications of phthalocyanines in industry……...7

Scheme 1.4: General synthesis of unsubstituted MPc…….....18

Scheme 1.5: Synthesis of substituted phthalonitriles…...……....20

Scheme 1.6: Synthesis of 3- and 4-tetrasubstituted MPcs……..….21

Scheme 1.7: Synthesis of peripheral octa-substituted MPcs……..….22

Scheme 1.8: Mechanistic scheme for formation of MPcs……23

Scheme 1.9: Jablonski diagram.…….……...37

Scheme 1.10: Possible reactions of MPc upon irradiation with singlet oxygen……..55

Scheme 3.1: Synthetic route for PbPc (**30**) and $[Sb(III)Pc]^{+}I_3^{-}$ (**61**)……84

Scheme 3.2: Synthetic pathway to 3-(**19a**) and 4-(**19b**) nitrophthalonitriles.....87

Scheme 3.3: Synthetic pathway to 4,5-dichlorophthalonitrile (**24**)……..88

Scheme 3.4: Synthesis of 3-monosubstituted (**25**) and 4-monosubstituted (**26**) and 4,5-disubstituted phthalonitrile (**28**)…...……90

Scheme 3.5A: Synthesis of phenoxy (**a**) and 4-*t*-butylphenoxy (**b**) tetra- and octa-substituted lead Phthalocyanines……..91

Scheme 3.5B: Synthesis of 4-benzyloxyphenoxy (**c**) tetra- and octa-substituted lead Phthalocyanines……92

Scheme 3.6: Synthesis of phenoxy (**a**), 4-*t*-butylphenoxy (**b**) and 4-benzyloxyphenoxy (**c**) tetra- and octa-substituted antimony Phthalocyanines……..103

LIST OF TABLES

Table 1.1: Known SbPc and PbPc complexes……..……..…….27

Table 3.1: Q-band spectral data of all PbPc complexes (**30**, **76-78**) in various solvents…….....99

Table 3.2: Q-band spectral data for all SbPc complexes (**61**, **79-81**) in DMSO, DMF and toluene……..……..……110

Table 3.3: Spectral, photophysical parameters of PbPc derivatives in various solvents……...121

Table 3.4: Nonlinear optical parameters of PbPc derivatives in DMSO……...….127

Table 3.5: Spectral, photophysical parameters of $Sb^{V}Pc$ derivatives in different solvents……...….131

Table 3.6: Spectral, photophysical parameters of $Sb^{III}Pc$ derivatives in DMSO, DMF and toluene…….135

Table 3.7: Photodegradation of PbPc derivatives in various solvents……...138

Table 3.8a: Photodegradation of $Sb^{III}Pc$ complexes in DMSO, DMF and toluene…139

Table 3.8b: Photodegradation of $Sb^{V}Pc$ complexes in DMSO, DMF and toluene…140

LIST OF FIGURES

Fig.1.1: Molecular structures of tetrapyrole macrocycles……4

Fig.1.2: Geometry of phthalocyanines……..……..…6

Fig. 1.3: Ground state electronic absorption of metallophthalocyanines..……8

Fig. 1.4: Electronic transitions in phthalocyanines.....9

Fig. 1.5: Absorption spectra of an unmetallated phthalocyanine (i) and metallated phthalocyanine (ii)……..……...10

Fig. 1.6: Charge transfer in metallophthalocyanines ……..11

Fig. 1.7: Absorption spectra of substituted MPcs substituted α and β positions. The insert shows the α and β positions for MPc……..……....12

Fig. 1.8: Absorption spectra of MPcs in different solvents…….....13

Fig. 1.9: Aggregation in phthalocyanines……...…….15

Fig. 1.10: Electronic transitions in phthalocyanines aggregates…….....16

Fig. 1.11: Structure of PbPc (**30**) and $[SbPc]I_3$ (**61**) studied in this thesis……..34

Fig. 1.12: Structure of the non-peripheral (3-) tetra substituted PbPc (**76**) and $[SbPc]I_3$ (**79**) studied ……...……...34

Fig. 1.13: Structure of the peripheral (4-) tetra substituted PbPc **(77**) and $[SbPc]I_3$ (**80**) studied.....35

Fig. 1.14: Structure of the peripheral octa-substituted PbPc (**78**) and $[SbPc]I_3$ (**81**) studied……..……36

Fig. 1.15: Expected fluorescence and absorption spectra of Pc…..……..……..39

Fig. 1.16: Triplet decay curve of phthalocyanine……42

Fig. 1.17: Laser light on aircraft……..45

Fig. 1.18: The response of an optical limiter…….……...47

Fig. 1.19: The physical processes forming the basis of the optical limiting effect (OL= optical limiter)……48

Fig. 1.20: Jablonski diagram for phthalocyanines showing the absorption and decay pathways...…...……..…….…..49

Fig. 1.21: Absorption cross sections for the ground and excited triplet state for Pc.……50

Fig. 2.1. Set-up for photoirradiation reactions……..……61

Fig. 2.2: Schematic diagram of a laser flash photolysis set-up for triplet quantum yield and lifetime determinations...…….……..62

Fig. 3.1: Ground state electronic absorption spectra of (i) PbPc (**30**) and (ii) $[Sb(III)Pc]^{+}I_3^{-}$ (**61**) in DMSO …….……86

Fig. 3.2: UV–Vis spectra for tetra- and octa-substituted lead phthalocyanines. Solvent = DMSO……...97

Fig. 3.3: Absorption spectra of compound **78a** in DMSO at different concentrations…….101

Fig. 3.4A: Absorption spectra of complex **77a** in different solvents ……..…..102

Fig. 3.4B: Absorption spectra of complex **78c** in different solvents …….102

Fig. 3.5: IR spectrum of complex **80b**……..…….105

Fig. 3.6: ^{1}H NMR spectrum of complex **81a** in DMSO……..……..….106

Fig. 3.7: UV–Vis spectra for tetra- and octa- substituted antimony phthalocyanines. Solvent = DMSO……...……...…..109

Fig. 3.8: Absorption spectra of compound **81a** in DMSO at different concentrations…….111

Fig. 3.9: Absorption spectra of complex **81b** in DMF, DMSO and Toluene……..112

Fig. 3.10a: Absorption spectra before (i) and after (ii) oxidation of (a) complex **80a** and (b) **81b** using TBHP in DMSO as an oxidant ……..……...114

Fig. 3.11a: Absorption, emission and excitation spectra of compound **76b** in toluene……117

Fig. 3.11b: Absorption, emission and excitation spectra of compound **76b** in DMSO……117

Fig. 3.11c: Absorption, emission and excitation spectra of compound **76b** in DMF……..118

Fig. 3.11d: Absorption, emission and excitation spectra of compound **78a** in DMSO.....118

Fig. 3.12a: Absorption, emission and excitation spectra of compound **76a** in DMF……...119

Fig. 3.12b: Absorption, emission and excitation spectra of compound **78a** in DMF……...119

Fig. 3.13: Transient absorption spectrum for **78a** in DMSO…….123

Fig. 3.14: Triplet decay curve for **78a** in DMF.....124

Fig. 3.15: Absorption cross sections for the ground (a) and excited triplet (b) state for compound **77b** in DMSO……..126

Fig. 3.16: Absorption, emission and excitation spectra of oxidized a) compound **61** and b) compound **81b** in DMSO using TBHP as oxidant.....130

Fig. 3.17. Triplet decay curve of complex **81a** in DMSO ……...133

Fig. 3.18: Photobleaching of complex **81a** in DMSO……137

CHAPTER ONE:

INTRODUCTION

1.1. PHTHALOCYANINES

Aim: To synthesize phthalocyanines containing large central metal atoms (lead and antimony) and to study their photophysical properties as well as their non-linear optical behaviour.

1.1.1. Discovery and history of phthalocyanines

A metal-free phthalocyanine (**3**) was accidentally discovered by Braun and Tcherniac in 1907 as a by-product during the preparation of ortho-cyanobenzamide (**2**) from phthalamide (**1**) in acetone (Scheme 1.1) [1]. However, no attention was given to the discovery at that time. Later, in 1927, an insoluble copper phthalocyanine was discovered by de Diesbach and von der Weid during the cyanation of ortho-dibromobenzene with copper (I) cyanide in an attempt to make a phthalonitrile [2]. A blue product was obtained, which was identified as copper phthalocyanine [2].

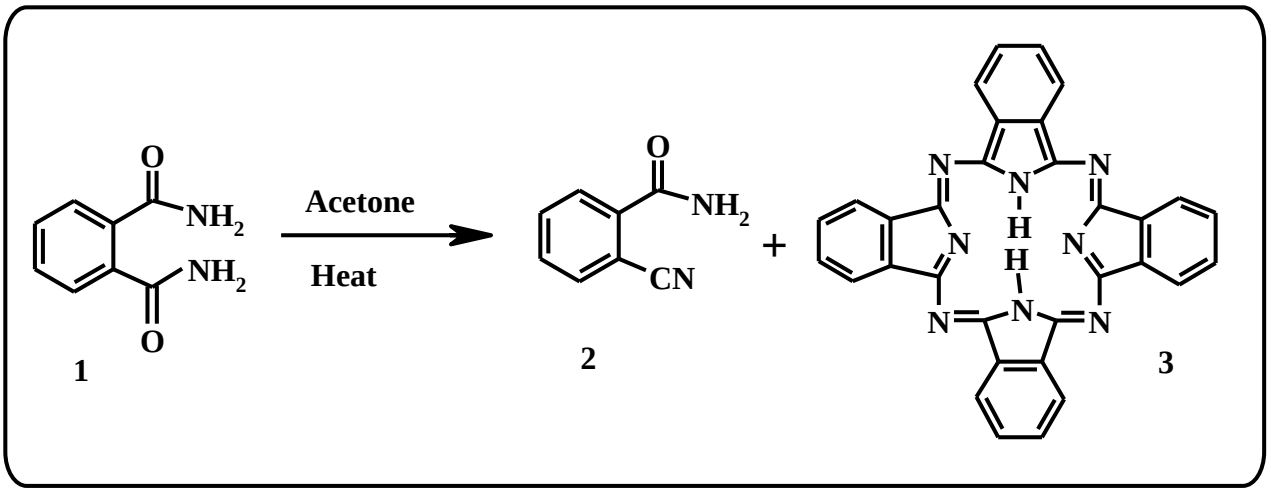

Scheme 1.1: First synthesis of a metal-free phthalocyanine

In 1928, Scottish Dyes Ltd prepared iron phthalocyanine (**6**) by chance during the preparation of phthalimide (**5**) from phthalic anhydride (**4**) and ammonia (Scheme 1.2) [3]. The product mixture contained traces of a dark blue compound, which was later shown to be iron phthalocyanine [3]. The blue product was a direct result of the iron vessel used in the production process [3].

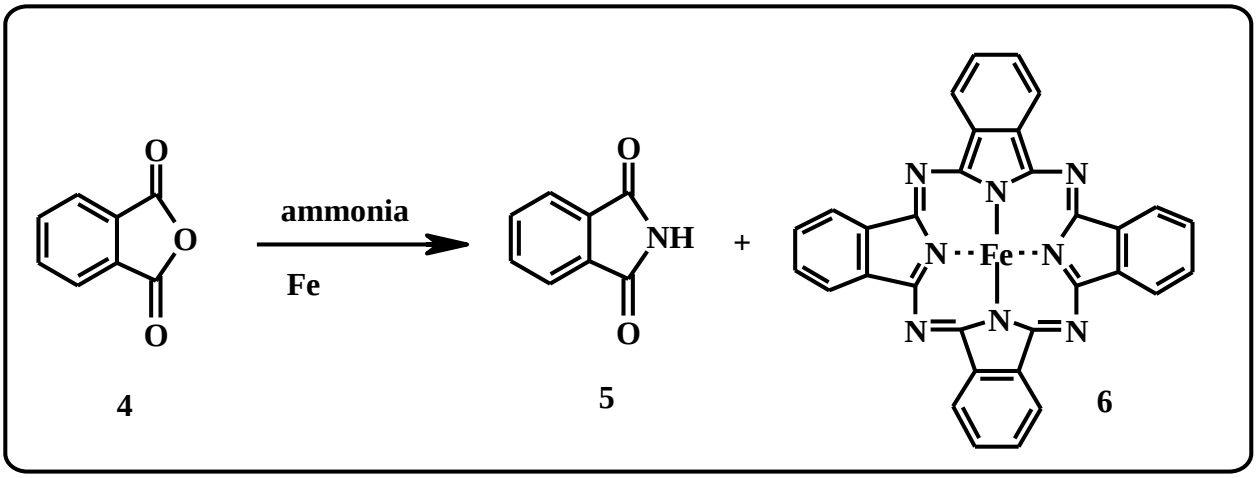

Scheme 1.2: Synthesis of iron phthalocyanine

This phthalocyanine compound was investigated meticulously by Linstead [4]. He was the first to use the term phthalocyanine [4], deriving the name from the Greek words *naphtha* (rock oil) and *cyanine* (blue). In subsequent years, using a variety of analytical techniques, the structure of phthalocyanine as well as procedures for obtaining several metal and metal-free phthalocyanines (Pcs) were clarified [5]. Robertson later confirmed Linstead's structure by using X-ray crystallography, showing that the Pc molecule is planar rather than three-dimensional [6].

1.1.2. Structure and applications of phthalocyanine

Phthalocyanines (**3**) belong to the tetrapyrrole macrocycle class, with the structure containing an alternating nitrogen atom-carbon atom ring. This class includes porphyrins (**7**) and porphyrazines (**8**) [7].

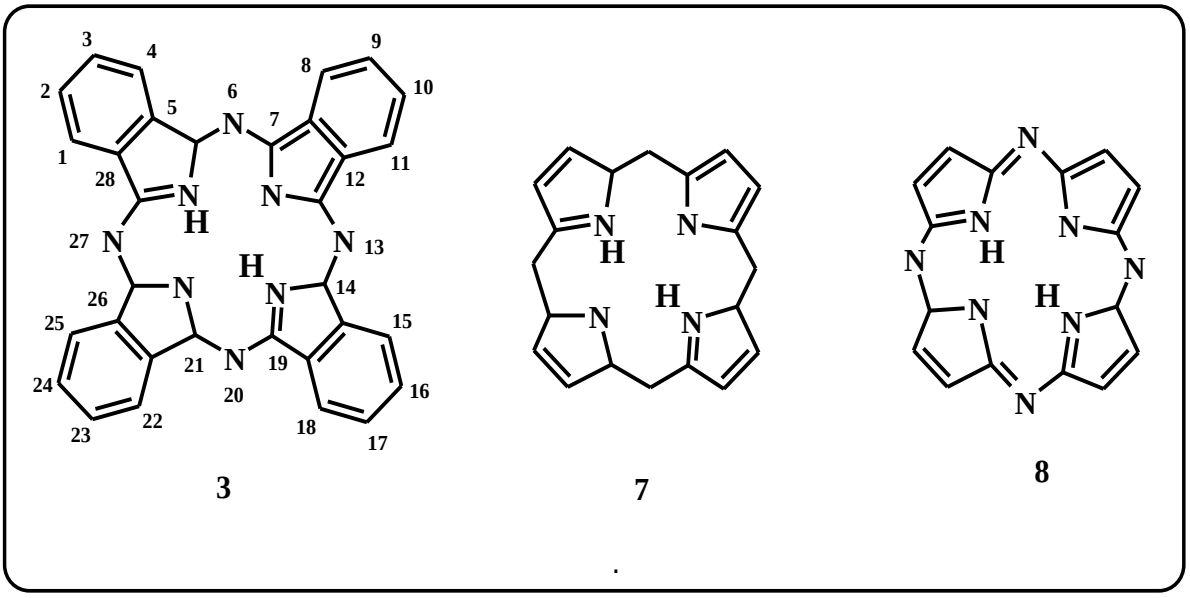

Fig.1.1: Molecular structures of tetrapyrole macrocycles

Phthalocyanines (**3**) consist of four isoindoline units linked together at the 1,3-positions by aza bridges. Pcs possess large nonlinearity, along with synthetic flexibility as well as thermal stability. The molecule has a conjugated, 18 π electron aromatic planar structure. This π system, which is localized over alternate carbon and nitrogen atoms, provide the unique chemical and physical properties attributed to Pcs. In addition, there are 16 possible sites of substitution on the fused benzene rings, which allow incorporation of different substituents on the peripheral {(2,3), (9,10), (16,17) or (23,14)} or non-peripheral {(1, 4), (8,11), (15,18) or (22,25)} positions of the ring (Fig.1.1).

Pcs can host different elements in the central cavity, with more than 70 different metals having been incorporated in the phthalocyanine core [8], forming metallophthalocyanines (MPcs). The presence of a metal atom in the Pc central core allows for axial ligation. Axial substitution in Pc complexes generally increases solubility, reduces molecular aggregation and evokes relevant changes to the electronic structure of the molecule by altering the π-electron distribution attributed to the dipole moment of the central metal–axial ligand bond [9].

The coordination of the Pc ligand with metal and metalloid elements results in an alteration of molecular conformation and several conformations are known [10]. The most common conformations are planar, ruffled, waved, domed, and skew domed. Pcs metallated with heavy metals show a domed conformation [10, 11]. The essentially planar conformation of Pcs can also be distorted by substituents alone, through conformational stress [12].

The geometry (Fig.1.2) of a metal-free phthalocyanine is square planar, i.e. D_{2h} symmetry. If the planarity is maintained when a metal, which fits inside the Pc cavity, is incorporated into the phthalocyanine ring, the symmetry increases from D_{2h} to D_{4h}. Larger metal ions (such as Pb, Sn, Sb, Hg and Cd) tend to distort the geometry of the macrocycle, forming a C_{4v} symmetry. This symmetry is a result of the rotation of the rigid isoindole units that reduce the internal stress induced by the large metal size.

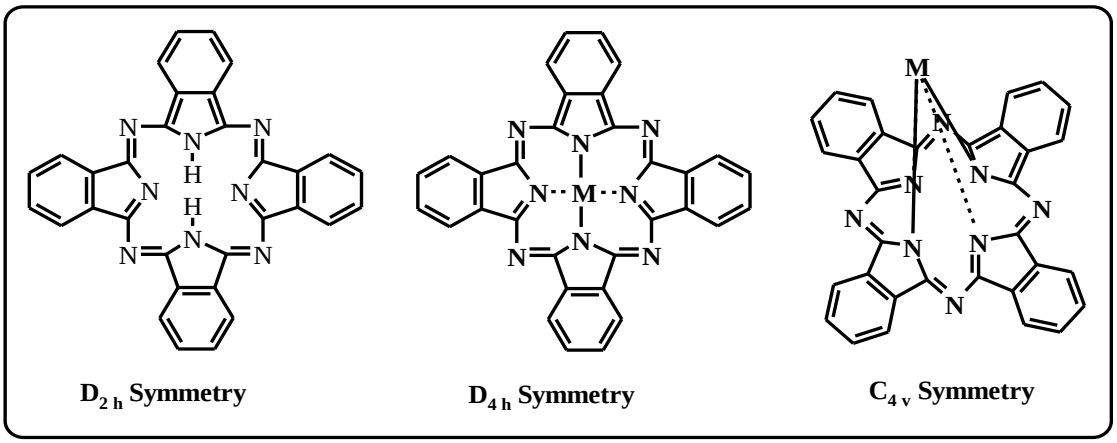

Fig.1.2: Geometry of phthalocyanines

In recent years there has been enormous interest in the fundamental properties of phthalocyanine chemistry. Traditional uses for phthalocyanines are as colorants and as blue and green pigments [7].

In addition, attention has also been focused on the potential applications of Pcs in industry (Scheme 1.3) due to their physical and chemical stability. Some of the potential uses for phthalocyanines include nonlinear optical materials [13], liquid crystals [14], Langmuir-Blodgett (LB) films [15], optical data storage (computer recordable DVDs) [16], as electrochromic substances [17], low dimensional metals [18], gas sensors [19], as photosensitizers [20], in photoelectrochemical cells [21] and electrophotographic applications [22]. Additionally, certain derivatives of phthalocyanines have shown promise as photodynamic reagents for cancer therapy and other medical applications [23].

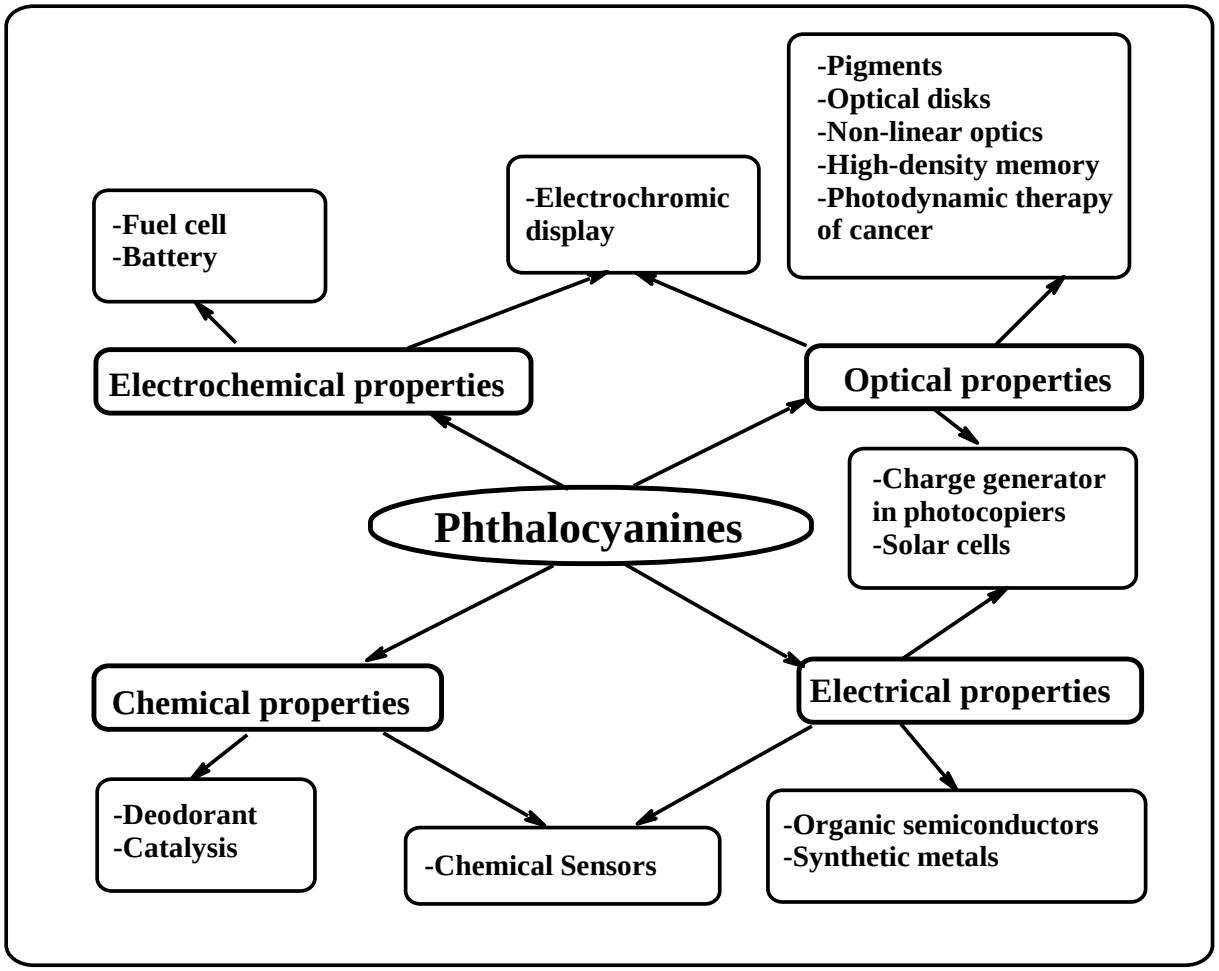

Scheme 1.3: Potential applications of phthalocyanines in industry

1.1.3. Origin of phthalocyanine spectra

Metallophthalocyanines (MPcs) show a characteristically strong, isolated absorption band in the red region of the electromagnetic spectrum with a corresponding high molar extinction coefficient [24]. This distinctive intense absorption peak at around 700 nm is called the Q-band and it is accompanied by vibrational bands (Fig.1.3). A second, less intense band, the B-band, appears between 300 and 400 nm (Fig.1.3). The B-band is broad due to the superimposition of the B_1 and B_2 bands. N, L, and C absorption bands are also present and commonly appear at the lower energy

wavelengths in UV transparent solvents. In some cases, a charge transfer band (CT) is also present (will be discussed in details below) (Fig.1.3).

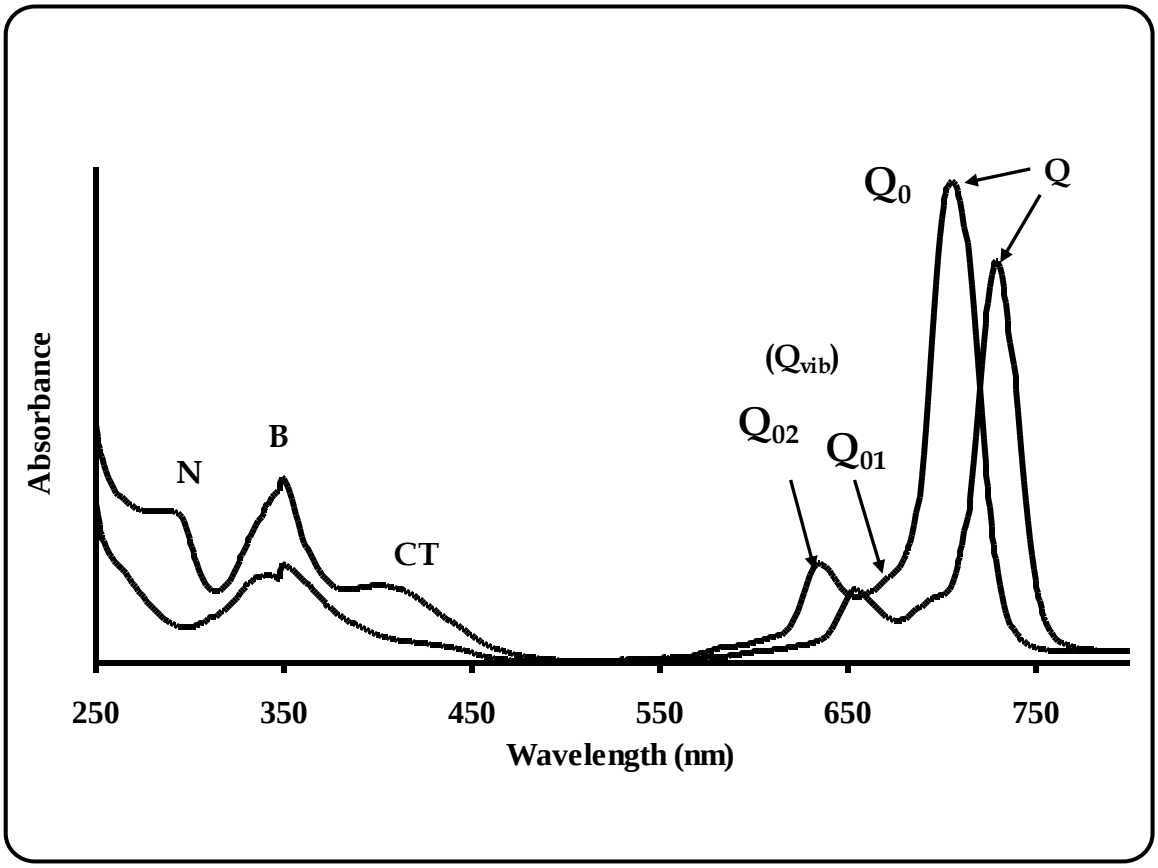

Fig. 1.3: Ground state electronic absorption of metallophthalocyanines

The bands in the absorption spectrum are primarily due to π-π* electronic transitions in the Pc ligand and the assignment of the Q and B bands are based on the four-orbital model proposed by Gouterman's group [25-27]. The model considers the top two highest occupied molecular orbitals (HOMO) and the degenerate lowest unoccupied molecular orbital (LUMO) [25] as shown in Fig.1.4. The Q-band absorption arises due to a transition from the a_{1u} of the HOMO to a doubly degenerate transition e_g of the LUMO, while a transition from a_{2u} or b_{2u} to the e_g of the LUMO results in the B-band absorption.

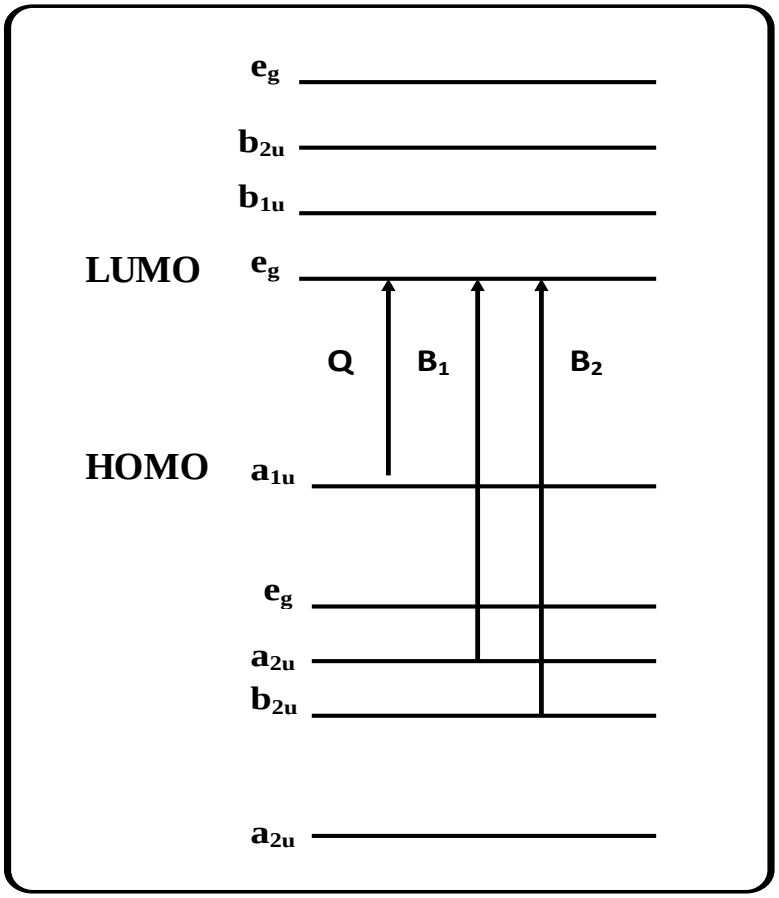

Fig. 1.4: Electronic transitions in phthalocyanines

The absorption spectrum of an unmetalled phthalocyanine is visibly different to that of MPc (Fig.1.5). The split Q-band is due to the presence of the core protons, which causes the LUMO to become nondegenerate, giving rise to two allowed electronic transitions of varying energy.

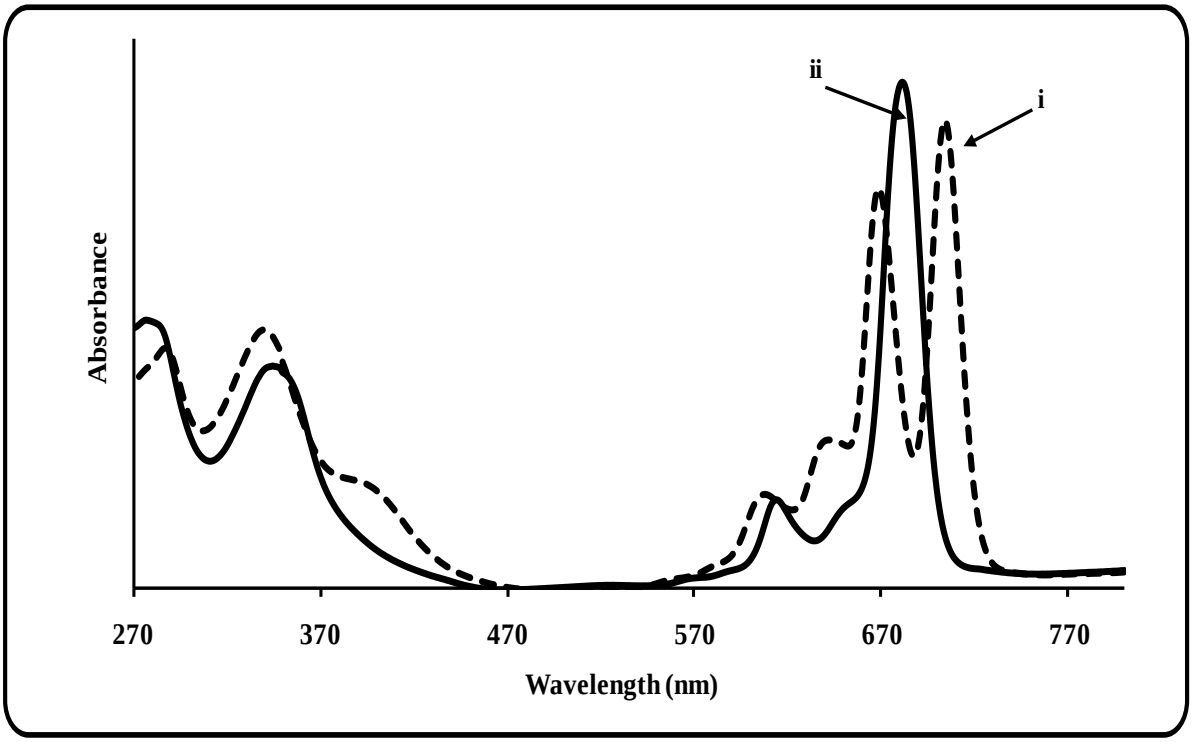

Fig. 1.5: Absorption spectra of an unmetallated phthalocyanine (i) and metallated phthalocyanine (ii)

The isolation, red shift and intensification of the Q-band relative to the B-band (Fig. 1.5) are due to the large energy gap between the a_{1u} and a_{2u} orbitals (Fig.1.4). Other absorption bands present between the Q and B bands occur when the metal d-orbitals lie within the HOMO-LUMO gap (Figs.1.3 and 1.6) of the Pc ring, and these are assigned as charge-transfer transitions (CT) [28]. A charge transfer (Fig.1.6) from an electron rich ligand to an electron poor metal is known as a ligand to metal charge transfer (LMCT) while a transfer from metal to ligand is a metal to ligand charge transfer (MLCT).

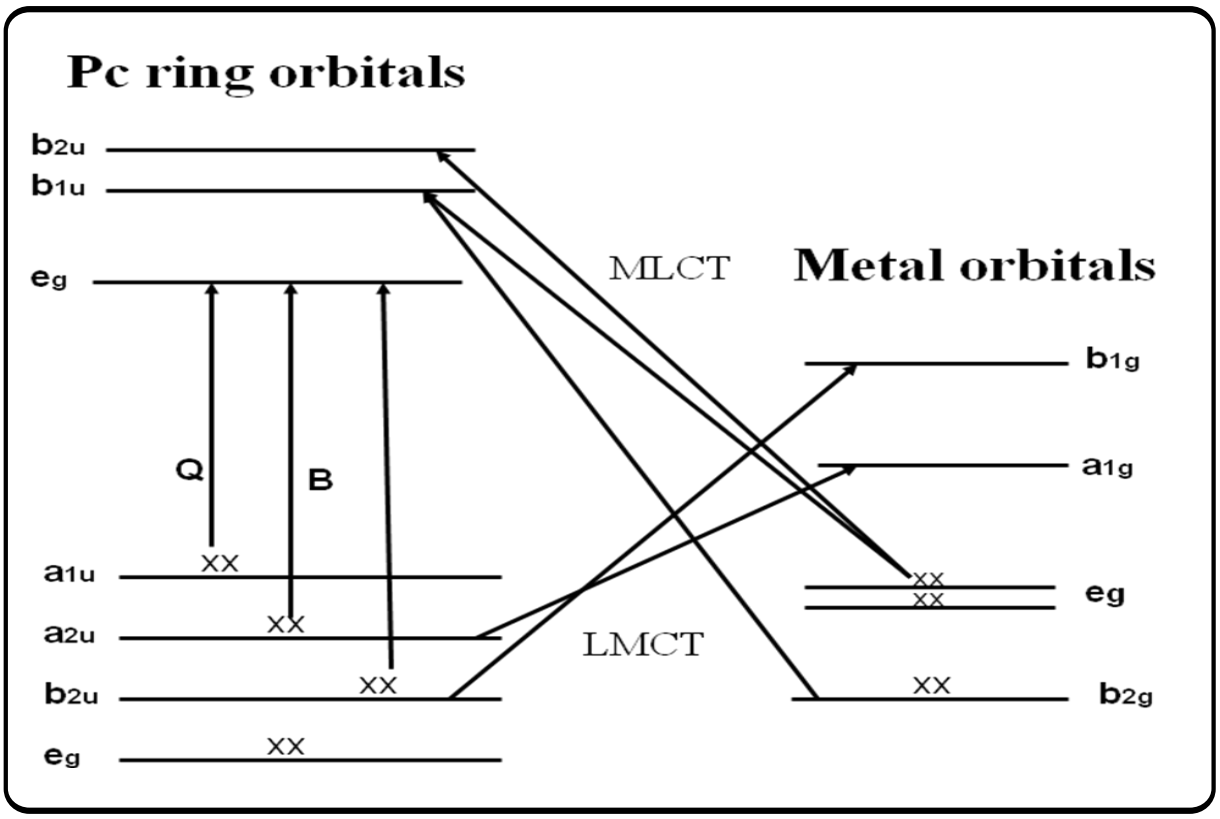

Fig. 1.6: Charge transfer in metallophthalocyanines

1.1.4. Solubilization of phthalocyanines

Unsubstituted metallophthalocyanines are known to have low solubility in most organic solvents. Solubility can be increased by the introduction of substituents into the phthalocyanine framework thus reducing the intermolecular attractions due to an increase in the distance between stacked molecules [29]. Two types of substituted macrocycles can be distinguished according to their substituent positions, and these also show significant differences in their chemical and physical behaviours. These are: substitution at the more sterically crowded α (non-peripheral) position and substitution at the β (peripheral) position (Fig. 1.7 insert). The former causes reduced aggregation tendencies to greater extent than the later [30].

The effect of substitution at the non-peripheral position (Fig.1.7) is much larger than that at the peripheral position as seen by a distinct red shift of the Q-band of the former relative to the latter. The spectral shift to the red is due to linear combinations of the atomic orbital (LCAO) coefficients at the non-peripheral positions of the HOMO being greater than those at the peripheral positions [31, 32].

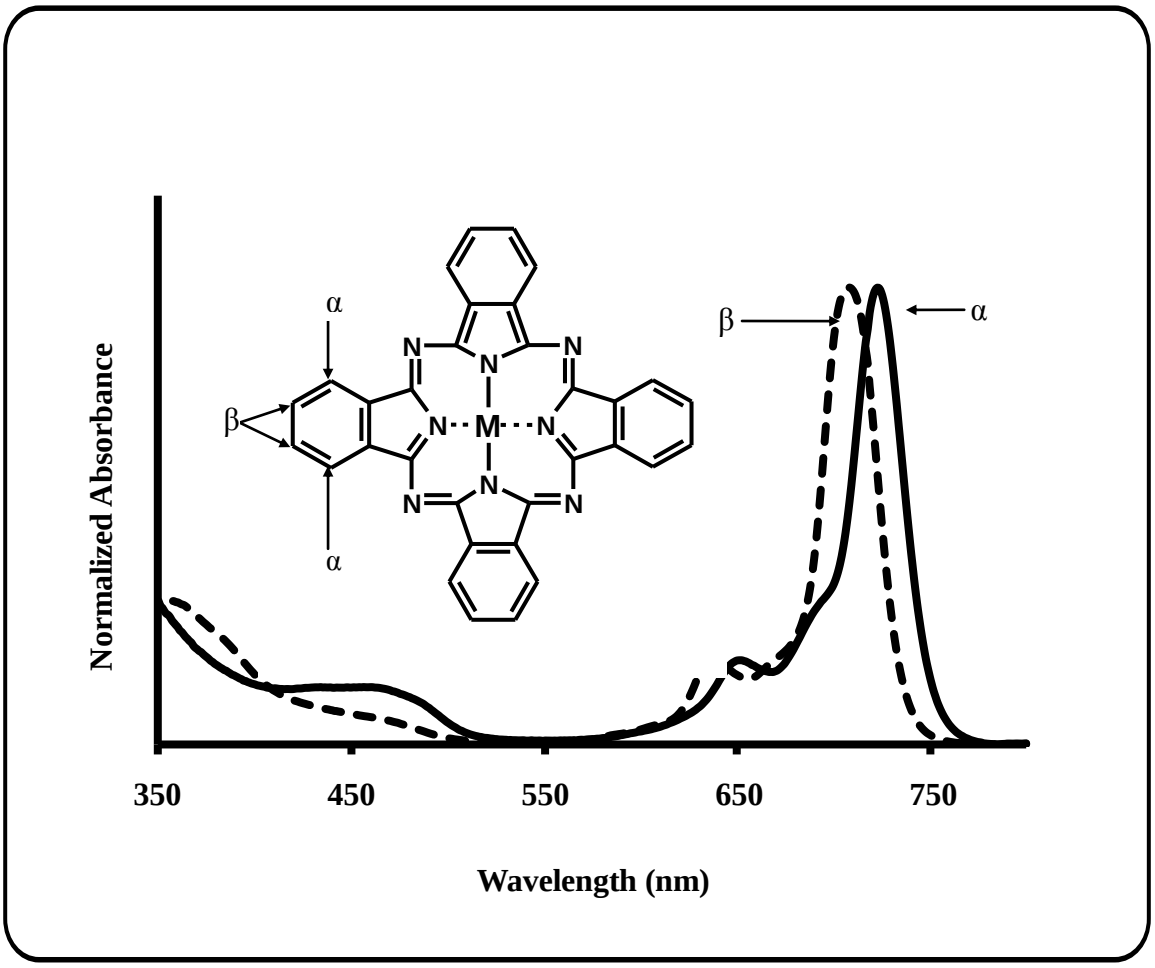

Fig. 1.7: Absorption spectra of substituted MPcs substituted α and β positions. The insert shows the α and β positions for MPc

Pcs may be tetra- or octa-substituted, where tetra-substituted phthalocyanines are usually more soluble than the corresponding octa-substituted phthalocyanines due to the formation of constitutional isomers and the high dipole moment that results from the unsymmetrical arrangement of the substituents at the periphery [33]. The

solubility and position of the Q-band of MPcs is thus governed by the nature of the substituents, the position of these substituents on the MPc ring, the central metal, solvent used and aggregation.

The solvent used has been shown to affect the wavelength and intensity of absorption bands due to the unequal perturbation of the two electronic states of the molecule, which depends on the nature of solvent-solute interactions in the states. The shifts in the position of Q absorption band are often interpreted in terms of the relative permittivity and also as a function of the solvent's refractive index (Fig.1.8) depending on the type of solvents [34].

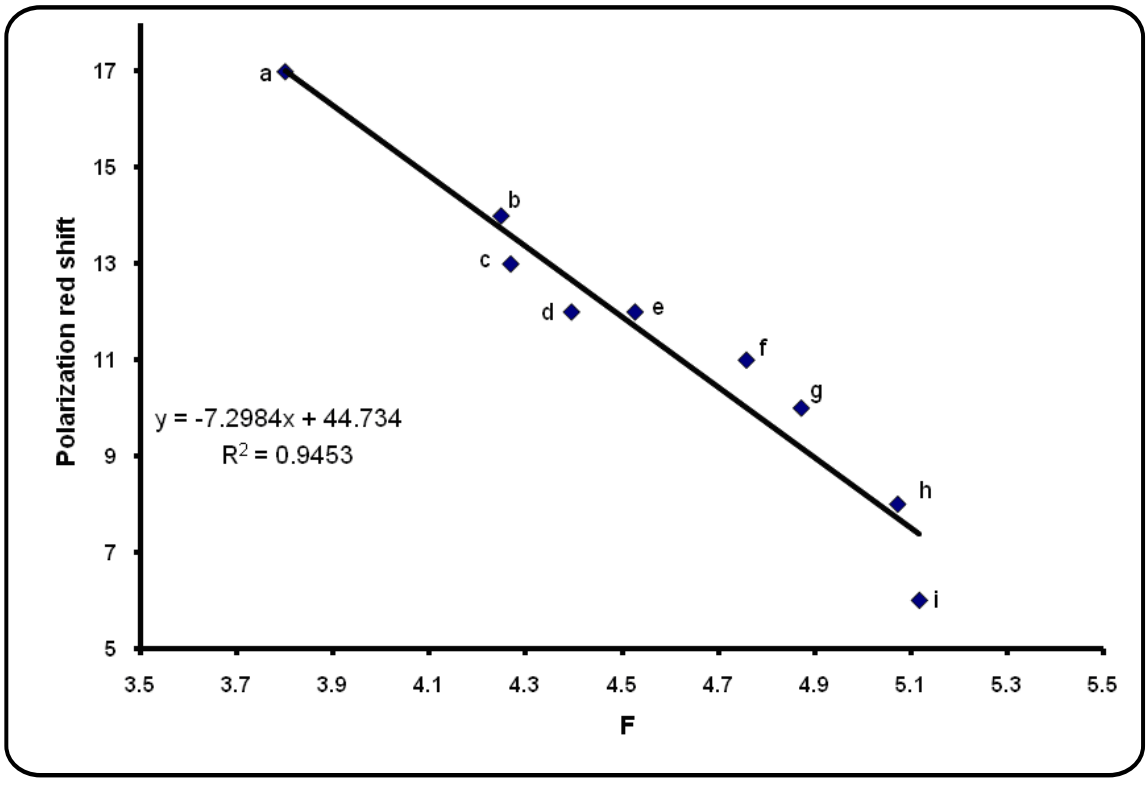

Fig. 1.8: Plot of polarization red shift vs. F (for ZnPc) where F = $(n^2-1)/(2n^2+1)$], and n is the refractive index of the solvent: (a)1-chloronaphthalene, (b) benzonitrile, (c) chlorobenzene, (d) benzene, (e) DMSO, (f) dichloromethane, (g) DMF, (h) THF, (i) triethylamine [34]

1.1.5. Aggregation of phthalocyanines

Phthalocyanines tend to aggregate in solution due to the strong electronic interactions present between planar macrocycles [35, 36]. Aggregation is usually depicted as a coplanar association of rings progressing from monomer to dimer and higher order complexes and is driven by enhanced van der Waals' attractive forces between phthalocyanine rings [37,38]. In the aggregated state, the electronic structure of the phthalocyanine rings is perturbed, resulting in an alteration of the ground and excited state properties. Aggregation in phthalocyanines (Fig.1.9 [39]) is characterized by a broadening of the Q-band with a corresponding blue- (H-aggregate [40]) or red-shift (J-aggregate [41]) in their wavelength values or by splitting of the Q-band. These spectral effects will depend on the proximity of the rings, the bulkiness of the substituents, the tilt angle of the rings, the overlap position, in addition to the other factors which determine the π-electron cloud overlap.

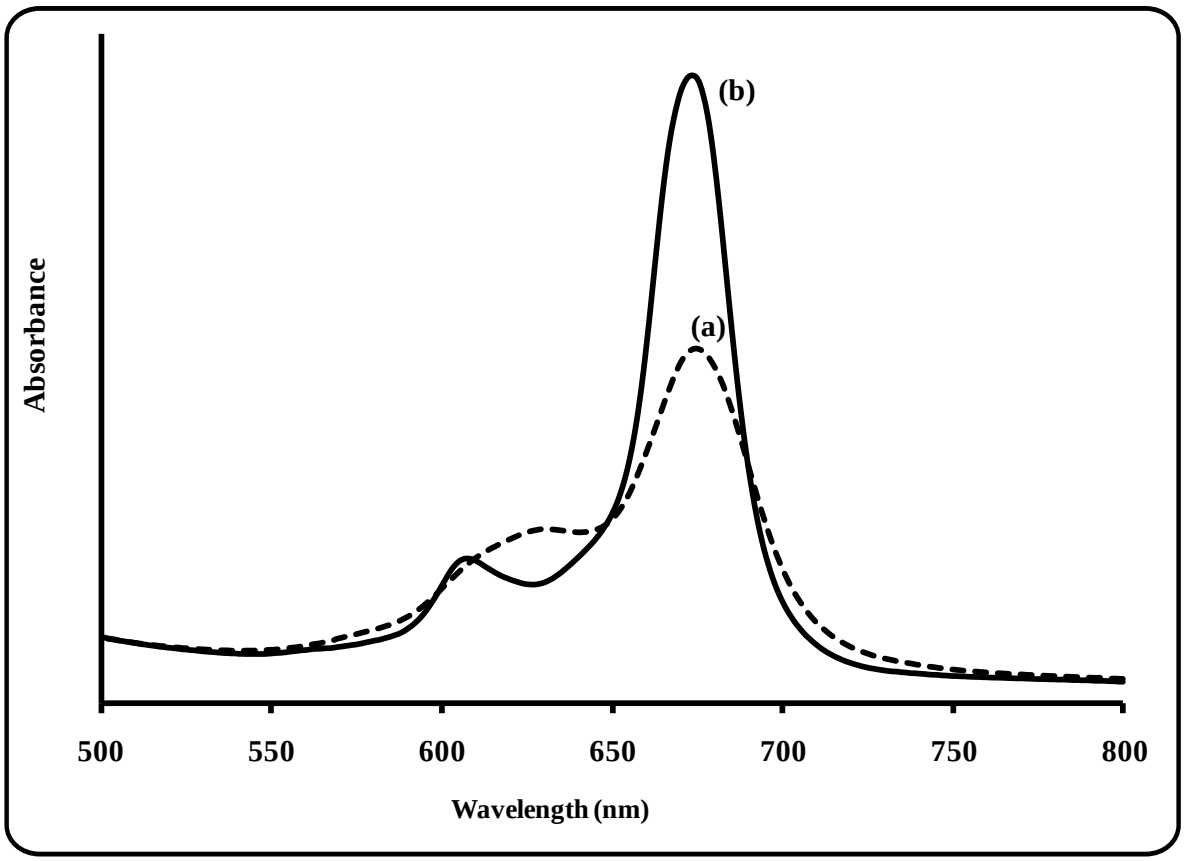

Fig. 1.9: Electronic absorption spectra of $ZnPcS_{mix}$ in PBS 7.4 (a) and in the presence of Triton X-100 (b). Concentration of $ZnPcS_{mix}$ = 5 x 10^{-6} M and for Triton X-100 = 0.02 M [39]

The H-aggregate [40] is a cofacial arrangement, which readily allows Pc macrocycles to stack on to top of each other. On the other hand, the J-aggregates are an edge-to-edge arrangement [41].

The overlap of π-electron clouds of dimers results in a split in the LUMO orbital (Fig. 1.10). According to the exciton coupling theory, transitions to higher energy states (^1E_u) are allowed (H-aggregates), whereas transitions to lower energy states (^1E_g) are forbidden (J-aggregates) [42]. The transitions to lower energy LUMO orbitals can still occur to a small extent, even though they are forbidden, resulting in a broad absorption band. It is thus rare to observe J-aggregates in phthalocyanines.

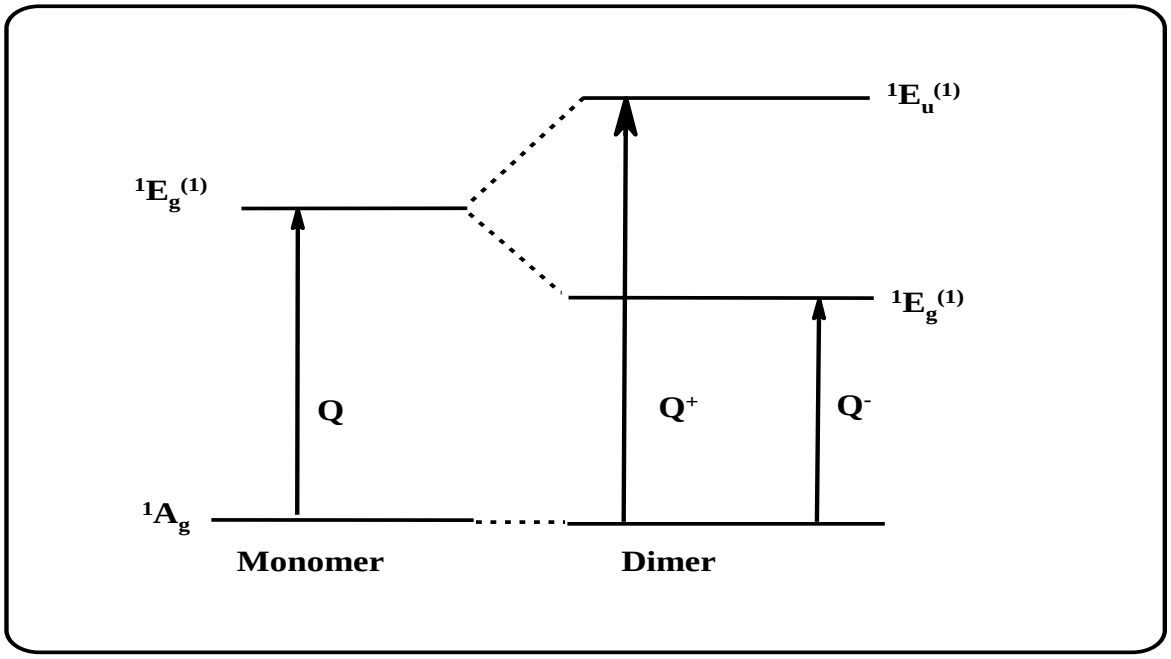

Fig. 1.10: Electronic transitions in phthalocyanines aggregates

Aggregation behaviour of Pcs is generally investigated by concentration-dependence, as well as, solvent studies. Dilution of the Pc solution generally leads to the formation of the monomeric species [43]. Addition of a surfactant, to an aggregated species can result in dissociation of the aggregates (Fig. 1.9) [39].

1.1.6. Synthesis of phthalocyanines

In general, phthalocyanines are prepared by cyclotetramerisation of the starting material. A number of ortho-disubstituted benzene derivatives can act as Pc starting materials. Most precursors are derived from phthalic acid (**12**), phthalic anhydride (**4**), phthalimide (**5**), *o*-cyanobenzamide (**2**), phthalonitrile (**10**), diiminoisoindoline (**9**) and o-dibromobenzene (**11**) [7,44], Scheme 1.4. Phthalonitrile (1,2-dicyanobenzene) (**10**) is generally the most used precursor in laboratory scale syntheses, because it

provides a mild, clean reaction process in high yields of pure MPcs (**13**) suitable for research purposes [45].

There are several methods of cyclotetramerisation of the phthalonitrile to form phthalocyanines. One approach involves the initial formation of diiminoisoindoline (**9**) by the reaction of phthalonitrile (**10**) with ammonia. A high boiling point solvent is often used in the synthesis of the desired MPc, in order to insert the metal ion into the central cavity. Furthermore, bases such as 1,8-diazabicylo-[5,4,0]-undec-7-ene (DBU) can also be used as powerful catalysts for the cyclotetramerisation of phthalonitriles in solution, where a metal ion is used as the template for the formation of metal phthalocyanines.

In some reactions, urea and hydroquinone (organic reducing agent) as sources of nitrogen and hydrogen, respectively, are used to enhance the formation of these macrocycles. MPcs can also be synthesized by the insertion of metal into a metal-free phthalocyanine (**3**) or by the replacement of lithium (Li) from Li_2Pcs. Aromatic solvents such as 1-chloronaphthalene, pentanol or quinoline then lead to the formation of MPcs in good yields. Microwave synthesis is another option in the synthesis of Pcs [46].

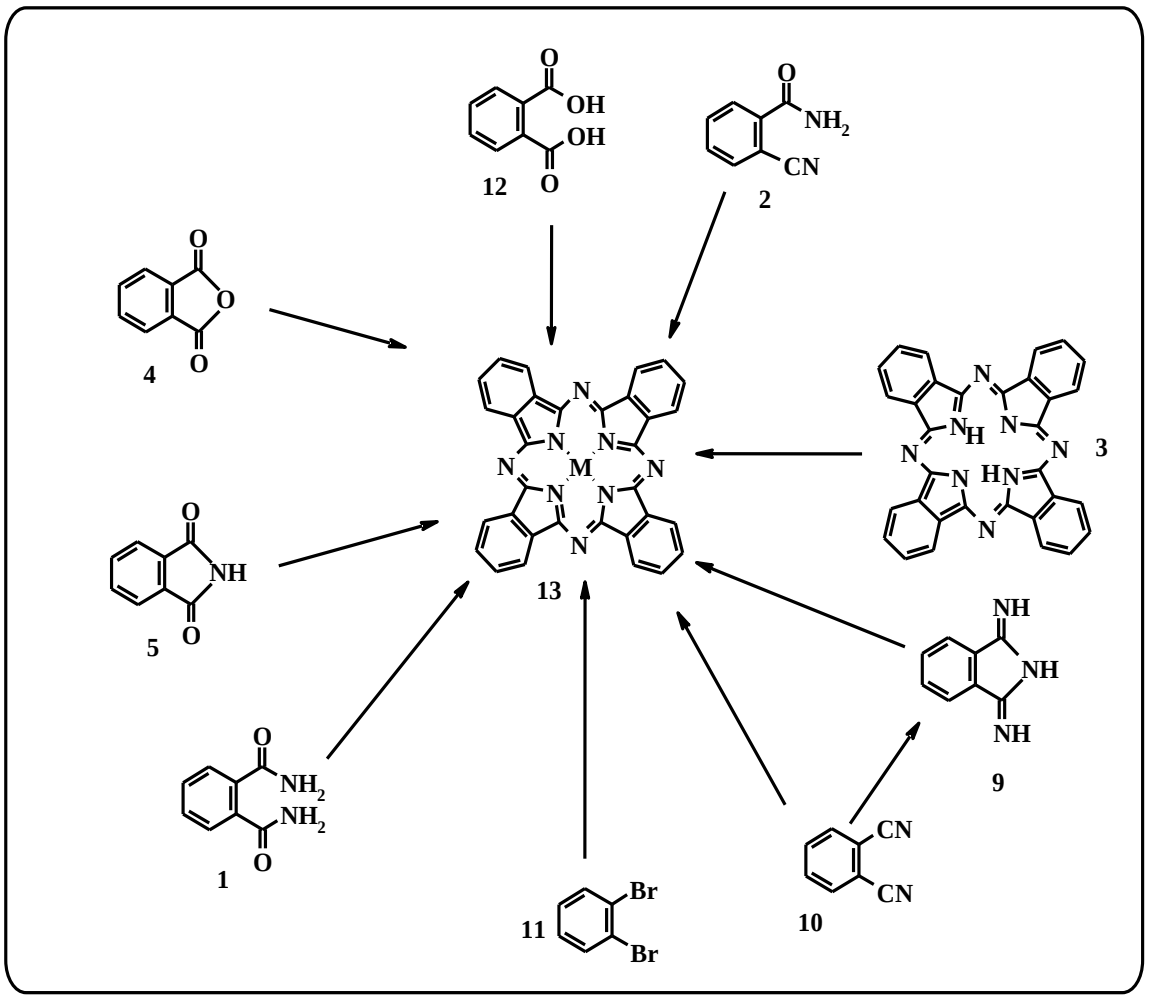

Scheme 1.4: General synthesis of unsubstituted MPc from different precursors and the presence of metal salt and heat, DBU, urea, catalyst or solvent (e.g.1-octanol)

Ring substituted Pcs are synthesized from precursors that contain the desired substituent. The use of a phthalonitrile precursor is preferred since control of the formation of particular substituted phthalocyanine is permitted through phthalonitrile substitution at 3- or 4-position. The challenge in the synthesis of ring substituted phthalocyanines is the preparation of an appropriate substituted phthalonitrile, which is the vital path in the preparation of new phthalocyanine derivatives.

The synthesis of a substituted phthalonitrile (**19**, Scheme 1.5A or **24**, Scheme 1.5B) is generally a stepwise reaction from commercially available appropriately substituted phthalic acids (such as 3-nitropthalic acid (**14**), 4,5-dichloropthalic acid (**20**)), followed by dehydration in acetic anhydride to afford substituted phthalic anhydride (**15** or **21**). The substituted phthalimide (**16**, **17** or **22**) is then formed from the anhydride by refluxing in formamide which acts as a solvent as well as source of nitrogen. Addition of ammonia to this phthalimide then forms the substituted phthalamide (**18** or **23**), which is subsequently dehydrated to form a desired substituted phthalonitrile (**19** or **24**).

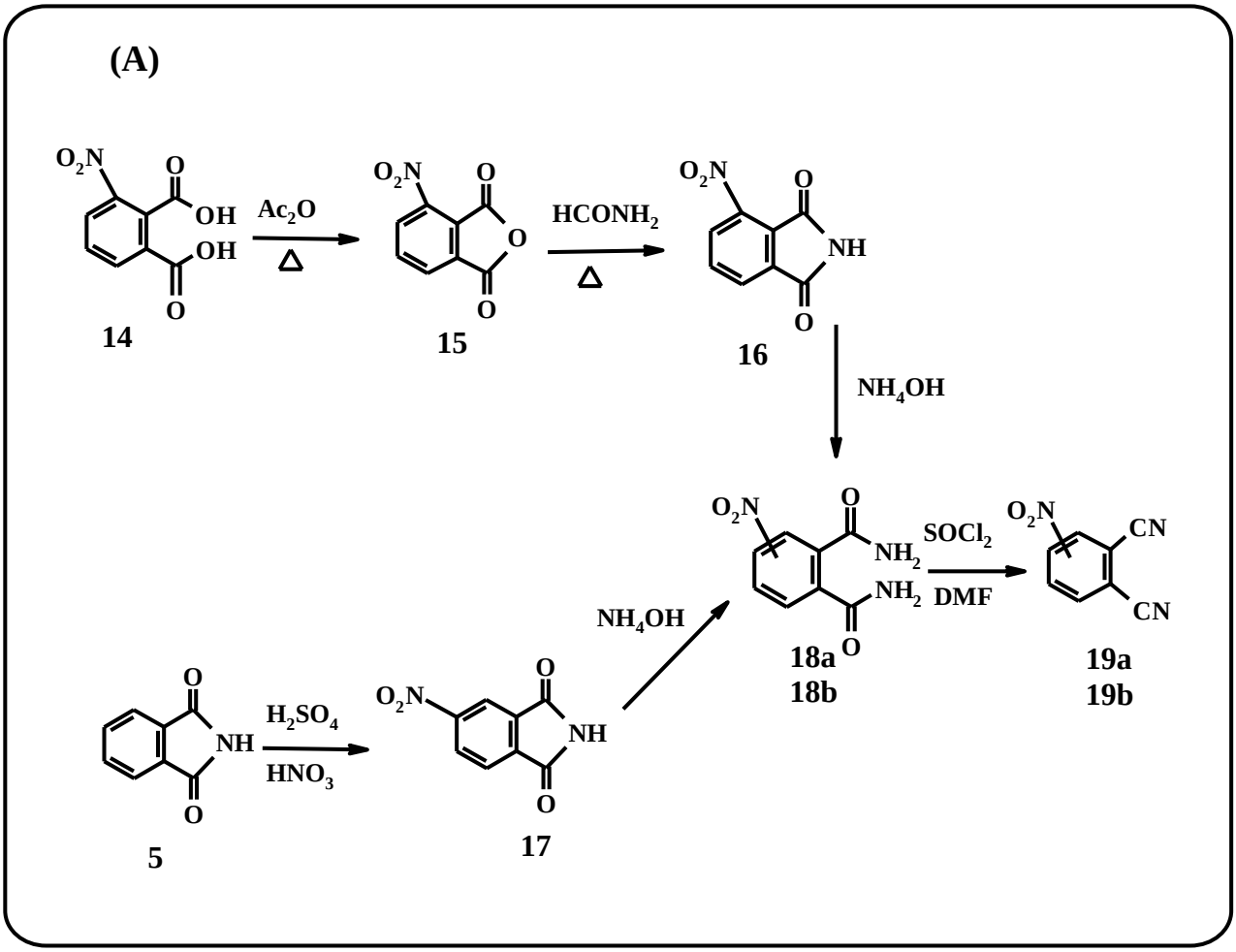

Scheme 1.5A: Synthesis of monosubstituted phthalonitriles (3- and 4-nitrophthalonitriles)

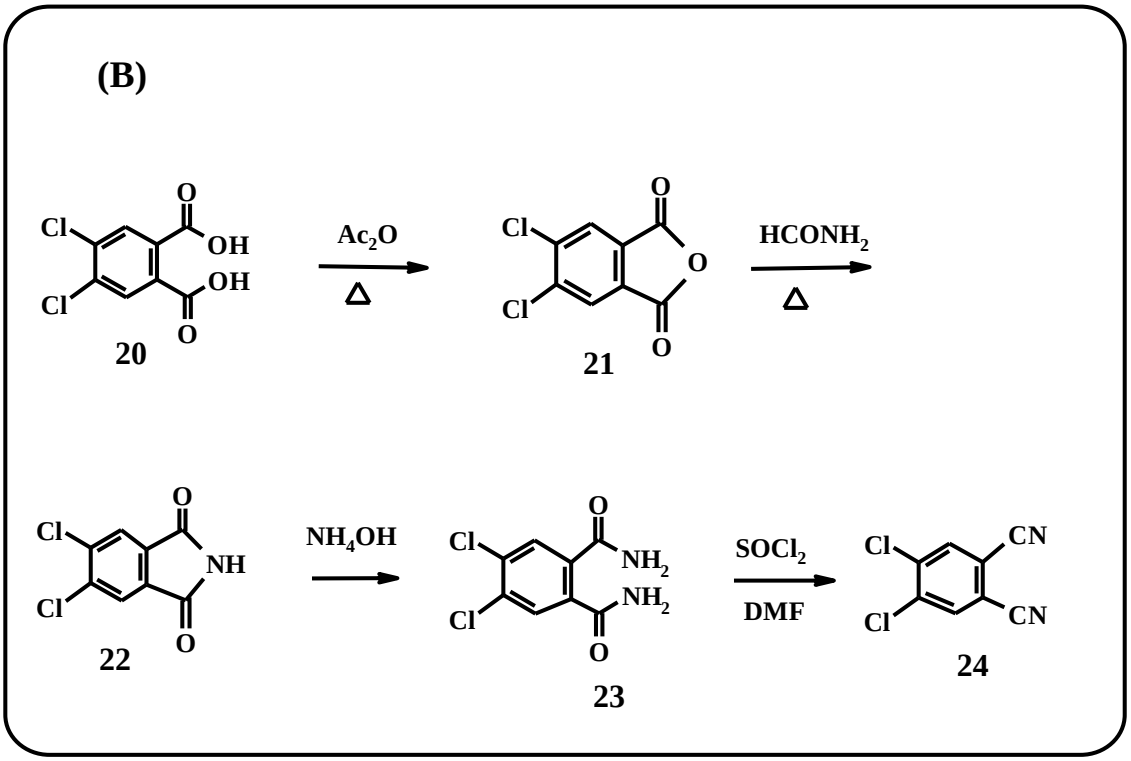

Scheme 1.5B: Synthesis of disubstuted phthalonitrile (4,5-dichlorophthalonitrile)

Once prepared, the 3- and 4-nitrophthalonitrile precursors can undergo a series of nucleophilic displacement reactions with a variety of alcohols or thiols to give the required monosubstituted phthalonitrile (Scheme 1.6) [47,48]. Treatment of the monosubstituted phthalonitrile with suitable reagents leads to formation of 3- or 4-tetrasubstituted MPc product (Scheme 1.6), depending on the position of the monosubstituted phthalonitrile. The product is thus expected to occur as a mixture of constitutional isomers. The product of the monosubstituted phthalonitrile at the 4-position for example leads to four single isomers with the following symmetry: (C_{4h}) 2,9,16,23-, (D_{2h}) 2,10,16,24-, (C_{2v}) 2,9,17,24- and (C_s) 2,9,16,24-tetrasubstituted Pcs, while phthalonitriles substituted at the 3-position leads to Pcs with the following symmetry: (C_{4h}) 1,8,15,22-, (D_{2h}) 1,11,15,25-, (C_{2v}) 1,11,18,22- and (C_s)1,8,18,22-tetrasubstituted Pcs. The major problem with these regioisomers is the difficulty in

separation, but they have been separated through techniques such as high performance liquid chromatography (HPLC) [49, 50].

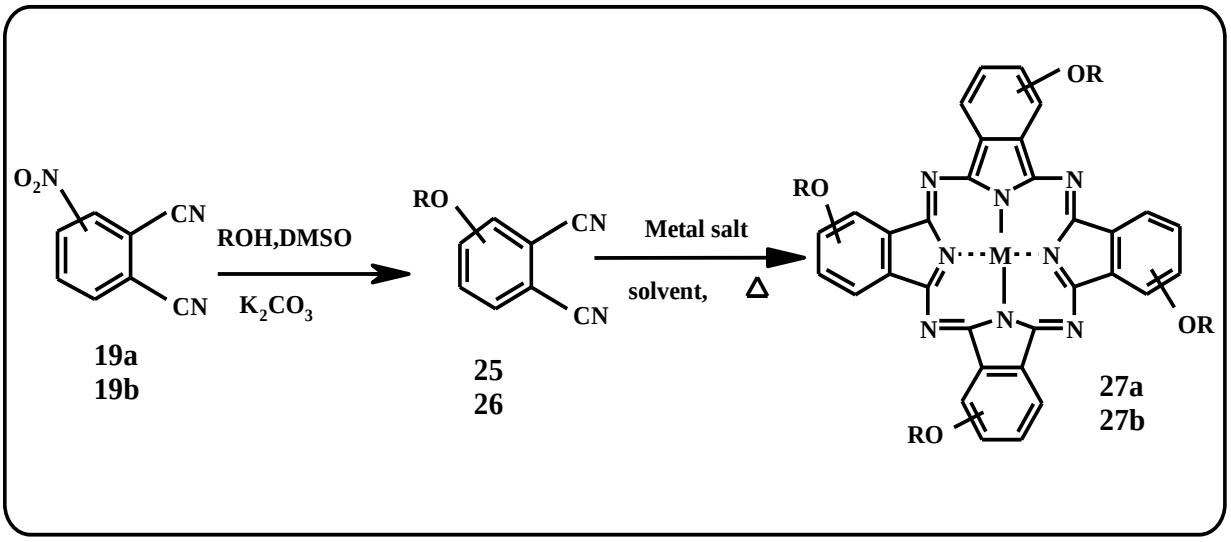

Scheme 1.6: Synthesis of 3- and 4-tetrasubstituted MPcs

4,5-Dichlorophthalonitrile is a precursor for the preparation of 4,5-disubstituted phthalonitriles and the subsequent formation of the symmetrically disubstituted phthalonitrile is achieved through the nucleophilic displacement of the chloro groups on the 4,5-dichloro phthalonitrile with alcohols or thiols in the presence of basic solvents such as DMSO (Scheme 1.7) [51].

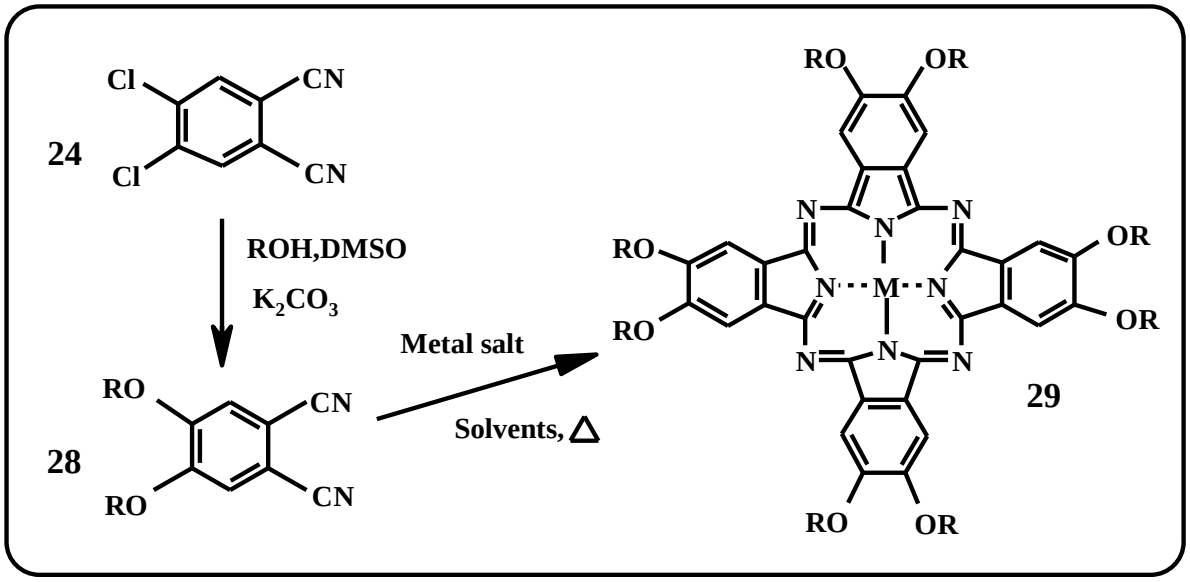

Scheme 1.7: Synthesis of peripheral octa-substituted MPcs

Condensation of these disubstituted phthalonitriles in the presence of a metal salt and solvent leads to formation of isomerically pure octasubstituted MPcs. The purification of octasubstituted complexes is thus considerably easier than their corresponding tetrasubstituted Pc complexes. They can be formed as non-peripherally (1,4,8,11,15,18,22,25) and peripherally (2,3,9,10,16,17,23,24)-octasubstituted MPcs. The former is formed by cyclotetramerisation of 3,6-disubstituted phthalonitrile derivatives, whereas the latter is formed by condensation of the 4,5-disubstituted phthalonitrile derivatives.

Scheme 1.8 describes the probable reaction sequence mechanism for the formation of metallophthalocyanines from a diiminoisoindoline precursor [52].

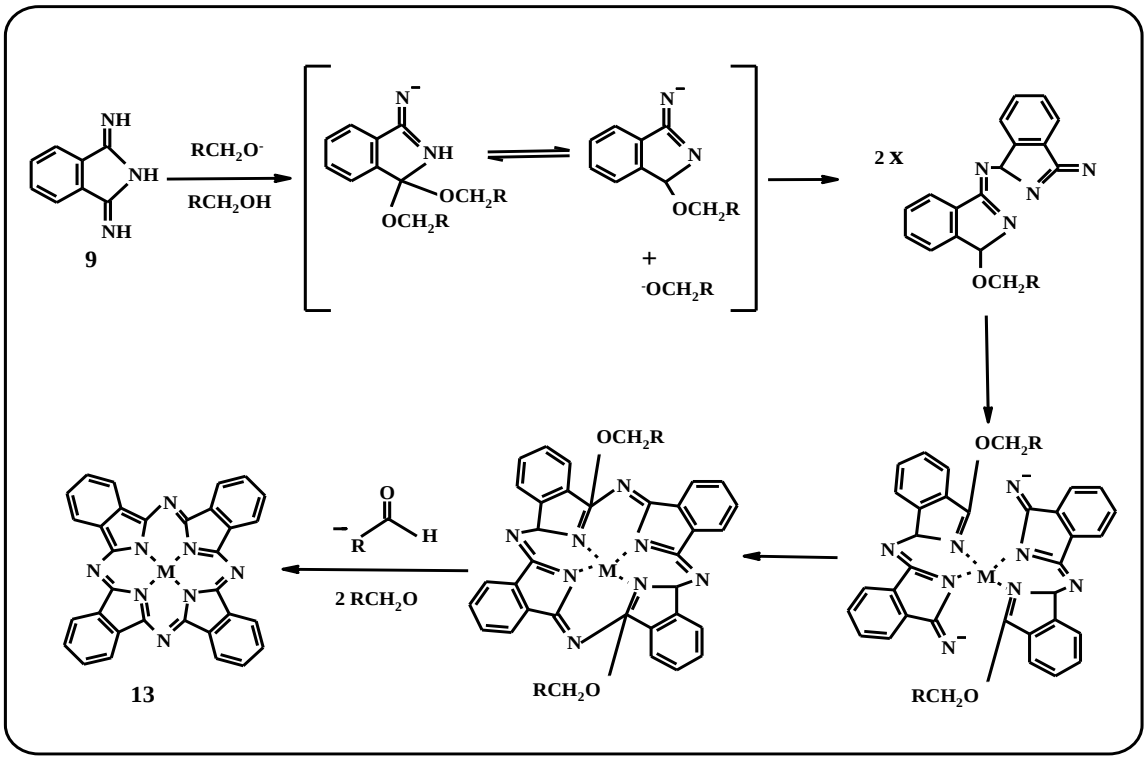

Scheme 1.8: Mechanistic scheme for formation of MPcs

The mechanism involves a condensation reaction between the phthalocyanine precursor leading to the formation of reactive intermediates with two isoindole units. The combination of the reactive isoindole species and the central metal ion coordination leads to formation of the MPc complex. In this mechanism, some intermediates have been isolated and have thus given some insights into how these complexes are formed [45, 52], even though the mechanism is not as yet fully understood.

Phthalocyanines may be characterized by several methods including infra red (IR) [53], nuclear magnetic resonance (NMR) [54,55] and UV-vis spectroscopies [38].

1.1.7. Review of lead (Pb) and antimony (Sb) phthalocyanines

Most MPc structures are essentially planar and therefore possess D_{4h} symmetry. However, for lead and antimony phthalocyanines, Pb^{2+} and Sb^{3+}, the metal ions are large with their ionic radii greater than the equilibrium cavity size of the ring, thus these ions protrude out of the cavity. PbPc and SbPc molecules have been shown to possess a domed shape and have an electric dipole moment perpendicular to the molecular plane owing to the C_{4v} symmetry [11, 56].

1.1.7.1. Lead phthalocyanines (PbPcs)

There are a number of reported lead phthalocyanine complexes [57-84], and they have potential use in fields such as non-linear optical limiting materials. Table 1.1 shows the structure of known PbPc complexes. Studies have focused mainly on the unsubstituted analogues [57-62], and while substituted lead phthalocyanines have been previously reported [63–84], these are generally concerned with the preparation mesomorphic lead phthalocyanines [64, 66-68, 73]. Unsubstituted Pb phthalocyanines in the monoclinic phase [74] have displayed an electrical switching effect.

PbPc can be prepared by three methods: i) heating the appropriate phthalonitrile with lead (II) monoxide (PbO) or lead (II) acetate without a solvent [65-71] or in the presence of a solvent [69-71], ii) addition of anhydrous lead(II) acetate or PbO to a solution of Li_2Pc or H_2Pc in anhydrous alcohol [69] (insertion method) or iii) the microwave method [75, 76].

Unsubstituted PbPc (**30**) was first prepared by Kroenke and Kenney [62] from a reaction of phthalonitrile and PbO in refluxing 1-chloronaphthalene.

Non-peripherally substituted tetranitro- (**31**) and tetraamino (**32**) substituted [72] PbPcs were synthesized by condensation of phthalonitrile in the presence of lead monoxide. Non-peripherally substituted tetra-(3-pentyl) (**33**), tetra-(2,4-dimethyl-3-pentyl) (**34**) and tetra-2-naphthyl (**35**) PbPcs were synthesized using the insertion method [69]. Non-peripherally substituted octakis(hexyl) (**36**) and (3-methylbutyl)-(**37**) substituted PbPcs were prepared by condensation of the prepared disubstituted phthalonitrile with lead acetate in 1-pentanol [77]. 1,4-Octakis(hexylsulfanyl) lead phthalocyanine (**38**) has been synthesized by treatment of the suitably prepared phthalonitrile with lead (II) acetate in the presence of 1-pentanol, and characterized by X-ray crystallography [63]. Octasubstituted polyether PbPc (**39**) was prepared from a reaction of disubstituted phthalonitrile and PbO in 1-chloronaphthalene [83]. The peripherally substituted 4-tetra(cumylphenoxy) (**40**) [65] PbPc was synthesized by condensation of the monosubstituted phthalonitrile with PbO or Pb acetate in solution. The octa-substituted PbPc complexes, substituted with F (**41**), Cl (**42**), Br (**43**), $–CH_3$ (**44**), $–C_2H_5$ (**45**), $–C_3H_7$ (**46**) at the peripheral positions have been reported by Zhang and Co-workers. [79, 80]. Peripherally substituted mesomorphic octakis(alkylthio)-substituted (**47**,**48**) PbPcs have been prepared by the microwave, as well as by the usual condensation methods in 1-pentanol [84]. The syntheses of tetra-(dihexeloxymalonyl)-tetrahexylthiophthalocyaninato lead (**49**), tetra-(dihexyloxymalonyl)-tetrachloro phthalocyaninato lead (**50**), tetra-(dihexyloxymalonyl) phthalocyaninato lead (**51**), tetra- (**52**) and octa- (**53**) diethoxymalonyl Pcs were reported by Dinçer and Co-workers [70, 71]. Peripherally substituted tetra-(1,1-(dicarbpentoxy)-2-(4-biphenyl)-ethyl) (**54**), tetra-(1,1-(dicarbpentoxy)-2-(1-naphthyl)-ethyl) (**55**) and tetra-(1,1,2-(tricarbpentoxyethyl)- (**56**) PbPcs were prepared by treatment of the disubstituted phthalonitrile with Pb acetate

and DBU in 1-pentanol [81], as was the peripherally substituted tetra-(1,1-(dicarbpenthoxy)-2-(4-biphenyl)-ethyl)-3,(9)10,(16)17,(23)24-tetrachloro PbPc (**57**) [82]. PbPcs substituted with siloxane chains (**58-60**) were synthesized in 2003 by Maya and Co-workers. [78].

1.1.7.2. Antimony phthalocyanines (SbPcs)

Less attention has been paid to SbPc derivatives than PbPc [85-99]. The first synthesis of SbPcs was reported by Linstead *et al.* [85]. Diantimony phthalocyanine ($PcSb_2$) (**75**) was obtained during preparation of metal-free phthalocyanines from o-cyanobenzamide and powdered antimony [85]. [Sb(III)Pc]Cl (**74**) was also synthesized by reaction of antimony trichloride and a metal-free Pc in refluxing chloronaphthalene [85]. The product obtained was unstable and gave the metal-free Pc upon treatment with sulphuric acid or upon heating with high-boiling point solvents. The crystals of the $[Sb(III)Pc]I_3$ (**61**) were isolated as a product of the reaction of a phthalonitrile with Sb_4O_6 under iodine vapour, and characterized by X-ray crystallography [86]. Sb(III)Pc]I (**62**) was reported in 1998 [93]. The [Sb(III)Pc]F (**63**) and [Sb(V)Pc]F (**64**) complexes were synthesized by condensation of a phthalonitrile with SbF_3 to form [Sb(III)Pc]F (**63**), and upon subsequent treatment of this [Sb(III)Pc]F (**63**) complex with hydrogen peroxide, the antimony ion was oxidized to [Sb(V)Pc]F (**64**), bearing two hydroxy axial ligands [87]. Dichloro (phthalocyanito) antimony(V) tetrachloroantimonate(III) ($[Sb(V)PcCl_2]SbCl_4$) (**65**) was synthesized from a phthalonitrile precursor with antimony trichloride [90]. $[(Cl)_2SbPc]SbCl_6$ (**66**), $[(Cl)_2SbPc]ClO_4$ (**67**), $[(Cl)_2SbPc]BF_4$ (**68**) and $[(Cl)_2SbPc]PF_6$ (**69**) have been prepared by Kagaya and Isago [88,89]. For the

substituted SbPcs, only Sb tetra-*tert*-butyl phthalocyanine [Sb(III)TBPc]I_3 (**70**) has been reported [88, 91], and the preparation involved the condensation of the 4-tert-butylphthalonitrile with antimony triiodide. Oxidation of [Sb(III)TBPc]I_3 (**70**), with the appropriate oxidant, gave [L_2Sb(V)TBPc]I_3 (where L= OH (**71**), Br (**72**), and Cl (**73**)) [88, 92].

Table 1.1: Known SbPc and PbPc complexes

(a) Lead Pcs

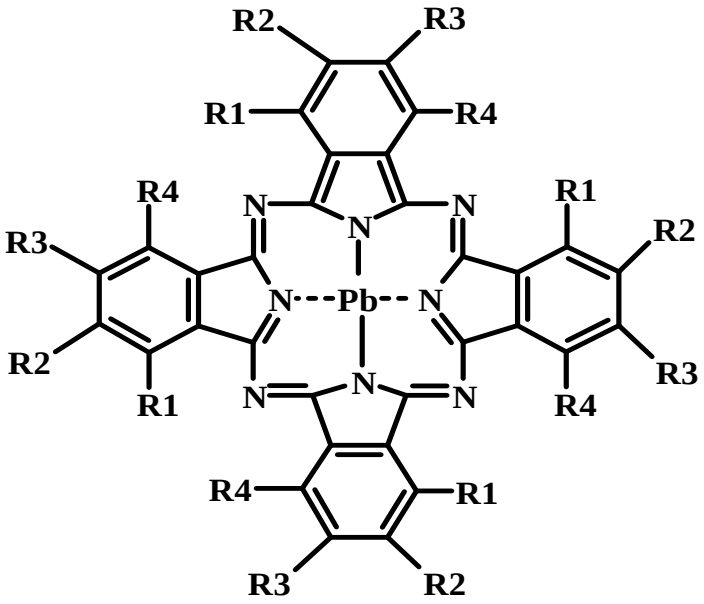

(**30**) R1 = H	R2 = H	R3 = H	R4 = H	[62]
(**31**) R1 = NO_2	R2 = H	R3 = H	R4 = H	[72]
(**32**) R1 = NH_2	R2 = H	R3 = H	R4 = H	[72]
(**33**) R1 =3-pentyl	R2 = H	R3 = H	R4 = H	[69]
(**34**) R1 =2,4dimethyl-3-pentyl	R2 = H	R3 = H	R4 = H	[69]

(**35**) R1 =2-naphthyl	R2 = H	R3 = H	R4 = H	[69]
(**36**) R1 = R4= hexyl	R2 = H	R3 = H		[77]
(**37**) R1 = R4= 3-methylbutyl	R2 = H	R3 = H		[77]
(**38**) R1 = R4= hexylsulfanyl	R2 = H	R3 = H		[63]
(**39**) R1 = R4= polyether	R2 = H	R3 = H		[83]
(**40**) R3 = cumylphenoxy	R1 = H	R2 = H	R4 = H	[65]
(**41**) R2 = R3= F	R1 = H	R4 = H		[79, 80]
(**42**) R2 = R3= Cl	R1 = H	R4 = H		[79, 80]
(**43**) R2 = R3= Br	R1 = H	R4 = H		[79, 80]
(**44**) R2 = R3= CH_3	R1 = H	R4 = H		[79, 80]
(**45**) R2 = R3= CH_3CH_2	R1 = H	R4 = H		[79, 80]
(**46**) R2 = R3= $CH_3CH_2CH_2$	R1 = H	R4 = H		[79, 80]
(**47**) R2 = R3= 13,17-dioxonacosane-15-sulfanyl			R1 = H	R4 = H	[84]
(**48**) R2 = R3= 13,17-dioxonacosane-15-sulfanylmethyl			R1 = H	R4 = H	[84]

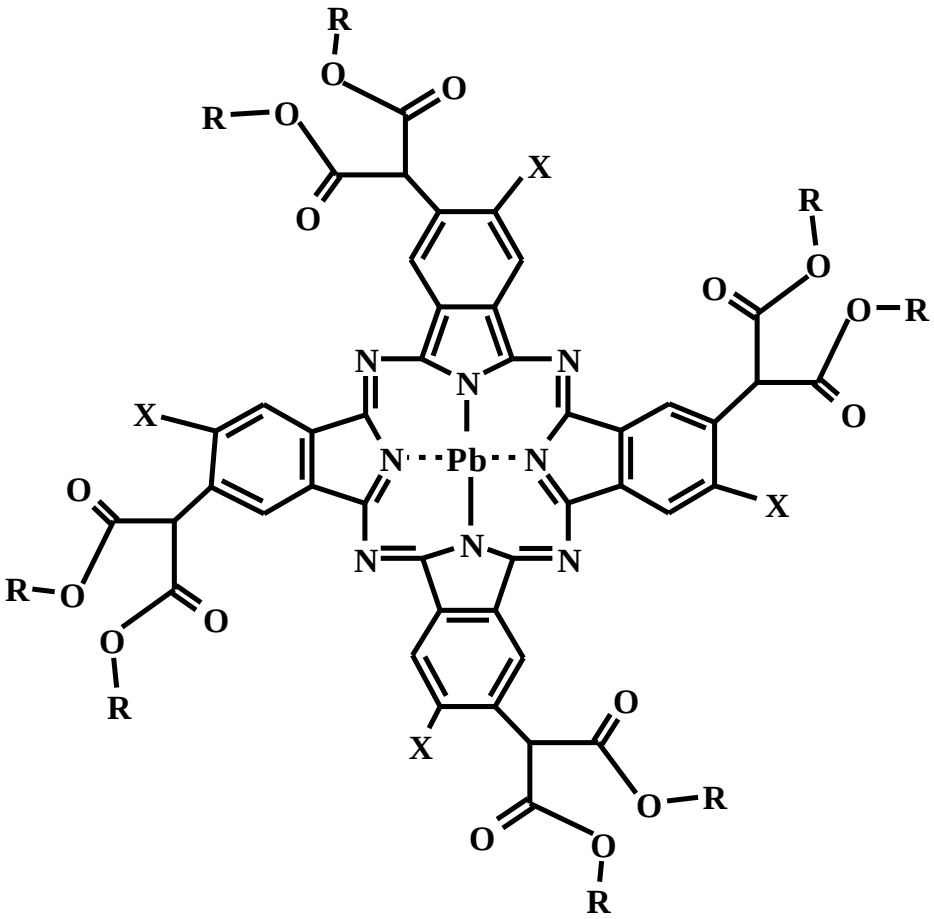

(**49**) R= C_6H_{13}	X= SC_6H_{13}	[71]
(**50**) R= C_6H_{13}	X= Cl	[71]
(**51**) R= C_6H_{13}	X= H	[71]
(**52**) R= C_2H_5	X= H	[70]
(**53**) R= C_2H_5	X= diethoxymalonyl	[70]

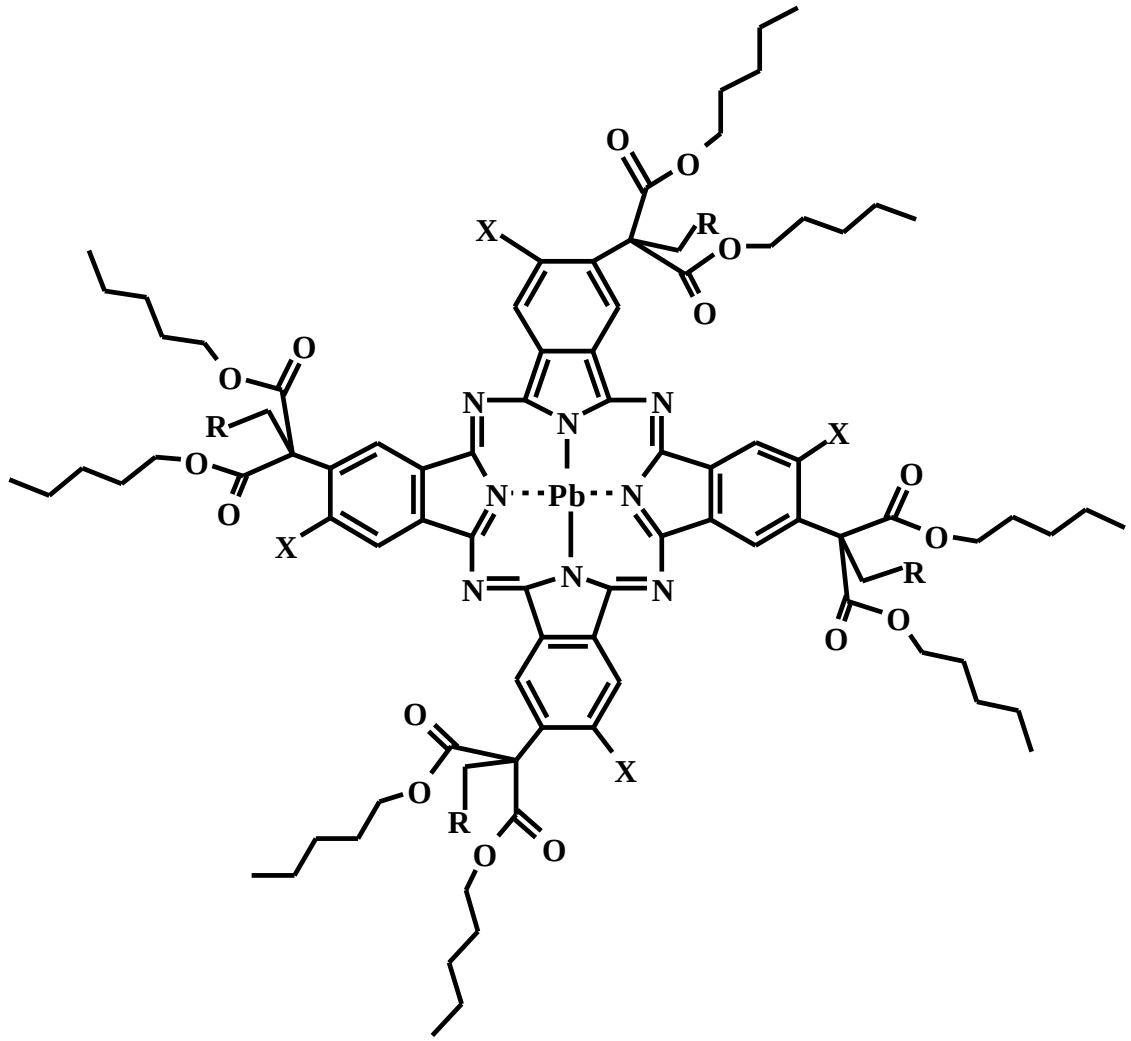

(**54**)R= bisphenyl	X= H	[81]
(**55**) R= naphthyl	X= H	[81]
(**56**) R= carbpentoxy	X= H	[81]
(**57**) R= bisphenyl	X= Cl	[81]

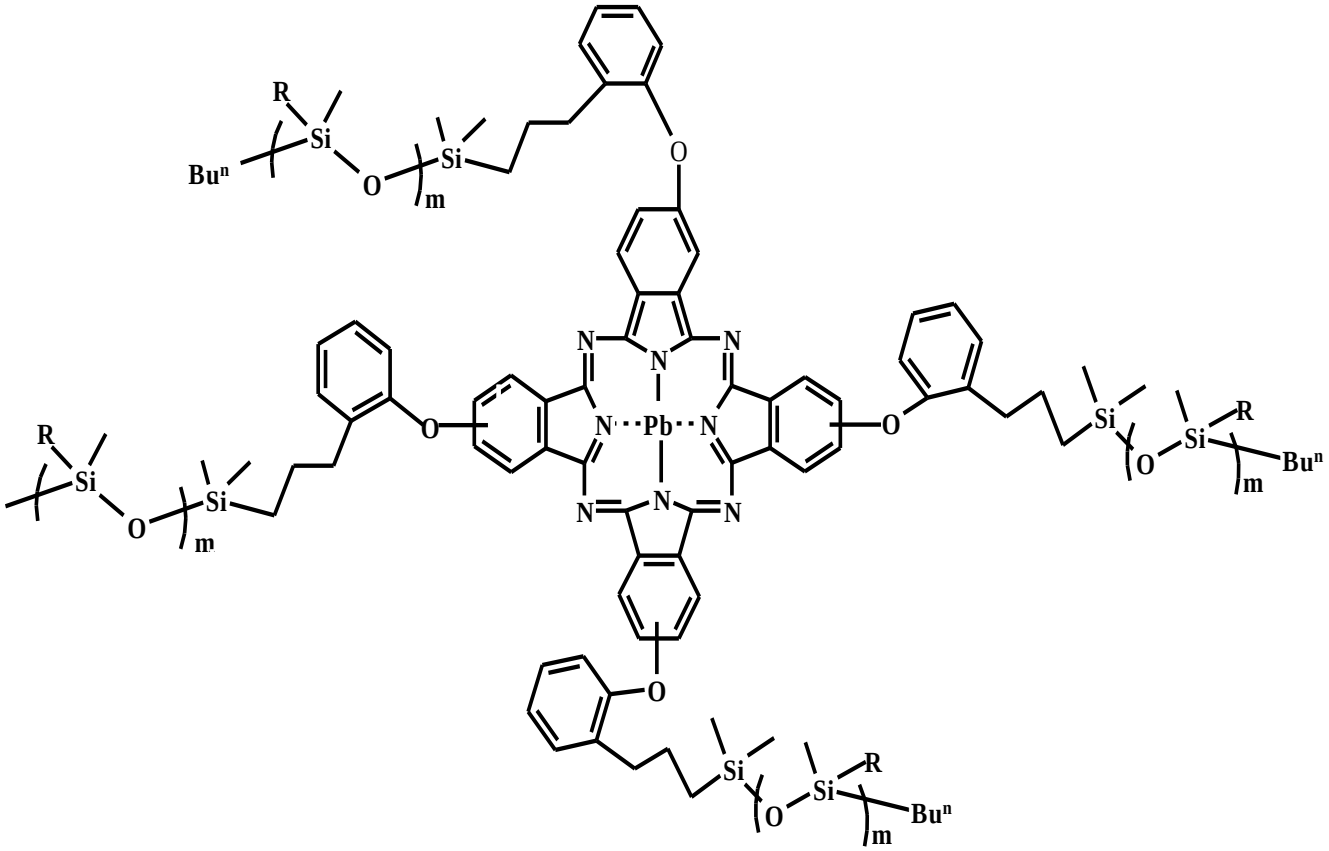

(**58**) R= methyl	m= 9	[78]
(**59**) R= methyl	m= 18	[78]
(**60**) R= phenyl	m= 9	[78]

b) antimony Pcs

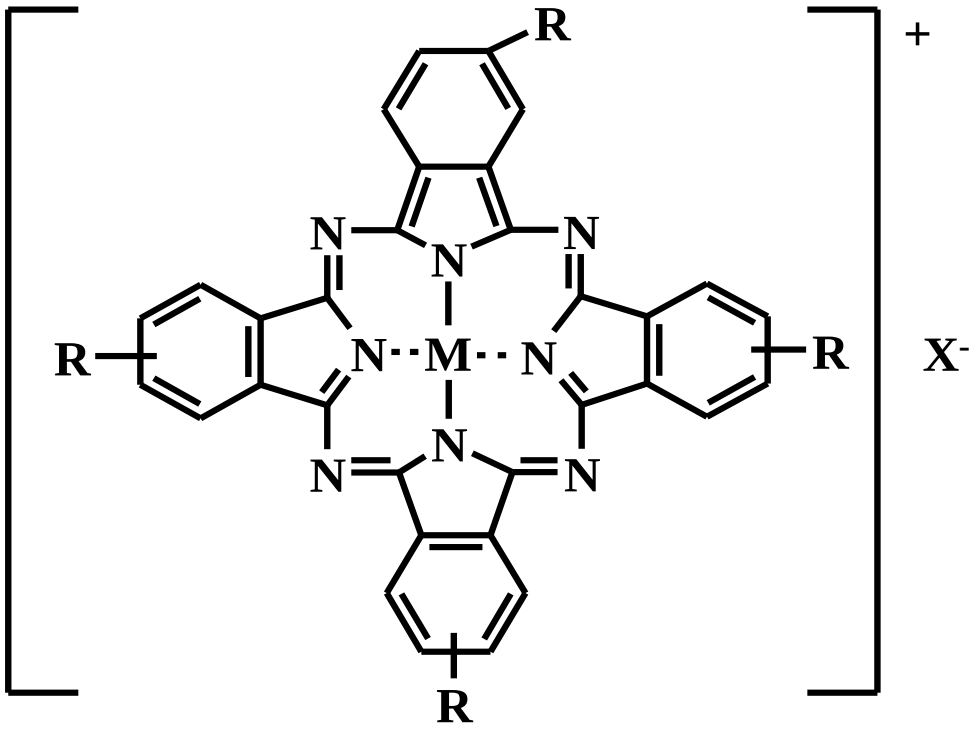

(**61**) M= Sb	R=H	X = I_3	[86]
(**62**) M= Sb	R=H	X = I	[93]
(**63**) M= Sb	R=H	X = F	[87]
(**64**) M= $Sb(OH)_2$	R=H	X = F	[87]
(**65**) M= $Sb(Cl)_2$	R=H	X = $SbCl_4$	[90]
(**66**) M= $Sb(Cl)_2$	R=H	X = $SbCl_6$	[89]
(**67**) M= $Sb(Cl)_2$	R=H	X = ClO_4	[89]
(**68**) M= $Sb(Cl)_2$	R=H	X = BF_4	[89]

(**69**) M= $Sb(Cl)_2$	R=H	X = PF_6	[89]
(**70**) M= Sb	R= t-C_4H_9	X = I_3	[88, 96]
(**71**) M= $Sb(OH)_2$	R= t-C_4H_9	X = I_3	[88, 96]
(**72**) M= $Sb(Br)_2$	R= t-C_4H_9	X = I_3	[88, 96]
(**73**) M= $Sb(Cl)_2$	R= t-C_4H_9	X= I_3	[88, 96]
(**74**) M= SbCl	R=H	X = -	[85]
(**75**) M= $(Sb)_2$	R=H	X =-	[85]

Aim of thesis

The aim of this thesis was to synthesize ring substituted Sb and Pb phthalocyanines, since as can seen from Table 1.1 above there are rare for SbPc complexes and to study their photophysical behaviour. Sb and Pb metals have been chosen as central atoms, because they are heavy atoms and they are diamagnetic, which plays a major role in the photosensitising and optical limiting abilities of complexes. Unsubstituted PbPc (**30**) and SbPc (**61**) complexes (Fig. 1.11) were synthesized for comparative purposes, even though it is well known that unsubstituted MPcs are insoluble in most organic solvents. Substituted MPcs will therefore be synthesized in order to overcome solubility problems. To the best of our knowledge, no SbPcs and PbPcs bearing aryloxy (phenoxy (**a**), 4-t-butylphenoxy (**b**) and 4-benzyloxyphenoxy (**c**)) substituents (Fig. 1.12-14) have been previously reported. Therefore, this project involves the synthesize of SbPcs and PbPcs that are tetra substituted (at the peripheral (**77** and **80**) and non-peripheral (**76** and **79**) positions) as well as octa-substituted (**78** and **81**) Pcs, Figs. 1.12-1.14, bearing aryloxy groups at the peripheral positions in addition to the

unsubstituted Pcs, Fig. 1.11. The photophysical properties of metallophthalocyanines as influenced by nature and position of these substituents will thus be studied.

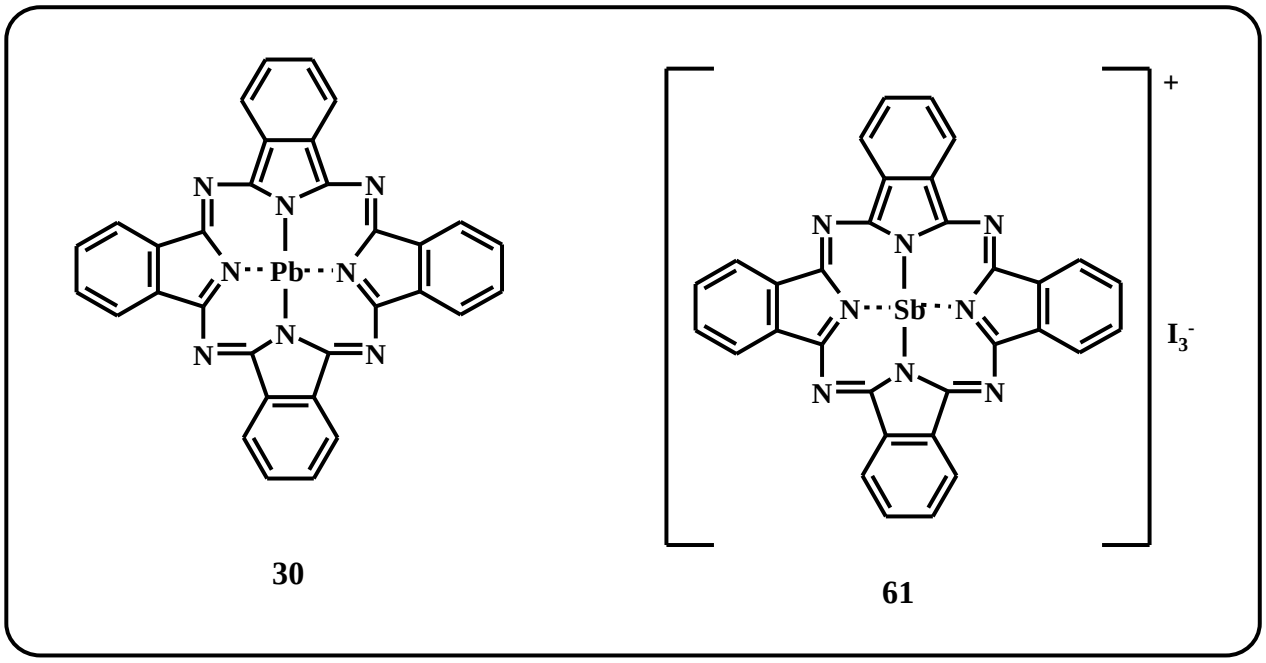

30 **61**

Fig. 1.11: Structure of PbPc (30) and [SbPc]I_3 (61) studied in this thesis

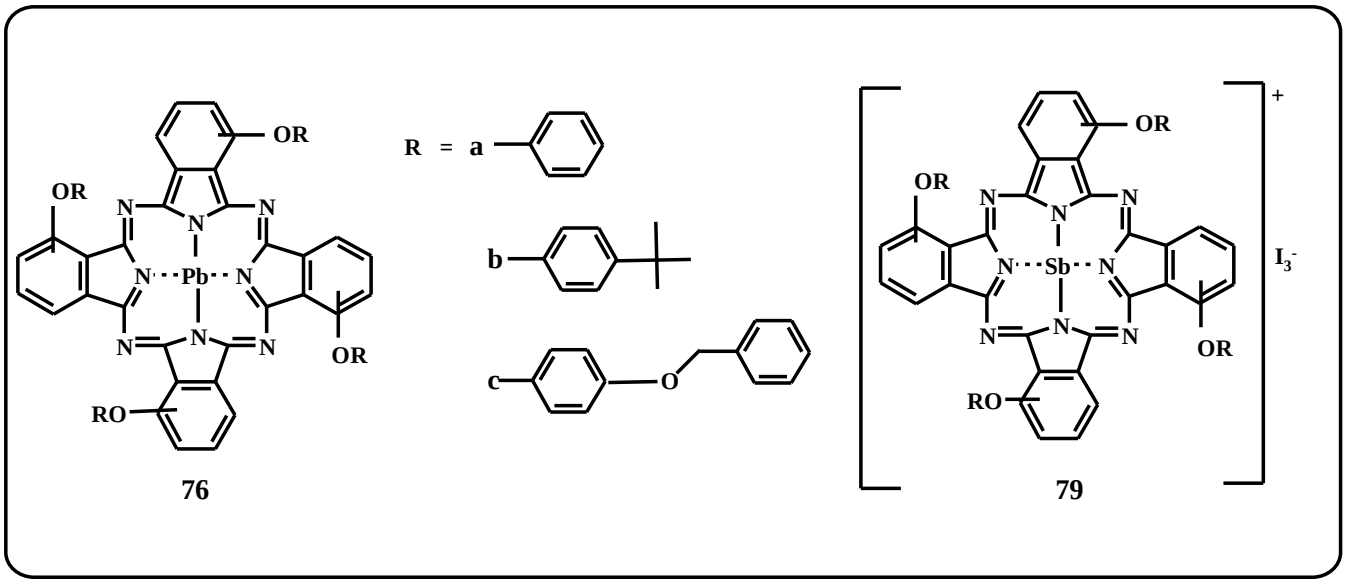

76 **79**

Fig. 1.12: Structure of the non-peripheral (3-) tetra substituted PbPc (76) and [SbPc]I_3 (79) studied

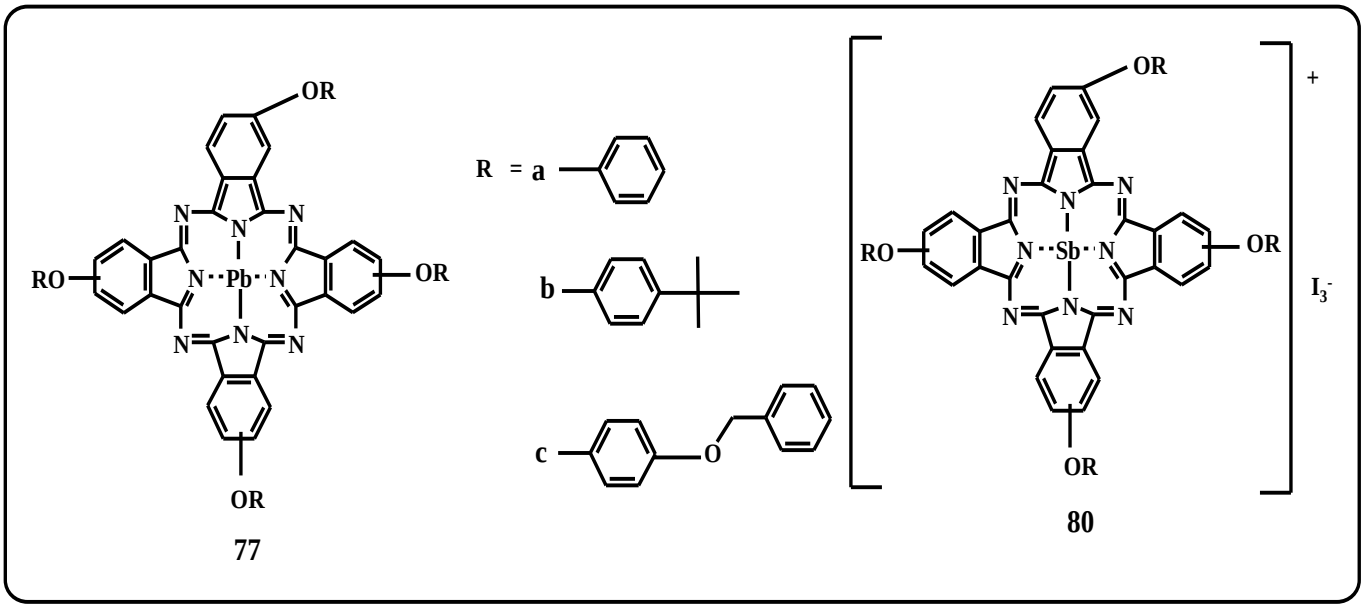

Fig. 1.13: Structure of the peripheral (4-) tetra substituted PbPc (77) and [SbPc]I_3 (80) studied

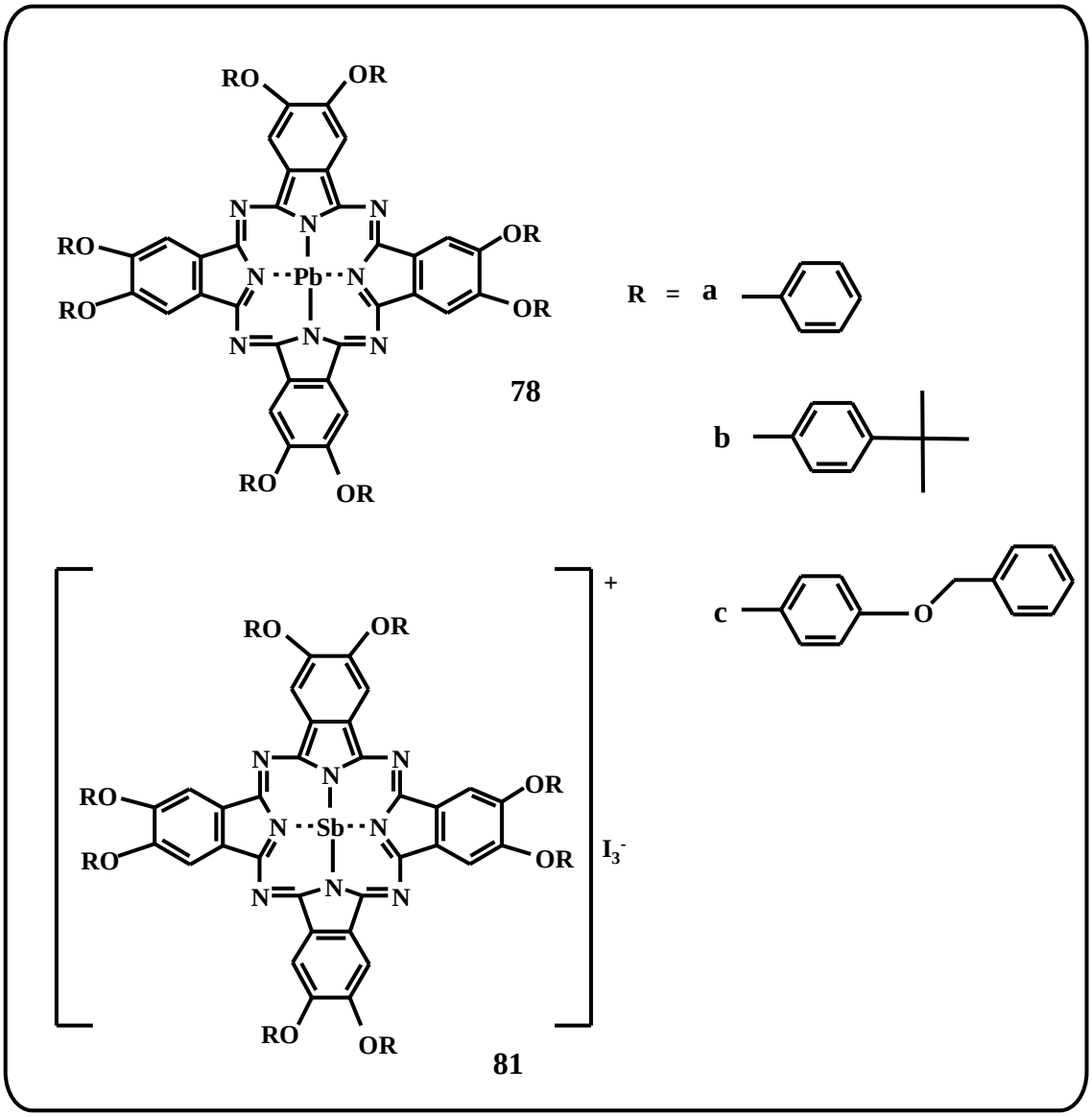

Fig. 1.14: Structure of the peripheral octa-substituted PbPc (78) and [SbPc]I_3 (81) studied

1.2. PHOTOPHYSICAL AND PHOTOCHEMICAL PROPERTIES

1.2.1. Photophysics

Photophysical processes may be defined as "the net physical changes that occur as a result of absorption of photon by Pc molecules" [100, 101].

1.2.1.1. Jablonski diagram

Jablonski diagram (Scheme 1.9) is often used to illustrate the physical changes following irradiation of Pc with light at an appropriate wavelength.

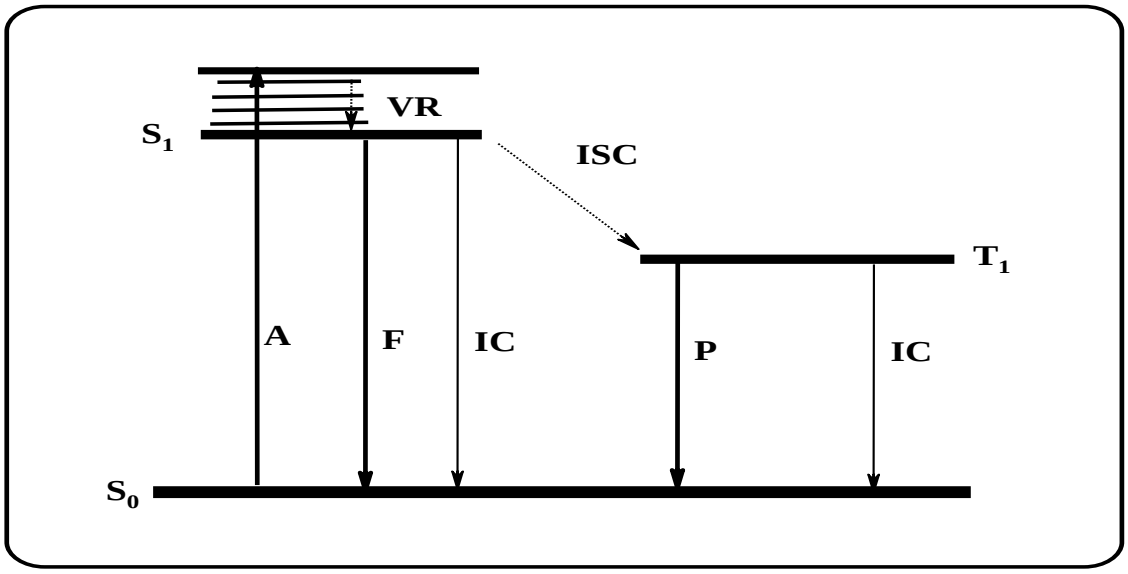

Scheme 1.9: Jablonski diagram showing transitions between the excited electronic state and the ground state. A = Absorption; VR = Vibrational relaxation, IC = Internal conversion, ISC = Intersystem crossing; F = Fluorescence; P = Phosphorescence

The molecule absorbs energy (A), causing the excitation of electrons from the singlet ground state (S_0) to the higher vibronic level of the first singlet excited state (S_1). From the higher vibronic level of S_1, the excited MPc (now ^{1}MPc*) loses some of

excitation energy, through vibrational relaxation processes, to the lowest vibronic level of S_1. The excited molecule, now at the lowest vibronic level of S_1, may then lose energy through the emission of light to S_0 (fluorescence (F)), by releasing heat to its surroundings via internal conversion (IC) or by undergoing intersystem crossing (ISC) to populate the triplet excited state (T_1). In the triplet state, the excited molecule may then lose energy by descending to S_0, and emit light to S_0 (phosphorescence (P)), or give its energy to another molecule through photosensitization.

1.2.1.2. Fluorescence

Fluorescence is short lived, with a typical time scale lying in the picosecond (10^{-12}) to nanosecond (10^{-9}) time range [102].

The energy involved in fluorescence is less than that of absorbance, thus the fluorescence emission spectrum is observed at longer wavelengths with respect to the absorption spectrum and is typically observed to be a mirror image of the absorption spectrum (Fig. 1.15). The difference between the spectral position of the Q-band maxima of absorbance and fluorescence is called Stoke's shift. Stokes shifts of less than 10 nm for MPcs signifies that the excited state has a geometry that is similar to that of the molecule in the ground state.

A fluorescence excitation spectrum (Fig. 1.15) provides information about the absorption spectrum of the excited fluorescent molecule in the excited state. The excitation spectrum is usually compared to the corresponding absorption spectrum and should ideally resemble the latter [103]. The excitation spectrum also shows if

the emitted molecule has a similar molecular geometry to that of the ground state or whether any geometrical changes have occurred in the molecule upon excitation.

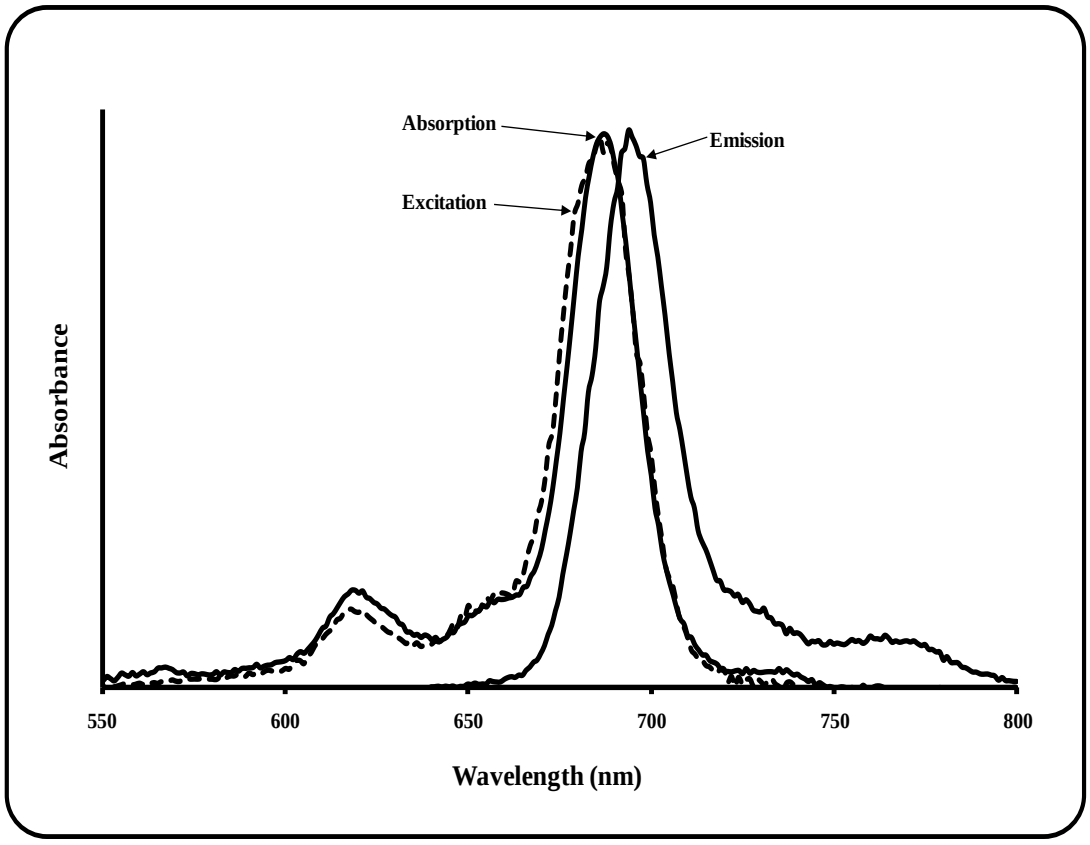

Fig. 1.15: An example of fluorescence and absorption spectra of MPc

The fluorescence properties of phthalocyanines are strongly influenced by factors such as temperature, molecular structure, solvent parameters (polarity, viscosity and refractive index), and the presence of heavy atoms in the solvent or in the molecule itself. Fluorescence spectral shifts, quantum yields and lifetimes are some of the photophysical properties that are measured [104, 105] and used to determine and quantify the efficiency of emission of a phthalocyanine.

Fluorescence quantum yield

Quantum yield is defined as "the number of molecules taking part in an event for every photon absorbed by the molecule", as given by Equation 1.1.

Φ = [number of molecules in an event] / [number of photons absorbed] **1.1**

Fluorescence quantum yield (Φ_F) is a measure of the efficiency of the fluorescence process and is usually determined by a comparative method [106, 107] and the method involves using a known fluorescence quantum yield as a standard, for example ZnPc in DMSO (Φ_F) = 0.20 [108], and is calculated according to Equation 1.2.

$$\Phi_F = \Phi_F^{std} \frac{F.A_{std}.n^2}{F_{std}.A.n_{std}^2} \qquad \textbf{1.2}$$

where F and F_{std} are the areas under the fluorescence curves of the MPc derivatives and the standard, respectively. A and A_{std} are the respective absorbances of the sample and standard at the excitation wavelengths and n and n_{std} are the refractive indices of the solvents used for the sample and standard, respectively.

Low concentrations of the compound with an absorbance of ~ 0.05 at the excitation wavelength of both sample and standard are necessary for these studies in order to avoid or minimise the re-absorption effect [109] which are due to inner filter effects that would result in erroneous quantum yield values. The inner filter effect is a phenomenon that decreases Φ_F values when the (exciting or emitting) light penetration through a spectrophotometric cell is hindered by strongly absorbing solutions. When using different solvents for the standard and sample, refractive indices are used as a correction measure [110]. Monomeric MPcs have similar

fluorescence quantum yields, ranging from 0.10 – 0.30 [111]. Aggregation [112], structural features such as double bond torsion, low-energy n to π* levels, heavy atoms, weak bonds and photoinduced electron transfer [113] reduce MPc fluorescence quantum yields.

1.2.1.3. Triplet quantum yield and lifetimes

The development of laser flash photolysis as a source of pulsed excitation has allowed the study of excited states, transient intermediates, triplet lifetime determinations and changes in absorbance in the triplet state, which is directly related to the triplet quantum yield [114]. Transient intermediates at the excited states are generated by a short and intense light pulse from a pulsed laser source.

The triplet quantum yields (Φ_T) may thus be defined as a measure of molecules that undergo intersystem crossing to occupy the triplet state. The triplet-triplet absorption of most Pcs occurs at approximately 500 nm and is due to transition from the lowest triplet state to higher triplet state of a molecule. A triplet decay curve is obtained by a plot of the difference between the absorbance before and after a laser pulse (ΔA), and time in seconds, following laser flash photolysis (Fig. 1. 16).

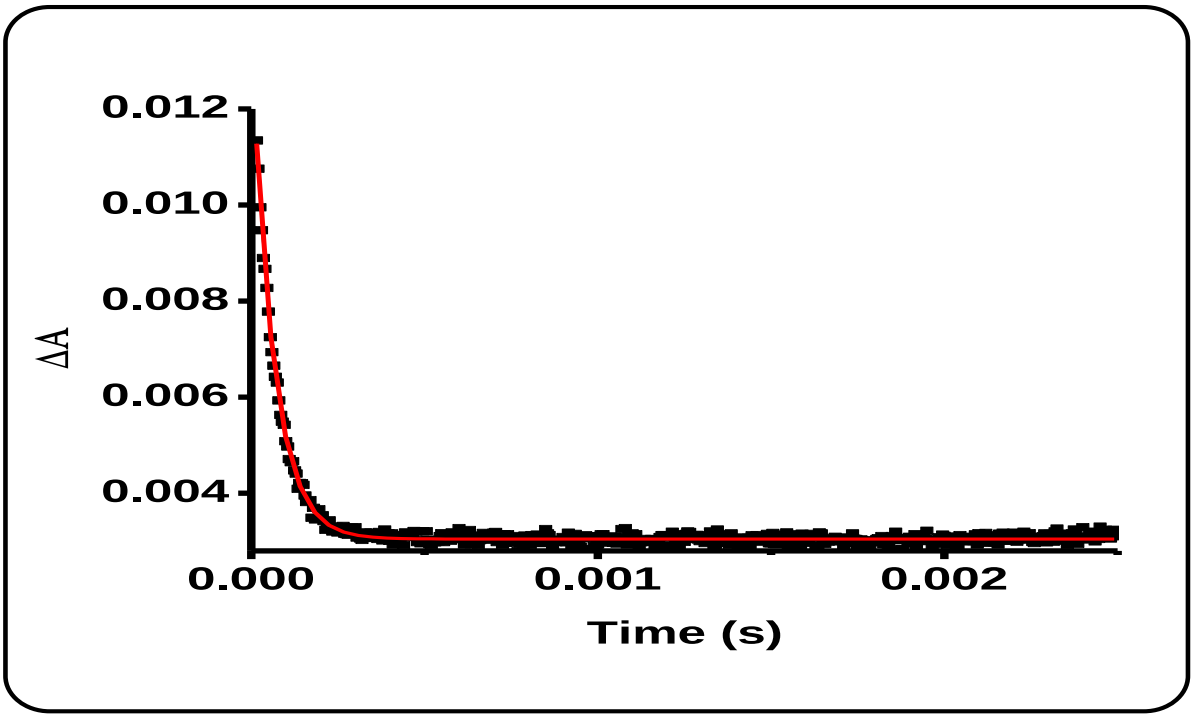

Fig. 1.16: Triplet decay curve of a typical phthalocyanine

The triplet lifetimes of the transient species are easily determined using a software program called OriginPro 7.5 via first or second order kinetics. A linear plot of ln *A* vs time may be used as alternative method to determine lifetime because the plot gives *k* as a gradient, the reciprocal of which gives the triplet lifetime (i.e. $\tau_T = 1/k$).

The triplet quantum yields (Φ_T) may be determined by using a comparative method [108, 115], which involves the use of a known Φ_T of a standard at a given wavelength, e.g. unsubstituted zinc phthalocyanine. The triplet quantum yield of a sample may be calculated using Equation 1.3

$$\Phi_T = \Phi_T^{std} \frac{\Delta A_T . \varepsilon_T^{std}}{\Delta A_T^{std} . \varepsilon_T} \qquad \textbf{1.3}$$

where ΔA_T and ΔA_T^{std} are the changes in triplet state absorbance of a Pc molecule and the standard, respectively. ε_T and ε_T^{std} are the triplet state molar extinction coefficients

for the Pc molecule and the standard, respectively. Φ_T^{std} is the triplet quantum yield for the standard, ZnPc (e.g. $\Phi_T = 0.65$ in DMSO [116]. The values of ε_T and ε_T^{std} are determined by the singlet depletion method, which involves the measurement of change in absorbance of the ground singlet states (ΔA_S and ΔA_S^{std}), the molar extinction coefficients at their respective ground singlet state (ε_S and ε_S^{std}) and changes in the triplet state absorptions, (ΔA_T and ΔA_T^{std}) according to Equations 1.3a and 1.3b:

$$\varepsilon_T = \varepsilon_S \frac{\Delta A_T}{\Delta A_S} \qquad \textbf{1.3a}$$

$$\varepsilon_T^{Std} = \varepsilon_S^{Std} \frac{\Delta A_T^{Std}}{\Delta A_S^{Std}} \qquad \textbf{1.3b}$$

Quantum yields of internal conversion (Φ_{IC}) may be obtained using Equation 1.4, which assumes that only three physical processes (fluorescence, intersystem crossing and internal conversion), jointly deactivate the excited singlet state of a Pc molecule.

$$\Phi_{IC} = 1 - (\Phi_T + \Phi_F) \qquad \textbf{1.4}$$

The triplet state generation properties of Pc macrocycles is useful in nonlinear optical processes, as well as PDT and photooxidation reactions. MPcs are capable of generating singlet oxygen since their triplet energy (110 – 126 kJ.mol^{-1}) is more than the required energy (94 kJ.mol^{-1}) to allow for efficient energy transfer to ground state oxygen [117].

1.2.2. Nonlinear optics

Nonlinear optics (NLO) is a sub-discipline of optics that is associated with the changes in the optical properties of a material when exposed to light [118]. There are several optical technologies based on nonlinear effects [119], these include optical rectifiers, optical switches, dynamic holography, and optical data-recording and optical limiters. An optical limiter is one of the powerful tools used for nonlinear optics. It is used in the protection of light sensitive elements such as optical sensors, human eyes and other light sensitive material.

Since the discovery and invention of intense light sources based on laser mechanisms in the 1960s [120], the need for the development of protective devices against laser radiation has stimulated essential research, due to the widespread use of laser weapons. Thus eye and sensor protection systems are required due to intentional laser misuse, which, for example, has resulted in temporary blindness of pilots upon approach to landing [121] (Fig 1.17). There have also been several laser induced eye injuries that have occurred in the U.S. military between 1984 and 2000 [122], caused by accidental exposure to a Q-switched, Neodynium:YAG (Nd:YAG) laser at 1064 nm wavelength.

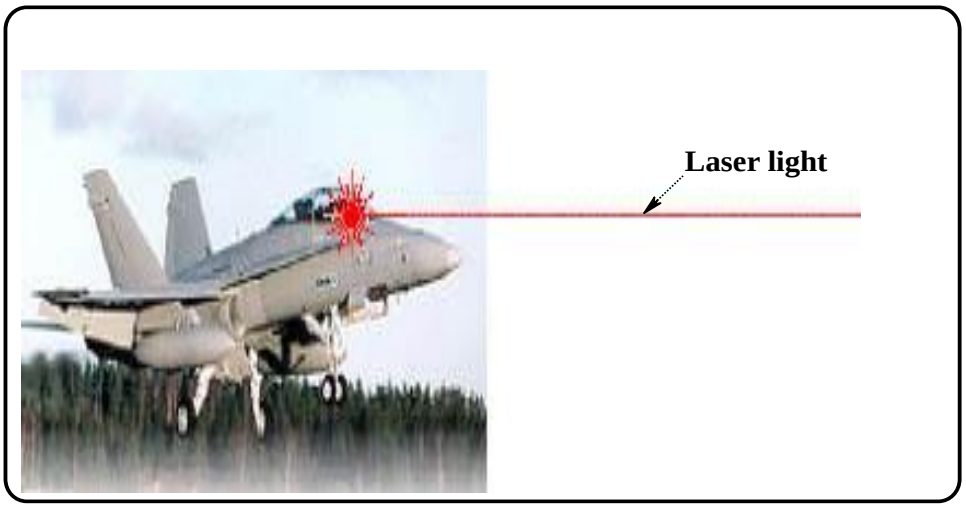

Fig. 1.17: Laser light on aircraft [121]

Consequently, there is a need to develop highly efficient protective devices, in order to provide protection to human eyes and sensitive sensor systems. For example, the reliance of the South African army on laser illumination [123] warning and on training air crew is not adequate because the sensors, which are currently in use, do not cover the complete range of laser threats and as a result they do not protect the eyes. Thus the interest in developing efficient and stable optical limiting material in South Africa.

The structural prerequisite for NLO material is the presence of a conjugated, delocalised π-electron orbital network. The conjugated structure affords high polarizability properties and thus fast charge redistribution on interaction with intense magnetic radiation, such as laser radiation [118,124,125]. Organic and organometallic materials have emerged as promising candidates for limiting laser radiation intensity. Among NLO materials, MPcs are of great interest because they have several advantages over the inorganic material currently in use for optical limiting (OL). The

advantages include: i) fast response times (subpicosecond) [126], the faster the response is, the better the optical limiter [126, 127], ii) small dielectric constants [119], and iii) ease of fabrication or processing and low cost of production [128].

The discovery of Pcs as active NLO materials in optical limiting applications have been widely recognised [129]. Up until recently, the feasibility of Pcs as NLO materials has been devoted to the measurements of NLO properties, together with a basic understanding of the origin of nonlinearities [130, 131].

1.2.2.1. Optical limiting effect

An optical limiter is a device that can limit the output intensity of a laser light to a maximum value. It has a transmission that varies with the intensity of incident light (Fig.1.18). The transmission is high for normal light and low for intense light. The optical limiting effect is observed when the intensity of laser light is strongly reduced by a system acting as an optical limiter once the input intensity exceeds a threshold value ($\mathbf{I_{lim}}$).

The ideal behaviour of an optical limiter is shown in Fig. 1.18, where $\mathbf{I_{out}}$ and $\mathbf{I_{in}}$ is the intensity of the light transmitted by the optical limiter and the intensity of the incoming light, respectively. Ideally, $\mathbf{I_{in}}$ increases linearly with $\mathbf{I_{out}}$ until a limiting point $\mathbf{I_{lim}}$ is reached [119, 132, 133]. The nonlinearity of optical limiting effect arises from the fact that the response $\mathbf{I_{out}}$ of the optical limiter is not directly proportional to the input values $\mathbf{I_{in}}$ in the operative range of $\mathbf{I_{in}}$ ($\mathbf{I_{in} >> I_{out}}$).

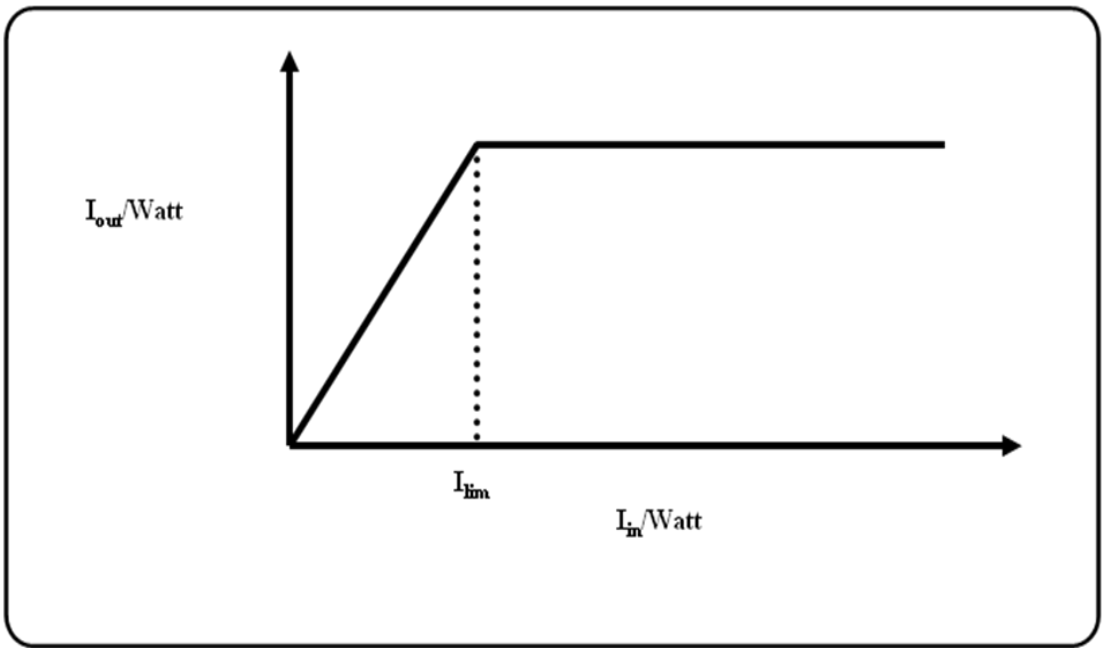

Fig. 1.18: The response of an optical limiter [119, 126, 132, 133]

The optical limiting effect can be produced through all the fundamental mechanisms which lie at the basis of the linear optical effects, i.e. absorption, refraction, reflection and scattering (Fig. 1.19). Among the listed optical limiters for the limiting of intense radiations, those based upon the phenomenon of absorption are the most desired [134], because the optical phenomenon of nonlinear absorption is based on the mechanism of excited-state absorption.

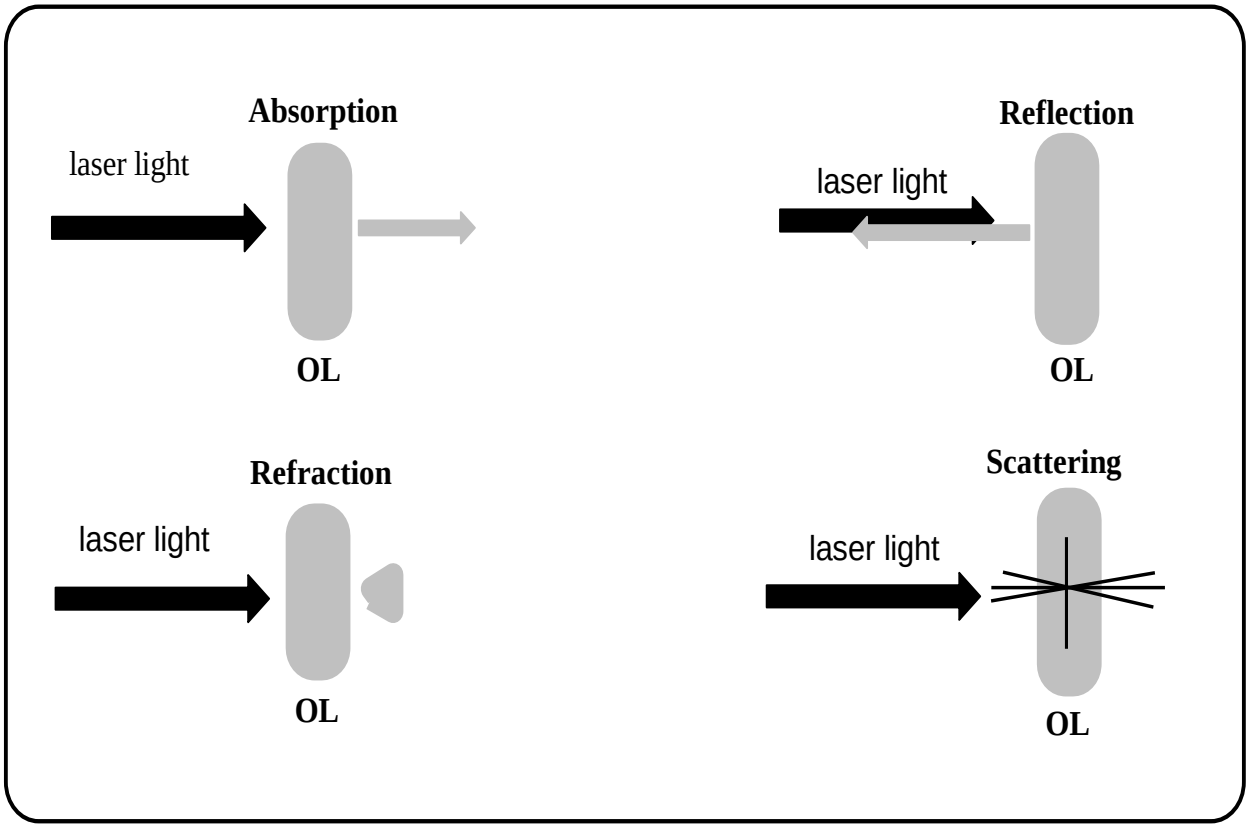

Fig. 1.19: The physical processes forming the basis of the optical limiting effect (OL= optical limiter) [133, 134]

Optical pumping [135] is the most effective process in producing good optical limiting effects. Optical pumping involves real transitions, where laser light interacts with the absorbing (optical limiting) material, producing the excited states, giving rise to reverse saturable absorption (RSA) and saturable absorption (SA).

The Jablonski diagram in Figure 1.20 describes the processes responsible for the optical limiting effects of RSA. The absorption cross section of the excited state, σ_{ex}, should exceed that of the ground state, σ_g in RSA.

In SA, the absorption cross section of the ground, σ_g , is larger than that of the state excited state, σ_{ex}, (Fig. 1.20).

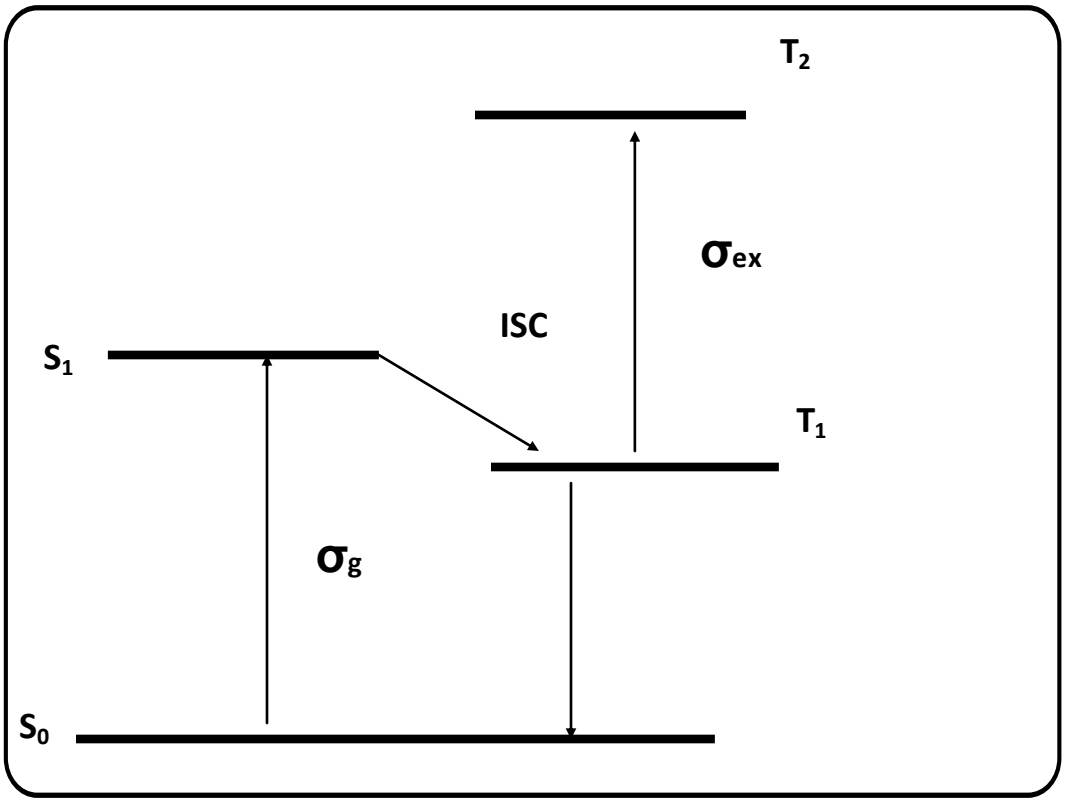

Fig. 1.20: Jablonski diagram for phthalocyanines showing the absorption and decay pathways. Where σ_g and σ_{ex} are absorption cross sections for the ground and excited states, respectively [119, 126]

An efficient optical limiter should, therefore, have: i) a triplet state cross section absorption that is larger than the ground state ($\sigma_{ex} >> \sigma_g$); ii) long lifetimes in the microsecond time range and a large population in the triplet state; iii) rapid intersystem crossing in order to populate the triplet state; iv) optical stability, to minimize degradation of the optical limiting material under laser irradiation; and v) good processibility [119, 126,127,133,135,136].

Pcs display optical limiting effects in the region between 400-600 nm, (Fig. 1.21), which shows that Pcs possess an RSA mechanism when $\sigma_{ex} >> \sigma_g$.

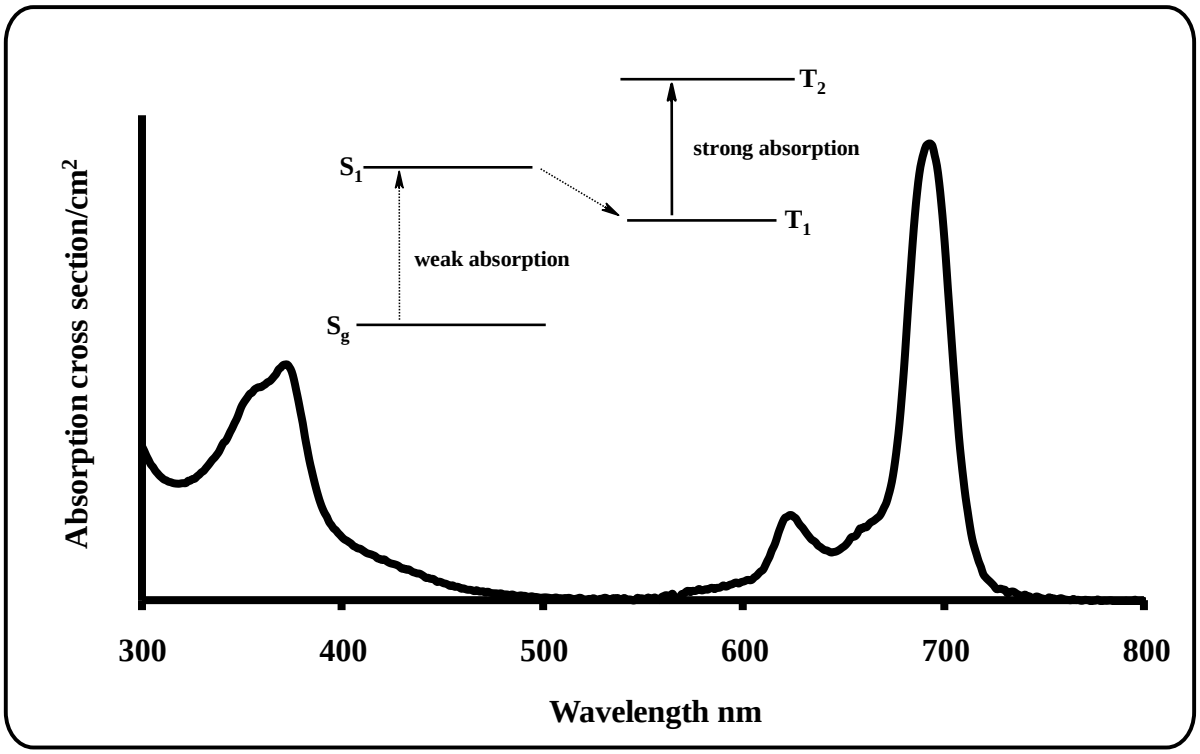

Fig. 1.21: Absorption cross sections for the ground and excited triplet state for Pc. The insert: Jablonski diagram showing weak and strong absorption under laser light

1.2.2.2. Nonlinear optical parameters

The important parameters in this section are i) *k*: the ratio of the absorption cross sections of the ground (σ_g) and excited (σ_{ex}) states; ii) I_{lim}, the safety threshold limiting intensity; and iii) $I_m[\chi^{(3)}]$ and γ, the third and second order susceptibilities, respectively.

k can be calculated using Equation 1.5 and a good optical limiter should have a *k* of more than one.

$$k = \frac{\sigma_{ex}}{\sigma_g} \qquad \textbf{1.5}$$

Limiting threshold intensity (I_{lim})

The limiting intensity values are calculated according to Equation 1.6 [119, 136]:

$$I_{lim} = \frac{h\omega^*}{2\pi\sigma_g\tau_{ex}} \qquad \textbf{1.6}$$

where ω^*, σ_g and τ_{ex} are the frequency at which the system absorbs, the singlet absorption cross section and the triplet lifetimes, respectively.

An ideal optical limiter should have a low threshold limit value (**l_{im}**), because if the value is too high, it becomes less reliable in terms of eye or light sensitive protection.

Third order susceptibility $\chi^{(3)}$ and second hyperpolarizability, γ

Calculation of the third order susceptibility, $I_m [\chi]^{(3)}$, is given by Equation 1.7 [136].

$$I_m[\chi^{(3)}] = \frac{2c^2n^2\beta}{\pi\omega^*} x10^{-22} \qquad \textbf{1.7}$$

where n and ω^* are, respectively, the linear refractive index (n = 1.478 for DMSO) and the frequency at the wavelength of interest. β represents a nonlinear absorption term which averages the molar extinction coefficients ε_g and ε_{ex} according to Equation 1.8 [136].

$$\beta = 5.3\varepsilon_g\varepsilon_{ex}[C]\Phi_{ISC} \qquad \textbf{1.8}$$

where ε_g and ε_{ex} are the molar extinction coefficients for the ground and excited state, respectively, [C] is the concentration of active species in the triplet state and Φ_{ISC} is the intersystem crossing quantum yield.

At a molecular level, $I_m [\chi]^{(3)}$ is directly related to the second hyperpolarizability, γ, through Equation 1.9 [119, 135, 136].

$$\gamma = \frac{I_m[\chi^{(3)}]}{f^4[C]N_a} \qquad \textbf{1.9}$$

where N_a is Avogadro's constant, C is the concentration of the active species in the triplet state and f is the Lorentz local field factor, $f = (\eta^2 + 2)/3$, where η is the viscosity.

These nonlinear parameters, $I_m[\chi^{(3)}]$ and γ, are used to quantify the nonlinear absorption.

1.2.3. Review of photophysical and nonlinear optical properties of PbPcs and SbPcs

PbPc and SbPc derivatives are considered to be excellent photosensitizers and optical limiters because of the presence of heavy atoms (Pb and Sb) which would facilitate singlet–triplet intersystem crossing (ISC) due to a strong metal-induced spin–orbit coupling [137], however, little information has been reported on the photophysical properties of SbPcs [87, 88, 91, 92, 97] and PbPcs [83] complexes.

1.2.3.1. Antimony phthalocyanines (SbPcs)

The fluorescence properties of Sb(III)Pcs were studied after oxidation to Sb(V)Pc derivatives, since Sb(III)Pc derivatives themselves do not fluoresesce [91]. The fluorescence quantum yield (Φ_F) of [Sb(V)Pc]F bearing OH axial ligands was found to be 0.076 in ethanol and showed a Q band at 699 nm in its emission spectrum [86]. $[Sb^{III}TBPc]I_3$, did not show fluorescence in the Q- band region, while a

$[Br_2Sb(V)TBPc]^+$ complex showed fluorescence (λ=753 nm, with fluorescence quantum yields (Φ_F) <0.001) in dichloromethane [97]. The Φ_F of $[Cl_2Sb(V)Pc]^+$, $[Cl_2Sb(V)TBPc]^+$, and $[(HO)_2Sb(V)TBPc]^+$ complexes were found to < 0.01 in dichloromethane [88, 92]. The Φ_F values were small and thought to be due to heavy atom effect. The behaviour of the triplet state of SbPc complexes has, as yet, not been explored. Hence, the aim of this thesis is to study the photophysical properties (triplet quantum yields, triplet lifetimes and fluorescence quantum yields) of SbPc complexes.

1.2.3.2. Lead phthalocyanines

The photophysical and nonlinear optical behaviour of PbPc complexes have not been fully explored. Polyether peripherally substituted PbPc complexes were found to give low triplet lifetimes in benzene (τ_T = 32 μs) and triplet quantum yields (Φ_T = 0.30), when compared to ZnPc (τ_T = 105 μs, Φ_T = 0.32) [83]. PbPc derivatives gave large rate constants of intersystem crossing due to the heavy Pb central atom.

Work on the nonlinear optical properties of Pb phthalocyanines has been reported [77, 78, 138 -142], with the PbPc derivatives showing good optical limiting properties [77, 78, 138 -142], when compared to NiPc and H_2Pc. However some of this work does not include all the nonlinear optical parameters that are of interest. These parameters include the absorption cross section ratio *k*, and limiting intensities (I_{lim}), also known as saturation energy density (F_{sat}), second (γ), and third order ($I_m[\chi^{(3)}]$), hyperpolarizabilities. Tetrakis(cumylphenoxy) PbPc has been shown to be a good optical limiter [138] as well as a derivative of PbPc with siloxane chains [78]. Both these complexes were studied with the aid of a Z-scan and f/5 focusing optics. The *k*

values for non-peripheral octakis(hexyl) PbPc and octakis(methylhexyl) PbPc were found to be 16.1 and 14.2, F_{sat} values (same as I_{lim}) were 9.8 and 7.1 $J.cm^{-2}$, while $I_m[\chi^{(3)}]$ were found to be 1.1 x 10^{-11} and 1.7 x 10^{-11} esu, respectively [77].

The aim of this thesis is to study these physical parameters for PbPc derivatives, as well as to determine the nonlinear optical parameters. Lead has been chosen for nonlinear optical studies because it has been shown to have good optical limiting due to the large ionic size of Pb and is therefore expected to give Pc complexes with high triplet quantum yields. The range of PbPc with known NLO parameters is limited, hence the work reported in this thesis.

1.2.4. Photodegradation/photobleaching

Photodegradation or photobleaching is a chemical process by which Pc macrocycles oxidatively decompose or degrade with time upon irradiation with visible light [143] in the presence of singlet oxygen.

In practice, there are two photobleaching processes [144], i.e. i) photomodification, where the chromophore of the phthalocyanine molecule is retained in a modified form during absorbance loss, e.g. a main absorption peak diminishes at a particular wavelength and a corresponding new absorption peak is concurrently observed at another wavelength; ii) true photobleaching, whereby the chromophore of the Pc ring is degraded into smaller molecular fragments. This chemical process is driven by singlet oxygen in the presence of light to give the photo-oxidation products, e.g. phthalamide, as suggested by Schnurpfeil *et al.* [145]. The mechanism (Scheme 1.10) suggests that singlet oxygen may add across the C=N bond followed by cleavage at

the meso position (mechanism A) [145]; or it may add across the carbons of the pyrrole by a Diels-Alder [4 + 2] cycloaddition (mechanism B) [143, 146].

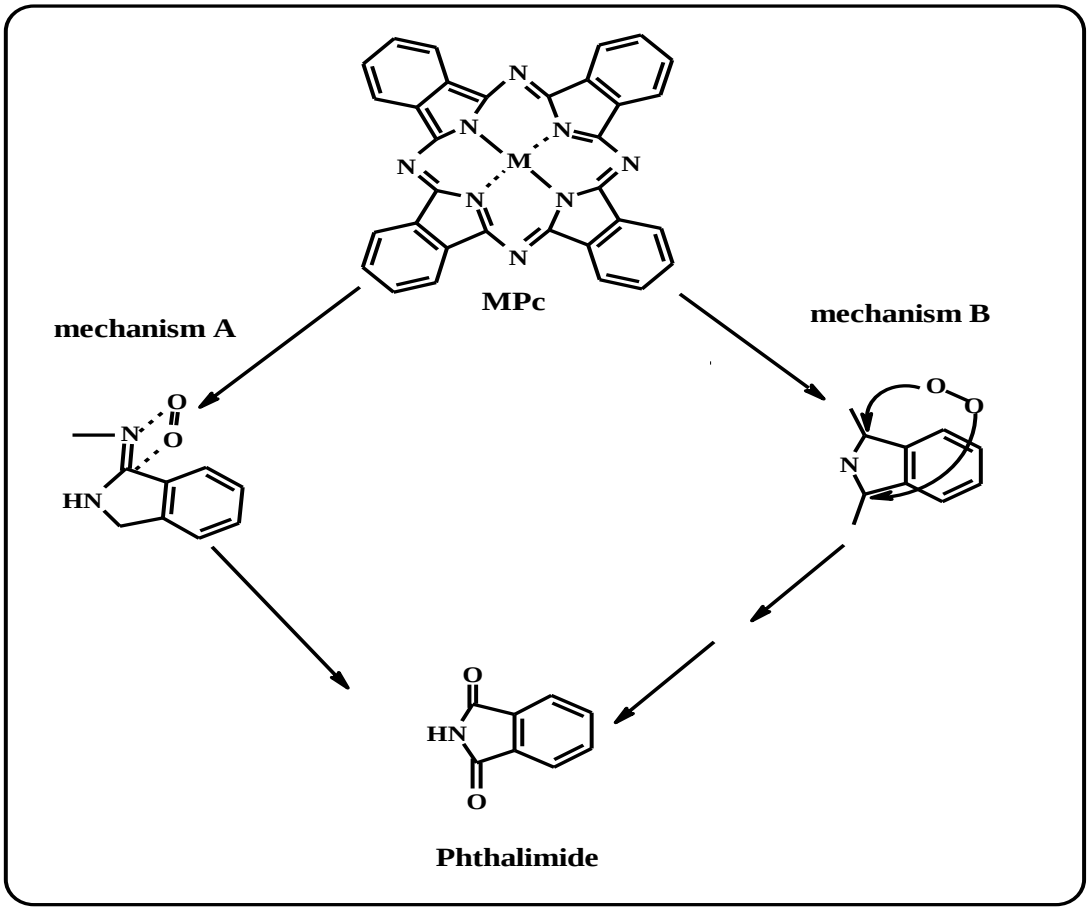

Scheme 1.10: Possible reactions of MPc upon irradiation with singlet oxygen [143, 145, 146]

Photodegradation/bleaching is a function of the nature of the substituents, the central metal, solvent and aggregation. It has been reported [147, 148] previously that the presence of electron-donating substituents on the MPc macrocycle brings about rapid degradation due to the ease of oxidation. On the other hand, electron-withdrawing substituents have the ability to stabilize the phthalocyanine ring, and thus to be resistant to oxidative attack. MPcs display different photodegration processes in different solvents. For example, photodegradation of phthalocyanines has been

observed to occur faster in chlorinated solvents such as chloroform ($CHCl_3$) and dichloromethane (DCM) because the radicals formed during C-Cl bond cleavage promote the photodegradation process. Photodegradation of MPcs in deuterated solvents is enhanced [147, 149], due to the long singlet oxygen lifetimes. In aqueous media, photodegradation rates of aggregated MPcs are low because the generation of singlet oxygen is very low in aggregated species [150, 151].

Photodegradation or photobleaching quantum yield (Φ_{Pd})

Photodegradation or photobleaching quantum yield (Φ_{Pd}) is defined as the ratio of the number of MPc molecules degraded per quantum of light absorbed. It is used to determine the photostability of MPc molecules and is identified by a decrease in the intensity of the Q-band absorption without the appearance of new peaks in the visible region. Photodegradation/photobleaching quantum yield may be calculated using the Equation 1.10 [36, 46, 152-154]:

$$\Phi_{Pd} = \frac{\Delta A}{\Delta t} \cdot \frac{V}{\varepsilon} \cdot \frac{1}{I_{abs}} \qquad \textbf{1.10}$$

where ΔA, Δt, V and ε are change in absorbance, change in time of irradiation, reaction volume and extinction coefficient of the Pc under investigation, respectively. I_{abs} is the overlap integral of the radiation source intensity and the absorption of the Pc in the region of the interference filter transmittance and may be calculated using Equation 1.11.

$$I_{abs} = \frac{\alpha S I}{N} \qquad \textbf{1.11}$$

where α is the fraction of light absorbed, I the light intensity, S and N_A are the irradiated cell area (cm^2) and Avogadro's constant ($mole^{-1}$), respectively.

1.2.4.1. Review of photodegration of SbPcs

Antimony (III)–Pcs are known to be readily oxidized to antimony (V) derivatives upon irradiation with visible light in aerated solutions [94]. The $[Sb(III)TBPc]I_3$ complex was found to be stable in the dark in chloroform and dichloromethane, but readily demetallated in donor solvents such as dimethylformamide (DMF) and tetrahydrofuran (THF) [98]. Photobleaching of this complex occurred under visible light irradiation in chloroform. Attempts to determine the singlet oxygen producing ability of $[Sb(III)TBPc]I_3$ using 1,3-diphenylisobenzofuran (DPBF) as a quencher resulted in oxidation of Sb(III) to Sb(V) [98]. The aim of the thesis is therefore to study the photodegration of the SbPc derivatives synthesized.

1.2.4.2. Review of photodegration of PbPcs

Sota and Dyrdra have reported on the photostability of PbPc in DMF, DMSO and pyridine [149]. The rate of photodegradation for PbPc was found to be 0.26, 0.10 and 1.34×10^{-2} min^{-1} in DMF, pyridine and DMSO, respectively [149]. The rate of this photochemical reaction was proven to be dependent on the solvent, as the photostability of this PbPc showed increasing stability in the order DMF < pyridine < DMSO [149]. Hence the objective of this thesis is to study the photodegradation of synthesized PbPc derivatives, in order to assess the stability of these complexes in the presence of light.

1.3. SUMMARY OF AIMS OF THE THESIS

The aims of the thesis discussed are summarized as follows:

1. To synthesize and spectroscopically characterize the peripherally octa-substituted (**78** and **81**) and tetra-substituted (at the nonperipheral (**76** and **79**) and peripheral (**77** and **80**) positions) PbPc and SbPc complexes with phenoxy (**a**), 4-t-butylphenoxy (**b**) and 4-benzyloxyphenoxy (**c**) groups (see Fig. 1.12-1.14). Furthermore, to synthesize unsubstituted PbPc (**30**) and SbPc (**61**) (Fig. 1.11) for comparative purposes.

2. To study the photophysical (fluorescence quantum yields, triplet quantum yields and triplet lifetimes) and photochemical (photobleaching/photodegradation quantum yield) properties of PbPc and SbPc complexes, the information derived will be essential for the characterization of nonlinear optical limiting material.

3. To study the nonlinear optical parameters of PbPc derivatives, these include *k*, which is the ratio of the absorption cross section of the singlet and triplet state; I_{lim}, the safety threshold limit intensity (limiting intensity); $I_m[\chi^{(3)}]$ and γ, the third and second order susceptibilities, respectively.

CHAPTER TWO:

EXPERIMENTAL

2.1. MATERIALS

Acetone, benzene, chloroform, 1-chloronaphthalene (1-CNP), dichloromethane (DCM), dimethylformamide (DMF), dimethylsulfoxide (DMSO), ethanol, hexane, methanol, 1-octanol and tetrahydrofuran (THF) were purchased from either SAARChem or Aldrich and were dried before use. Deuterated chloroform ($CDCl_3$), deuterated dimethylsulfoxide (DMSO- d_6), acetic anhydride (Ac_2O), ammonia (25 % or 32 %), antimony triiodide (SbI_3), 4-(benzyloxy)phenol, bromine, 4-*tert*butylphenol, 4,5-dichlorophthalic acid, formamide, hydrochloric acid (32 % HCl), tert-butylhydroperoxide (TBHP), magnesium sulphate, lead acetate, nitric acid (55 % HNO_3), 3-nitrophthalic acid, phenol, phthalimide, phthalonitrile (recrystallised from ethanol), potassium bromide, potassium carbonate, sodium carbonate, sulphuric acid (98 % H_2SO_4), thionyl chloride, urea, were purchased from Sigma-Aldrich, SAARChem or Merck. All other reagents were of analytical grade and were used as received from the suppliers. Column chromatography was performed on silica gel 60 (0.04 – 0.063 mm).

2.2. EQUIPMENT

Ground state electronic absorption spectra were performed on a Varian Cary 500 UV–Vis–NIR spectrophotometer; infrared spectra (KBr pellets) on Perkin Elmer Spectrum 2000 FT-IR Spectrometer and ^{1}H nuclear magnetic resonance (^{1}H NMR) signals on a Bruker AMX 400 MHz NMR spectrometer. Elemental analysis was performed at the University of Cape Town, South Africa, using a Thermo Flash EA 1112 series elemental analyzer and also using Elementar Vario Micro Cube CHNS Analyser. Microwave irradiations were carried out in a Defy DM206T microwave oven at a

power of 1000 W. Fluorescence excitation and emission spectra were recorded on a Varian Cary Eclipse Fluorescence spectrophotometer using 1 cm pathlength cuvettes.

Photo-irradiations for photodegradation quantum yield determinations were performed using a General electric Quartz line lamp (300W) as has been reported previously [108]. A 600 nm glass cut off filter (Schott) and water were used to filter off ultraviolet and infrared radiations respectively. An interference filter (Intor, 700 nm with a band width of 40 nm) was additionally placed in the light path before the sample. Light intensities were measured with a POWER MAX5100 (Molelectron detector incorporated) power meter and were found to be 5.14 x 10^{16} photons $s^{-1}.cm^{-2}$ for the photobleaching studies. A schematic representation of the set-up for photo-irradiation reactions is shown below (Fig. 2.1).

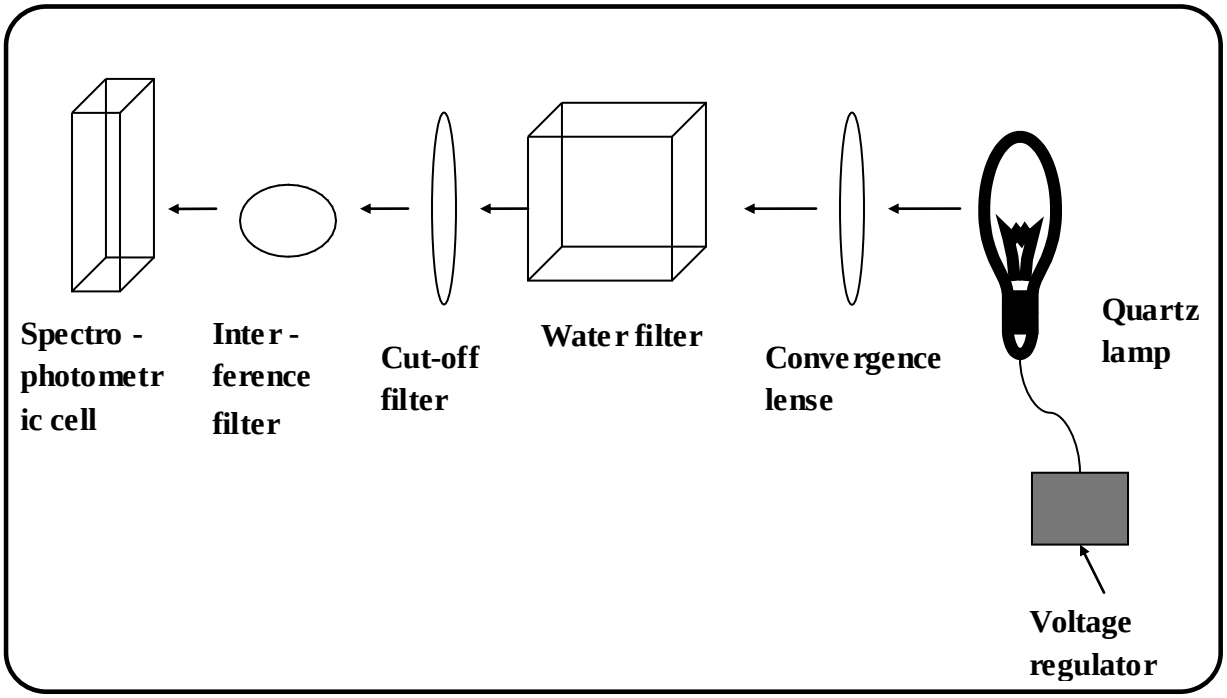

Fig. 2.1: Set-up for photoirradiation reactions

Triplet quantum yields and lifetimes were determined by recording the triplet absorption and decay kinetics from a laser flash photolysis system shown in Fig. 2.2. The excitation pulses were produced by a Nd: YAG laser (Quanta-Ray, 1.5 J / 90 ns) pumped tunable dye laser (Lambda Physic FL 3002, Pyridin 1 dye in methanol). The analyzing beam source was derived from a Thermo Oriel xenon arc lamp, and a photomultiplier tube (PMT) was used as detector. Signals were recorded with a Tektronix TDS 360 two-channel digital real-time oscilloscope. Triplet lifetimes were determined by exponential fitting of the kinetic curves using OriginPro 7.5 software.

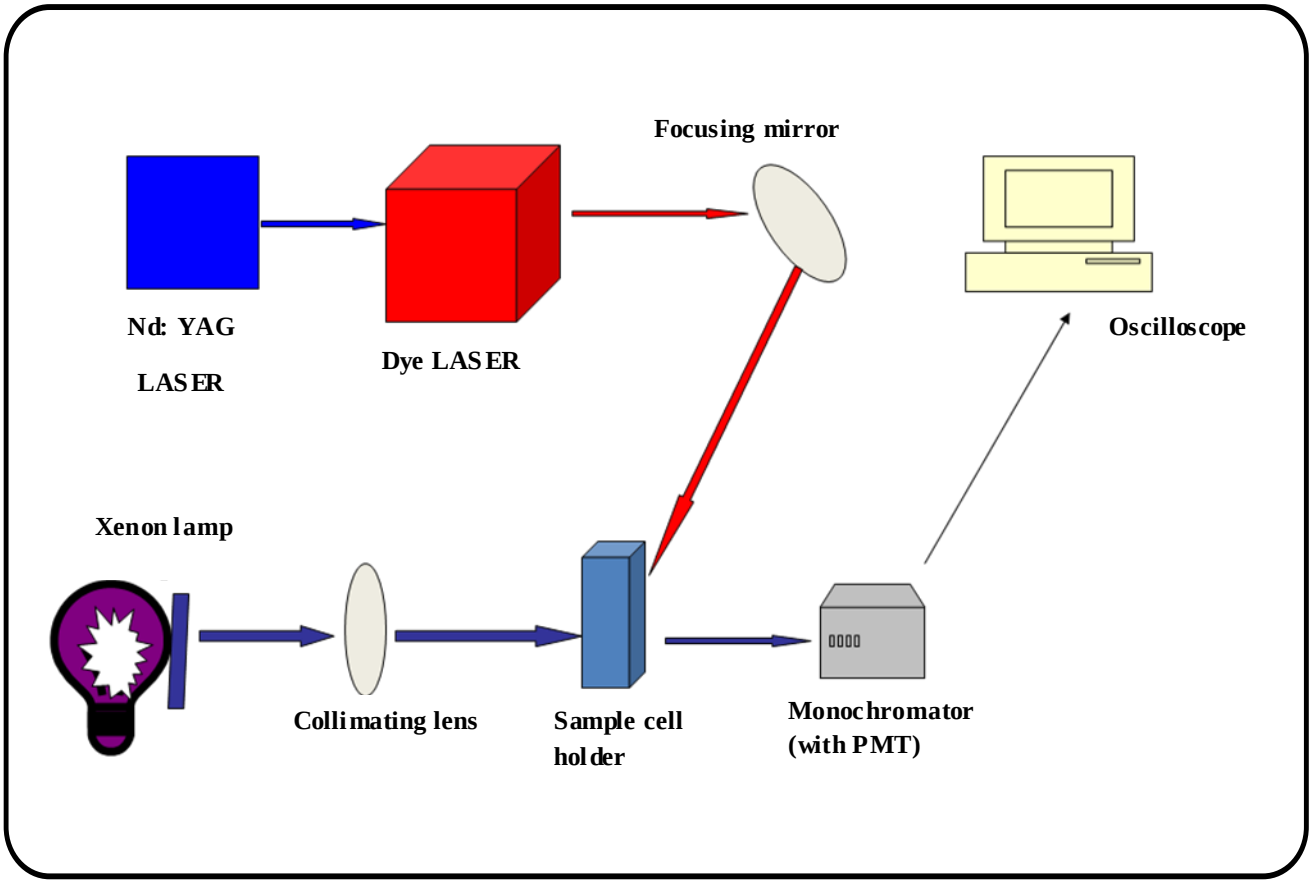

Fig. 2.2: Schematic diagram of a laser flash photolysis set-up for triplet quantum yield and lifetime determinations

Triplet quantum yields (Φ_T) were calculated using Eq. 1.3 with unsubstituted ZnPc (Φ_T = 0.65 in DMSO [116], 0.58 in DMF [155] and 0.65 in toluene [156] employed as a standard. Triplet lifetimes were determined by exponential fitting of the kinetic curves using OriginPro 7.5 software. Fluorescence quantum yields were determined using Eq. 1.2, with unsubstituted ZnPc in DMSO (Φ_F = 0.20 [108]. Nonlinear optical parameters and photodegradation quantum yields (Φ_P) were calculated using Eqs. 1.5-1.9 and Eq. 1.10, respectively.

2.3. SYNTHESIS

2.3.1. Phthalonitriles

The phthalonitriles were characterized by IR and/ or NMR spectroscopies

2.3.1.1. 3-Nitrophthalonitrile (Scheme 3.2 A) [47, 157]

3-Nitrophthalic anhydride (15):

3-Nitrophthalic acid (**14**) (45.0 g, 0.21 mol) in acetic anhydride (40 ml) was refluxed in a round-bottomed flask with gentle boiling until the acid completely dissolved. The reaction mixture was refluxed for a further 10 minutes, poured into a porcelain dish and allowed to cool. The resulting yellow product was filtered. The crystals were then washed with diethyl ether until the unreacted acid could not be detected. The resulting yellow crystals were allowed to dry in air. Yield: 37.0 g (90 %). IR [(KBr) ν_{max}/cm^{-1}]: 1722, 1699 (C=O), 1529 (NO_2 asym), 1334 (NO_2 sym).

3-Nitrophthalimide (16):

3-Nitrophthalic anhydride (**15**) (35 g, 0.26 mol) in formamide (45 ml) was heated under reflux for 3 hours. The reaction mixture was cooled, filtered, thoroughly washed with water and dried at 60 °C, thus yielding the title compound. Yield: 32.0 g (95 %). IR [(KBr) ν_{max}/cm^{-1}]: 3433 (N-H), 1531 (NO_2 asym), 1345 (NO_2 sym).

3-Nitrophthalamide (18a):

3-Nitrophthalimide (**16**) (30 g, 0.16 mol) was stirred in 32 % ammonia solution (660 ml) for 24 hours. The resulting deep yellow product was filtered and washed with cold water until the excess ammonia could not be detected. The title compound was dried at 110 ^{o}C. Yield: 28.0 g (92 %). IR [(KBr) ν_{max}/cm^{-1}]: 3433 (N-H), 1532 (NO_2 asym), 1345 (NO_2 sym).

3-Nitrophthalonitrile (19a):

DMF (208 ml) was placed in a three-necked flask under nitrogen and cooled to 0 °C with an ice bath. Thionyl chloride (21 ml) was slowly added to DMF (while the temperature was maintained at 0 °C), thereafter, the mixture was allowed to reach room temperature and stirred for 30 minutes. The mixture was cooled to 0 °C and 3-nitrophthalamide (**18a**) (25g, 0.12 mol) was slowly added to the mixture while stirring. The slurry was then stirred at room temperature for 3 hours, slowly poured onto crushed ice (~ 1.3 kg), filtered under reduced pressure and thoroughly washed with cold water. The pale yellow product was then dried at 110 °C. Yield: 18.0 g (82 %). IR [(KBr) ν_{max}/cm^{-1}]: 2231 (C≡N), 1531 (NO_2 asym), 1341 (NO_2 sym). ^{1}H-NMR

(400 MHz, DMSO-d_6): δ, ppm 8.48 (1-H, d, Ar H), 8.32 (1-H, d, Ar-H), 8.06 (1-H, t, Ar-H).

2.3.1.2. 4-Nitrophthalonitrile (Scheme 3.2) [48]

4-Nitrophthalimide (17):

To concentrated H_2SO_4 (200 ml) was slowly added 55 % HNO_3 (40 ml). The mixture was then allowed to cool to 15 °C in an ice bath. Thereafter, phthalimide (**5**) (40.0 g, 0.26 mol) was added portion-wise to the acid mixture while stirring and maintaining the temperature between 10 and 15 ^oC. The temperature was then taken up to 35 °C and the slurry stirred at that temperature for 1 hour. After cooling to 0 °C, the yellow reaction mixture was poured onto crushed ice (~ 2 kg) while stirring to yield a beige suspension. After filtration, the solid was thoroughly washed with cold water and the product was dried at 110 °C. Yield: 31.0 g (59 %). IR [(KBr) ν_{max}/cm^{-1}]: 2233 (C≡N), 1537 (NO_2 asym), 1338 (NO_2 sym). ^{1}H-NMR (400 MHz, DMSO-d_6): δ, ppm 8.76 (1-H, s, Ar-H), 8.48 (1-H, d, Ar-H), 8.10 (1-H, d, Ar-H).

4-Nitrophthalamide (18b) and **4-nitrophthalonitrile** (**19b**) were synthesised by following methods similar to **3-nitrophthalamide (18a**) and **3-nitrophthalonitrile** (**19a**).

4-Nitrophthalamide (18b): Yield: 30.0 g (88 %). IR [(KBr) ν_{max}/cm^{-1}]: 3433 (N-H), 1535 (NO_2 asym), 1334 (NO_2 sym).

4-Nitrophthalonitrile (19b): Yield**:** 20.0 g (80 %). IR [(KBr) ν_{max}/cm^{-1}]: 2232 (C≡N), 1535 (NO_2 asym), 1337 (NO_2 sym). ^{1}H-NMR (400 MHz, DMSO-d_6): δ, ppm 9.02 (1-H, s, Ar-H), 8.38 (1-H, d, Ar-H), 8.12 (1-H, d, Ar-H).

2.3.1.3. 4,5-Dichlorophthalonitrile (Scheme 3.3) [75]

4,5-Dichlorophthalic anhydride (21):

A mixture of 4,5-dichlorophthalic acid (**20**) (45 g, 0.19 mol) and acetic anhydride (75 ml) was heated under weak reflux for 5 hours. After cooling, a greyish white product was filtered, thoroughly washed with petroleum ether (40–60 °C) and air-dried to yield 4,5-dichlorophthalic anhydride. Yield: 39.0 g (94 %). IR [(KBr) ν_{max}/cm^{-1}]: 1828, 1786 (C=O).

4,5-Dichlorophthalimide (22):

4,5-dichlorophthalic anhydride (**21**) (38 g, 0.18 mol) in formamide (51 ml) was refluxed for 3 hours. After cooling the greyish white product was filtered, thoroughly washed with water and dried at 110 °C for 3 hours, thus yielding **22**. Yield: 36.0 g (96 %). IR [(KBr) ν_{max}/cm^{-1}]: 1772, 1713 (imide).

4,5-Dichlorophthalamide (23):

A solution of 4,5-dichlorophthalimide (**22**) (35 g, 0.16 mol) in 25 % ammonia (428 ml) was stirred for 24 hours and then stirred for a further 24 hours after addition of 33

% ammonia (159 ml). The product was filtered, thoroughly washed with water and dried at 60 ^{o}C. Yield: 26.0 g (70 %). IR [(KBr) ν_{max}/cm^{-1}]: 1642, 1623 (amide).

4,5-Dichlorophthalonitrile (24):

At 0 °C was added thionyl chloride (88 ml) under nitrogen and stirring to dry DMF (125 ml). After two hours, dry 4,5- dichlorophthalamide (**23**) (25.0 g, 0.11 mol) was added and the mixture stirred at 0 – 5 °C for 5 hours and then at room temperature for 24 hours. The product was slowly added to ice water, filtered, thoroughly washed with water and recrystallised from methanol to yield a pale white product. Yield: 17.0 g (78 %). IR [(KBr) ν_{max}/cm^{-1}]: 2230 (C≡N). ^{1}H-NMR (400 MHz, DMSO-d_6): δ, ppm 8.48 (2-H, s, Ar-H).

2.3.1.4. Phthalonitriles mono-substituted with phenoxy derivatives (Scheme 3.4)

3-Phenoxyphthalonitrile (25a)

Under a blanket of nitrogen, phenol (1.75 g, 18.5 mmol) and **19a** (2.75 g, 13 mmol) were dissolved in dry DMSO (26 ml). To this suspension was added anhydrous K_2CO_3 (3.595g, 25.5 mmol) and the mixture stirred at room temperature. Further K_2CO_3 (0.165 g, 1.2 mmol) was added portion-wise after 4 and 24 hrs of stirring. After 48 hrs total reaction time, the mixture was poured into 1 M HCl (130 ml), thus forming a precipitate that was recrystallised from methanol/water (1:1) to yield a brownish yellow product. Yield: 1.62 g (57 %), IR [(KBr)ν_{max}/cm^{-1}]: 3039-3048 (Ar-H), 2233 (C≡N), 1201 (C-O-C). ^{1}H NMR (400 MHz, $CDCl_3$): δ, ppm 7.52-7.57 (1H,

t, Ar–H), 7.43–7.47 (3H, m, Ar–H), 7.24–7.31 (1H, m, Ar–H), 7.06-7.10 (3H, m, Ar-H).

3-(4-*tert*-Butylphenoxy)phthalonitrile (25b)

Synthesis and purification was as described for complex **25a**, using 4-*tert*-butylphenol (3.45 g, 19.5 mmol) and **19a** (2.75g, 13 mmol). Yield: 1.50 g (42 %). IR [(KBr) ν_{max}/cm^{-1}]: 3041-3050 (Ar-H), 2230 (C≡N), 1209 (C–O–C), 2964 (Bu^t). ^1H NMR (400 MHz, $CDCl_3$): δ, ppm 7.52-7.56 (1H, m, Ar–H), 7.41–7.45 (3H, m, Ar–H), 7.00–7.10 (3H, m, Ar–H), 1.34 (9H, s, Bu^t).

3-[4-(Benzyloxy)phenoxy]phthalonitrile (25c)

Under a stream of nitrogen, 4-(benzyloxy)phenol (4.21 g, 21.0 mmol) and **19a** (3.00 g, 17.5 mmol) were dissolved in dry DMSO (15 ml). To this suspension was added anhydrous K_2CO_3 (4.85 g, 35.0 mmol) and the mixture stirred at room temperature. Further K_2CO_3 (1.22 g, 9.00 mmol) was added after 4 hours and again after 24 hours of stirring. After 48 hours total reaction time, the mixture was poured into water (100 ml), thus forming a precipitate that was thoroughly washed with water and recrystallised from methanol to yield a brownish yellow title compound. Yield: 2.32 g (40 %). IR [(KBr) ν_{max}/cm^{-1}]: 3043-3052 (Ar-H), 2237 (C≡N), 1260 (C-O-C). ^1H-NMR (400 MHz, DMSO-d_6): δ, ppm 7.63 (1-H, s, Ar-H), 7.37-7.39 (6-H, m, Ar-H), 7.03 (5-H, m, Ar-H), 5.16 (2-H, s, CH_2).

4–Phenoxyphthalonitrile (26a)

Synthesis and purification was as described for complex **25a**, using phenol (2.66 g, 30 mmol) and **19b** (3.00 g, 17.5 mmol). Yield: 1.60 g (42 %), IR [(KBr)ν_{max}/cm^{-1}]: 3037-3046 (Ar-H), 2233 (C≡N), 1231 (C-O-C). ^{1}H NMR (400 MHz, $CDCl_3$): δ, ppm 7.69-7.71 (1H, m, Ar–H), 7.43–7.47 (2H, t, Ar–H), 7.21–7.31 (3H, m, Ar–H), 7.05-7.07 (2H, m, Ar-H).

4-(4-tert-Butylphenoxy)phthalonitrile (26b)

Synthesis and purification was as described for complex **25a**, using 4-*tert*-butylphenol (3.905 g, 26 mmol) and **19b** (3.00 g, 17.5 mmol). Yield: 1.68 g (35 %), IR [(KBr) ν_{max}/cm^{-1}]: 3040-3051 (Ar-H), 2230 (C≡N), 1247 (C–O–C), 2989 (Bu^t). ^{1}H NMR (400 MHz, $CDCl_3$): δ, ppm 7.73-7.75 (1H, d, Ar–H), 7.48–7.51 (2H, m, Ar–H), 7.01–7.04 (4H, m, Ar–H), 1.39 (9H, s, Bu^t).

4-[4-(Benzyloxy)phenoxy]phthalonitrile (26c):

Synthesis and purification of **26c** was as described for compound **25c**, using 4-(benzyloxy)phenol (4.2 g, 21.0 mmol), **19b** (3.00 g, 17.5 mmol) and DMSO (15 ml). Yield: 2.82 g (49 %). IR [(KBr) ν_{max}/cm^{-1}]: 3039-3050 (Ar-H), 2236 (C≡N), 1253 (C-O-C). ^{1}H-NMR (400 MHz, DMSO-d_6): δ, ppm 7.52 (1-H, d, Ar-H), 7.49-7.32 (5-H, m, Ar-H), 7.21 (2-H, m, Ar-H), 7.00 (4-H, q, Ar-H), 5.10 (2-H, s, CH_2).

2.3.1.5. Phthalonitriles disubstituted with phenoxy derivatives (Scheme 3.3)

4,5-Diphenoxyphthalonitrile (28a)

A mixture of 4,5-dichlorophthalonitrile (**24**) (3.00 g, 15.25 mmol), phenol (4.30 g, 45.7 mmol) and dry DMSO (23 ml) was stirred at 90 °C, while anhydrous K_2CO_3 (8 × 4.215 g, 8 × 30.5 mmol) was added every 5 min until eight portions had been added. The reaction mixture was stirred at 90 °C for an additional 45 min and allowed to cool. Thereafter, the mixture was added to ice water (100 ml) and the aqueous phase extracted with $CHCl_3$ (3× 50 ml). The solvent was evaporated and the product recrystallised from ethanol and dried at room temperature. Yield: 3. 00 g (63%). IR [(KBr) ν_{max}/cm^{-1}]: 3039-3050 (Ar-H), 2237 (C≡N), 1212 (C–O–C). ^{1}H NMR (400 MHz, $CDCl_3$): δ, ppm 7.50-7.54 (4H, m, Ar–H), 7.27–7.37 (2H, m, Ar–H), 7.25 (2H, s, Ar–H), 7.12-7.16 (4H,m,Ar-H).

4,5-Bis(4-*tert*-butylphenoxy)phthalonitrile (28b)

Synthesis and purification of **28b** was as described for compound **28a**, using 4-*tert*-butylphenol (5.18 g, 34.5 mmol), 4,5-dichlorophthalonitrile (**24**) (2.25 g, 11.5 mmol) and K_2CO_3 (8 × 3.18 g, 8 × 22.5 mmol), DMSO (23 ml). Yield: 3.50 g (72 %). IR [(KBr) ν_{max}/cm^{-1}]: 3040-3052 (Ar-H), 2224 (C≡N), 1225 (C–O–C), 2961 (Bu^t). ^{1}H NMR (400 MHz, $CDCl_3$): δ, ppm 7.43-7,53 (4H, m, Ar–H), 7.18 (2H, s, Ar–H), 7.04-7.06 (4H, m, Ar–H), 1.19 (18H, s, Bu^t).

4,5-bis[4-(Benzyloxy)phenoxy]phthalonitrile (28c):

Synthesis and purification of **28c** was as described for compound **28a**, using 4-(benzyloxy)phenol (19.16 g, 45.7 mmol), **24** (3.00g, 15.0 mmol) and K_2CO_3 (8 x 4.21 g, 8 x 30.0 mmol), DMSO (23 ml). Yield: 4.19 g (57 %). IR [(KBr) ν_{max}/cm^{-1}]: 3037-3053 (Ar-H), 2232 (C≡N), 1244 (C-O-C). ^{1}H-NMR (400 MHz, DMSO-d_6): δ, ppm 8.50 (2-H, s, Ar-H), 7.45 (8-H, br, Ar-H), 7.10 (10- H, d, Ar-H), 5.21 (4-H, s, CH_2).

2.3.2. Unsubstituted metallophthalocyanines (Scheme 3.1)

2.3.2.1. Lead (II) phthalocyanine (30) [62, 72]

Lead phthalocyanine was synthesized by modifying the procedure described in the literature [72]. Under a blanket of nitrogen, phthalonitrile (**10**) (2.5 g, 20.00 mmol) was heated to 180 °C until it completely melted. Then lead acetate (1.63 g, 5.00 mmol) was added in small portions to the molten solution. The reaction mixture was maintained at 180 ^{0}C for 90 min with constant stirring. The product was finely ground and washed with glacial acetic acid, methanol three times, ethanol and then with acetone, respectively, until the washings turned essentially colourless. The solid product was further purified by washing with methanol, ethanol and then with acetone in a Soxhlet apparatus. Yield: 0.78 g (49 %), UV-Vis (DMSO): λ_{max} (log ε); 702 nm (4.98), 6.35 (4.33), 435 (4.37), 350 (4.70). IR (KBr): ν_{max}/cm^{-1}; 3038-3049 (Ar-H), 1603 (C=C), 1479 (C=C); 952, 871, 816, 772, 725 (Pc skeletal). ^{1}H NMR (400 MHz, DMSO-d_6) δ, ppm; 9.29-9.32 (8H, d, Pc), 8.27-8.43 (8H, d, Pc).

2.3.2.2. Antimony (III) phthalocyanine triiodide (61) [86]

Synthesis and purification was as outlined for **30 (**stoppend flask). The amounts of the reagents employed were as follows: phthalonitrile (**10**) (0.83 g, 6.50 mmol) and antimony iodide (0.90 g, 1.80 mmol). Yield: 0.88 g (13 %), UV-Vis (DMSO): λ_{max} (log ε) 732 nm (4.99), 660 (4.25), 385 (4.35), 348 (4.60). IR (KBr): ν_{max}/cm^{-1}; 3041-3055 (Ar-H), 1606 (C=C), 1501 (C=C); 875, 813, 801, 770, 746, 722 (Pc skeletal). ^{1}H NMR (400 MHz, DMSO-d_6) δ, ppm; 7.77 (8H, d, Pc), 7.67 (8H, d, Pc).

Since both SbPc and PbPc are not new, no elemental or mass spectral analyses was done, satisfactory ^{1}H NMR and UV/vis were obtained.

2.3.3. Aryloxy substituted Pb phthalocyanines (Sheme 3.5A and 3.5B)

2.3.3.1. 1,(4)-(Tetraphenoxyphthalocyaninato)lead (76a)

Under a blanket of nitrogen, **25a** (1.60 g, 7.30 mmol) was dissolved in 1-CNP (8 ml). Pb acetate (0.91 g, 2.40 mmol) was then added to the solution and the reaction mixture refluxed at 180 °C for 7 h under nitrogen. After cooling, the solution was chromatographed with hexane as eluent to remove 1-CNP. The column was then eluted with $CHCl_3$ which was evaporated off, thus affording **76a**. Yield: 1.27 g (49%). UV–Vis (DMSO): λ_{max} nm (log ε) 723 (5.33), 652 (4.65), 460 (4.41), 347 (4.77). IR [(KBr) ν_{max}/cm^{-1}]: 3035-3051 (Ar-H), 1578 (C=C), 1249 (C–O–C), 970, 924, 877, 830, 818, 799, 788, 782, 742, 712, 702 (Pc skeletal). ^{1}H NMR (400 MHz, $CDCl_3$): δ, ppm 9.04– 9.06 (4H, d, Pc–H), 8.89–8.92 (4H, m, Pc–H), 8.60–862 (4H, m, Pc–H), 7.78–8.01 (20H, m, phenyl–H). *Anal.* Calc. for $C_{56}H_{32}N_8O_4Pb$: C, 61.87; H, 2.97; N, 10.31. Found: C, 61.81; H, 3.59; N, 10.07%.

2.3.3.2. 1,(4)-(Tetra-tert-butylphenoxyphthalocyaninato)lead (76b)

Synthesis and purification was as outlined for 7**6a** except **25b** instead of **25a** was employed. The amounts of the reagents employed were as follows: **25b** (1.25 g, 4.55 mmol), lead acetate (0.62 g, 1.65 mmol) and 1-CNP (4.5 ml). Yield: 0.80 g (37%). UV–Vis (DMSO): λ_{max} nm (log ε) 724 (5.22), 652 (4.64), 460 (4.34), 347 (4.67). IR [(KBr) ν_{max}/cm^{-1}]: 3037-3049 (Ar-H), 1584 (C=C), 1251 (C–O–C), 999, 970, 944, 869, 827, 750 (Pc skeletal), 2960 (t-Butyl-H). ^{1}H NMR (400 MHz, $CDCl_3$): δ, ppm 8.40–9.06 (12H, m, Pc–H), 7.73–8.00 (16H, m, phenyl–H), 1.27– 1.32 (36H, m, ^{t}Bu). *Anal.* Calc. for $C_{72}H_{64}N_8O_4Pb$: C, 65.95; H, 4.92; N, 8.55. Found: C, 67.76; H, 6.14; N, 7.14%.

2.3.3.3. 2,(3)-(Tetraphenoxyphthalocyaninato)lead (77a)

Synthesis and purification was as outlined for 7**6a** except **26a** instead of **25a** was employed. The amounts of the reagents employed were as follows: **26a** (1.25 g, 5.50 mmol), lead acetate (0.7 g, 1.85 mmol) and 1-CNP (6 ml). Yield: 0.92 g (46%). UV–Vis (DMSO): λ_{max} nm (log ε) 708 (4.95), 638 (4.26), 346 (4.52). IR [(KBr) ν_{max}/cm^{-1}]: 3038-3050 (Ar-H), 1593 (C=C), 1229 (C–O–C), 960, 942, 928, 904, 886, 869, 856, 781,759,743, 724 (Pc skeletal). ^{1}H NMR (400 MHz, $CDCl_3$): δ, ppm 8.69–8.78 (4H, m, Pc–H), 8.48–8.61 (4H, m, Pc–H), 8.26–8.31 (4H, m, Pc–H), 7.73–7.97 (20H, m, phenyl–H). *Anal.* Calc. for $C_{56}H_{32}N_8O_4Pb$.2acetate: C, 59.27; H, 3.23; N, 9.54. Found: C, 57.37; H, 3.04; N, 8.85%.

2.3.3.4. 2,(3)-(Tetra-tert-butylphenoxyphthalocyaninato)lead (77b)

Synthesis and purification was as outlined for **76a** except **26b** instead of **25a** was employed. The amounts of the reagents employed were as follows: **26b** (1.05 g, 3.80 mmol), lead acetate (0.57 g, 1.25 mmol) and 1-CNP (4 ml). Yield: 0.75 g (46%). UV–Vis (DMSO): λ_{max} nm (log ε) 709 (5.00), 638 (4.37), 347 (4.42) IR [(KBr) ν_{max}/cm^{-1}]: 3038-3051 (Ar-H), 1596 (C=C), 1240 (C–O–C), 978, 963, 943, 930, 879, 855, 843, 828, 823, 752, 729 (Pc skeletal), 2967 (t-butyl-H). ^{1}H NMR (400 MHz, $CDCl_3$): δ, ppm 8.43–9.01 (12H, m, Pc–H), 7.52–7.55 (16H, m, phenyl– H), 1.33 (36H, s, ^{t}Bu). *Anal*. Calc. for $C_{72}H_{64}N_8O_4Pb$: C, 65.96; H, 4.92; N, 8.55. Found: C, 67.64; H, 5.90; N, 7.19%.

2.3.3.5. 2,3-Octaphenoxyphthalocyaninatolead (78a)

In 1-octanol (8 ml), compound **28a** (2.00 g, 6.40 mmol), lead acetate (0.85 g, 2.12 mmol) and urea (0.50 g, 8.50 mmol) were stirred under a blanket of nitrogen at 150 °C for 14 h. The reaction mixture was allowed to cool, thereafter, methanol (80 ml) was added and the mixture was refluxed for 2 h. After cooling, the mixture was filtered, and the resulting solid sequentially washed with methanol and water and then dried. The crude product was purified by column chromatography, using $CHCl_3$ as the eluting solvent. After evaporation of solvent, the product was further purified by column chromatography (using chloroform as eluent) to afford the title compound as a dark green solid. Yield: 1.00 g (32%). UV–Vis (DMSO): λ_{max} nm (log ε) 707 (5.18), 637 (4.41), 348 (4.65). IR [(KBr) ν_{max}/cm^{-1}]: 3040-3051 (Ar-H), 1601 (C=C), 1269 (C–O–C), 998, 880, 841, 787, 768, 744, 726 (Pc skeletal). ^{1}H NMR (400 MHz,

$CDCl_3$): *δ*, ppm 8.50 (8H, s, Pc H), 7.23–7.44 (40H, m, phenyl–H). *Anal.* Calc. for $C_{80}H_{48}N_8O_8Pb$: C, 65.91; H, 3.32; N, 7.69. Found: C, 65.44; H, 3.73; N, 8.06%.

2.3.3.6. 2,3-[Octakis(4-t-butylphenoxyphthalocyaninato)] lead (78b)

Synthesis and purification was as outlined for **78a** except **28b** instead of **28a** was employed. The amounts of the reagents employed were: **28b** (2.00 g, 4.75 mmol), lead acetate (0.10 g, 1.19 mmol) and urea (0.285 g, 4.75 mmol) in 1-octanol (8.75 ml). Yield: 1.00 g (44%). UV–Vis (DMSO): λ_{max} nm (log ε) 709 (4.94), 638 (4.17), 358 (4.41). IR [(KBr) ν_{max}/cm^{-1}]: 3040-3050 (Ar-H), 1598 (C=C), 1269 (C–O–C), 889, 884, 827, 828, 769, 751,744 (Pc skeletal), 2961 (t-butyl-H). ^{1}H NMR (400 MHz, $CDCl_3$): *δ*, ppm 8.91 (8H, s, Pc–H), 7.13–7.43 (32H, m, phenyl–H), 1.38 (72H, s, tBu). *Anal.* Calc. for $C_{112}H_{112}N_8O_8Pb$: C, 70.68; H, 5.93; N, 5.89. Found: C, 69.88; H, 5.92; N, 5.91%.

Complexes containing 4-benzyloxyphenoxy (**c**) in Scheme 3.5B were synthesized in the microwave, hence are discussed separately from the rest.

2.3.3.7. 1, (4)-tetrakis(4-benzyloxyphenoxy)phthalocyaninato lead (76c)

A mixture of compound **25c** (0.10 g, 0.29 mmol), lead acetate (0.05 g, 0.14 mmol), DBU (0.2 ml) and 5 ml n-pentanol was irradiated at 1000 W in a microwave for 15 min. After cooling, the product was washed with methanol and chromatographed with hexane as eluent to remove impurities. The column was then eluted with THF which was evaporated off, thus affording **76c**. Yield: 0.09 g (23 %). UV–Vis (DMSO):

λ_{max} nm (log ε) 725 (5.01), 657 (4.42), 362 (4.56). IR [(KBr) ν_{max}/cm^{-1}]: 3037-3049 (Ar-H), 2951 (CH_2), 1608 (C=C), 1225 (C–O–C), 961, 848, 745, 712 (Pc skeletal). ^{1}H NMR (400 MHz, DMSO-d_6): δ, ppm 7.64-7.68 (4H, m, Pc–H), 7.59-7.63 (8H, m, Pc–H), 7.51–7.58 (20H, m, phenyl–H), 7.43–7.49 (16H, m, phenyl–H), 5.42 (8H, s, CH_2). *Anal*. Calc. for $C_{84}H_{56}N_8O_8Pb$: C, 66.70; H, 3.73; N, 7.41. Found: C, 66.35; H, 3.70; N, 7.06%.

2.3.3.8. 2, (3)-tetrakis(4-benzyloxyphenoxy)phthalocyaninato lead (77c)

Synthesis and purification of **77c** was as outlined for **76c** except **26c** instead of **25c** was employed. The amounts of the reagents employed were as follows: **26c** (0.25 g, 0.36 mmol), lead acetate (0.06 g, 0.18 mmol) DBU (0.2 ml) and n-pentanol (5 ml) for 5 min. Yield: 0.08 g (19 %). UV–Vis (DMSO): λ_{max} nm (log ε) 709 (4.98), 641 (4.32), 346 (4.46). IR [(KBr) ν_{max}/cm^{-1}]: 2948 (CH_2), 3041-3050 (Ar-H), 1605 (C=C), 1218(C–O–C), 941, 827, 734, 696 (Pc skeletal). ^{1}H NMR (400 MHz, DMSO-d_6): δ, ppm 7.52-7.58 (4H, m, Pc–H), 7.44-7.49 (8H, m, Pc–H), 7.35–7.42 (20H, m, phenyl–H), 7.22–7.28 (16H, m, phenyl–H), 5.20 (8H, s, CH_2). *Anal*. Calc. for $C_{84}H_{56}N_8O_8Pb$.hexane: C, 67.63; H, 4.38; N, 7.01. Found: C, 68.35; H, 4.70; N, 7.33%.

2.3.3.9. 2,3-Octakis(4-benzyloxyphenoxy)phthalocyaninato lead (78c)

Synthesis and purification of **78c** was as outlined for **76c** except **28c** instead of **25c** was employed. The amounts of the reagents employed were as follows: **28c** (0.25 g, 0.36 mmol), lead acetate (0.06 g, 0.18 mmol) DBU (0.2 ml) and n-pentanol (5 ml) for

5 min. Yield: 0.75 g (46%). UV–Vis (DMSO): λ_{max} nm (log ε) 712 (5.01), 638 (4.34), 347 (4.45). IR [(KBr) ν_{max}/cm^{-1}]: 3041-3051 (Ar-H), 2925 (CH_2), 1504 (C=C), 1231 (C–O–C), 1000, 875, 839, 739, 694 (Pc skeletal). ^{1}H NMR (400 MHz, DMSO-d_6): δ, ppm 7.54-7.56 (8H, br, Pc–H), 7.44–7.48 (32H, br, phenyl–H), 7.22–7.38 (40H, br, phenyl–H), 5.09-5.26 (16H, m, CH_2). *Anal.* Calc. for $C_{136}H_{96}N_8O_{16}Pb$.hexane: C, 71.33; H, 4.60; N, 4.69. Found: C, 71.31; H, 6.30; N, 5.38%.

2.3.4. Aryloxy substituted Sb phthalocyanines (Sheme 3.6)

2.3.4.1. 1,(4)-(Tetraphenoxyphthalocyaninato)antimony triiodide (79a)

3-phenoxyphthalonitrile **25a** (0.25 g, 1.23 mmol) was heated to 180 °C until it completely melted. Then antimony iodide (0.15 g, 0.31 mmol) was added in small portions to the completely molten solution. The reaction mixture in a stoppend flask was maintained at 180 °C for 24 hrs with constant stirring. The solid product was dissolved in CH_2Cl_2 and precipitated from the solution by addition of methanol. The product was washed with methanol three times, ethanol and then with acetone, respectively, until the washings turned essentially colourless. The solid product was further purified by washing with methanol, ethanol and then with acetone in a Soxhlet apparatus. Yield: 0.15 g (35 %). UV–Vis (DMSO): λ_{max} nm (log ε) 759 (4.98), 686 (4.48), 418 (4.66), 363 (4.67). IR [(KBr) ν_{max}/cm^{-1}]: 3035-3051 (Ar-H), 1603 (C=C), 1261 (C–O–C), 955, 893, 876, 759, 738 (Pc skeletal). ^{1}H NMR (400 MHz, DMSO-d_6): δ, ppm 8.78–9.19 (12H, m, Pc–H), 7.45–7.88 (20H, m, phenyl–H). *Anal.* Calc. for $C_{56}H_{32}N_8O_4Sb\ I_3$: C, 48.59; H, 2.31; N, 8.10. Found: C, 48.03; H, 1.98; N, 7.34%.

2.3.4.2. 1,(4)-(Tetra-tert-butylphenoxyphthalocyaninato)antimony triiodide (79b)

Synthesis and purification of **79b** was as outlined for **79a** except **25b** instead of **25a** was employed. The amounts of the reagents employed were: **25b** (0.25 g, 0.95 mmol) and antimony iodide (0.12 g, 0.24 mmol). Yield: 0.12 g (31 %). UV–Vis (DMSO): λ_{max} nm (log ε) 761 (4.99), 686 (4.49), 420 (4.67), 363 (4.67). IR [(KBr) ν_{max}/cm^{-1}]: 3037-3048 (Ar-H), 1598 (C=C), 1273 (C–O–C), 945, 883, 816, 749, 733 (Pc skeletal), 2978 (t-Butyl-H). ^{1}H NMR (400 MHz, DMSO-d_6): δ, ppm 8.81–9.20 (12H, m, Pc–H), 7.34–7.61 (16H, m, phenyl–H) 1.21– 1.34 (36H, m, ^{t}Bu). *Anal*. Calc. for $C_{72}H_{64}N_8O_4SbI_3$: C, 53.76; H, 3.98; N, 6.97. Found: C, 53.79; H, 3.16; N, 6.58%.

2.3.4.3. 1,(4)-tetrakis(4-benzyloxyphenoxy)phthalocyaninatoantimony triiodide (79c)

Synthesis and purification of **79c** was as outlined for **79a** except **25c** instead of **25a** was employed. The amounts of the reagents employed were: **25c** (0.19 g, 0.56 mmol) and antimony iodide (0.05 g, 0.14 mmol). Yield: 0.09 g (36 %). UV–Vis (DMSO): λ_{max} nm (log ε) 762 (5.02), 687 (4.69), 422 (4.87), 368 (4.87). IR [(KBr) ν_{max}/cm^{-1}]: 3038-3051 (Ar-H), 2948 (CH_2), 1655 (C=C), 1275 (C–O–C), 991, 887, 784, 732 (Pc skeletal). ^{1}H NMR (400 MHz, DMSO-d_6): δ, ppm 7.72-7.78 (4H, m, Pc–H), 7.68-7.71 (8H, m, Pc–H), 7.57–7.61 (20H, m, phenyl–H), 7.53–7.56 (16H, m, phenyl–H), 5.20 (8H, s, CH_2). *Anal*. Calc. for $C_{84}H_{56}N_8O_8SbI_3.2H_2O$: C, 54.69; H, 3.04; N, 6.08. Found: C, 52.89; H, 2.70; N, 5.83%.

2.3.4.4. 2,(3)-(Tetraphenoxyphthalocyaninato)antimony triiodide (80a)

Synthesis and purification of **80a** was as outlined for **79a** except **26a** instead of **25a** was employed. The amounts of the reagents employed were: **26a** (0.25 g, 1.23 mmol) and antimony iodide (0.15 g, 0.31 mmol). Yield: 0.17 g (38 %). UV–Vis (DMSO): λ_{max} nm (log ε) 738 (5.00), 665 (4.60), 411 (4.76), 354 (4.76). IR [(KBr) ν_{max}/cm^{-1}]: 3037-3051 (Ar-H), 1628 (C=C), 1251 (C–O–C), 1000, 888, 858, 759, 738 (Pc skeletal). ^{1}H NMR (400 MHz, DMSO-d_6): δ, ppm 8.52–8.69 (12H, s, Pc–H), 7.35–7.76 (20H, m, phenyl–H). *Anal.* Calc. for $C_{56}H_{32}N_8O_4SbI_3$: C, 48.59; H, 2.31; N, 8.10. Found: C, 48.49; H, 2.88; N, 8.34%.

2.3.4.5. 2,(3)-(Tetra-tert-butylphenoxyphthalocyaninato)antimony triiodide (80b)

Synthesis and purification of **80b** was as outlined for **79a** except **26b** instead of **25a** was employed. The amounts of the reagents employed were: **26b** (0.25 g, 0.95 mmol) and antimony iodide (0.12 g, 0.24 mmol). Yield: 0.17 g (44 %). UV–Vis (DMSO): λ_{max} nm (log ε) 739 (4.97), 666 (4.47), 411 (4.64), 354 (4.64). IR [(KBr) ν_{max}/cm^{-1}]: 3040-3053 (Ar-H), 1608 (C=C), 1243 (C–O–C), 995, 873, 826, 769, 743 (Pc skeletal), 2981 (t-Butyl-H). ^{1}H NMR (DMSO-d_6): δ, ppm 8.31–8.80 (12H, m, Pc–H), 7.14–7.51 (16H, m, phenyl–H) 1.13– 1.36 (36H, m, ^{t}Bu. *Anal.* Calc. for $C_{72}H_{64}N_8O_4SbI_3$: C, 53.76; H, 3.98; N, 6.97. Found: C, 53.09; H, 4.01; N, 7.28%.

2.3.4.6. 2, (3)-tetrakis(4-benzyloxyphenoxy)phthalocyaninato antimony triiodide (80c)

Synthesis and purification of **80c** was as outlined for **79a** except **26c** instead of **25a** was employed. The amounts of the reagents employed were: **26c** (0.19 g, 0.56 mmol) and antimony iodide (0.05 g, 0.14 mmol). Yield: 0.07 g (28 %). UV–Vis (DMSO): λ_{max} nm (log ε) 738 (5.00), 665 (4.60), 413 (4.76), 356 (4.76). IR [(KBr) ν_{max}/cm^{-1}]: 3042-3051 (Ar-H), 2943 (CH_2), 1648 (C=C), 1235 (C–O–C), 999, 877, 764, 742 (Pc skeletal). ^{1}H NMR (400 MHz, DMSO-d_6): δ, ppm 7.57-7.61 (4H, m, Pc–H), 7.53-7.56 (8H, m, Pc–H), 7.47–7.51 (20H, m, phenyl–H), 7.41–7.46 (16H, m, phenyl–H), 5.09 (8H, s, CH_2). *Anal*. Calc. for $C_{84}H_{56}N_8O_8SbI_3.2H_2O$: C, 54.69; H, 3.04; N, 6.08. Found: C, 52.99; H, 2.56; N, 5.63%.

2.3.4.7. 2,3-Octaphenoxyphthalocyaninatoantimony triiodide (81a)

Synthesis and purification of **81a** was as outlined for **79a** except **28a** instead of **26a** was employed. The amounts of the reagents employed were: **28a** (0.62 g, 1.99 mmol) and antimony iodide (0.25g, 0.50 mmol). Yield: 0.05 g (18 %). UV–Vis (DMSO): λ_{max} nm (log ε) 740 (5.03), 667 (4.62), 411 (4.78), 356 (4.78). IR [(KBr) ν_{max}/cm^{-1}]: 3041-3050 (Ar-H), 1511 (C=C), 1271 (C–O–C), 1000, 883, 856, 749, 732 (Pc skeletal). ^{1}H NMR (400 MHz, DMSO-d_6): δ, ppm 8.75 (8H, s, Pc–H), 7.35–7.76 (40H, m, phenyl–H). *Anal*. Calc. for $C_{80}H_{48}N_8O_8SbI_3.2H_2O$: C, 53.75; H, 2.71; N, 6.27. Found: C, 53.80; H, 3.17; N, 6.60%.

2.3.4.8. 2,3-[Octakis(4-*t*-butylphenoxyphthalocyaninato)]antinomy triiodide (81b)

Synthesis and purification of **81b** was as outlined for **79a** except **28b** instead of **25a** was employed. The amounts of the reagents employed were: **28b** (0.84 g, 1.99 mmol) and antimony iodide (0.25g, 0.50 mmol). Yield: 0.01 g (2.7 %). UV–Vis (DMSO): λ_{max} nm (log ε) 740 (5.02), 667 (4.44), 411 (4.73), 356 (4.64). IR [(KBr) ν_{max}/cm^{-1}]: 3039-3052 (Ar-H), 1508 (C=C),1270 (C–O–C), 883, 827, 769, 751,749 (Pc skeletal), 2965 (*t*-butyl-H). ^{1}H NMR (400 MHz, DMSO-d_6): δ, ppm 8.70 (8H, s, Pc–H), 7.01–7.40 (32H, m, phenyl–H), 1.11-1.40 (72H, s, ^{t}Bu). *Anal.* Calc. for $C_{112}H_{112}N_8O_8SbI_3.2H_2O$: C, 60.15; H, 5.05; N, 5.01. Found: C, 60.57; H, 5.61; N, 5.09%.

2.3.4.9. 2,3-[Octakis(4-benzyloxyphenoxy)phthalocyaninato]antinomy triiodide (81c)

Synthesis and purification of **81c** was as outlined for **79a** except **28c** instead of **25a** was employed. The amounts of the reagents employed were: **28c** (0.84 g, 1.99 mmol) and antimony iodide (0.25g, 0.50 mmol). Yield: 0.06 g (4.6 %). UV–Vis (DMSO): λ_{max} nm (log ε) 742 (5.01), 669 (4.46), 414 (4.71), 360 (4.66). IR [(KBr) ν_{max}/cm^{-1}]: 3039-3053 (Ar-H), 2935 (CH_2), 1514 (C=C), 1238 (C–O–C), 995, 893, 859, 769, 724 (Pc skeletal). ^{1}H NMR (400 MHz, DMSO-d_6): δ, ppm 7.62-7.68 (8H, br, Pc–H), 7.51–7.59 (32H, br, phenyl–H), 7.38–7.49 (40H, br, phenyl–H), 4.98-5.16 (16H, m, CH_2). *Anal.* Calc. for $C_{136}H_{96}N_8O_{16}SbI_3.2H_2O$: C, 61.94; H, 3.64; N, 4.25. Found: C, 59,98; H, 2.30; N, 5.18%.

CHAPTER THREE:

RESULTS

AND

DISCUSSION

PUBLICATIONS

The results presented in this thesis have been published in journals listed below:

1. "Synthesis and Photophysical properties of lead phthalocyanines". **Desmond Kwena Modibane** and Tebello Nyokong. *Polyhedron* **27** (2008) 1102.

2. "Synthesis, photophysical and photochemical properties of octa-substituted antimony phthalocyanines". **Desmond Kwena Modibane** and Tebello Nyokong, (2008), *Polyhedron* (2008) **in press**.

3. "Synthesis, photophysical and nonlinear optical properties of microwave synthesized 4-tetra and octa-substituted lead phthalocyanines", **Desmond Kwena Modibane** and Tebello Nyokong, (2008), submitted for publication in *Polyhedron*.

3.1. SYNTHESIS AND CHARACTERIZATION

3.1.1. Unsubstituted lead and antimony phthalocyanines

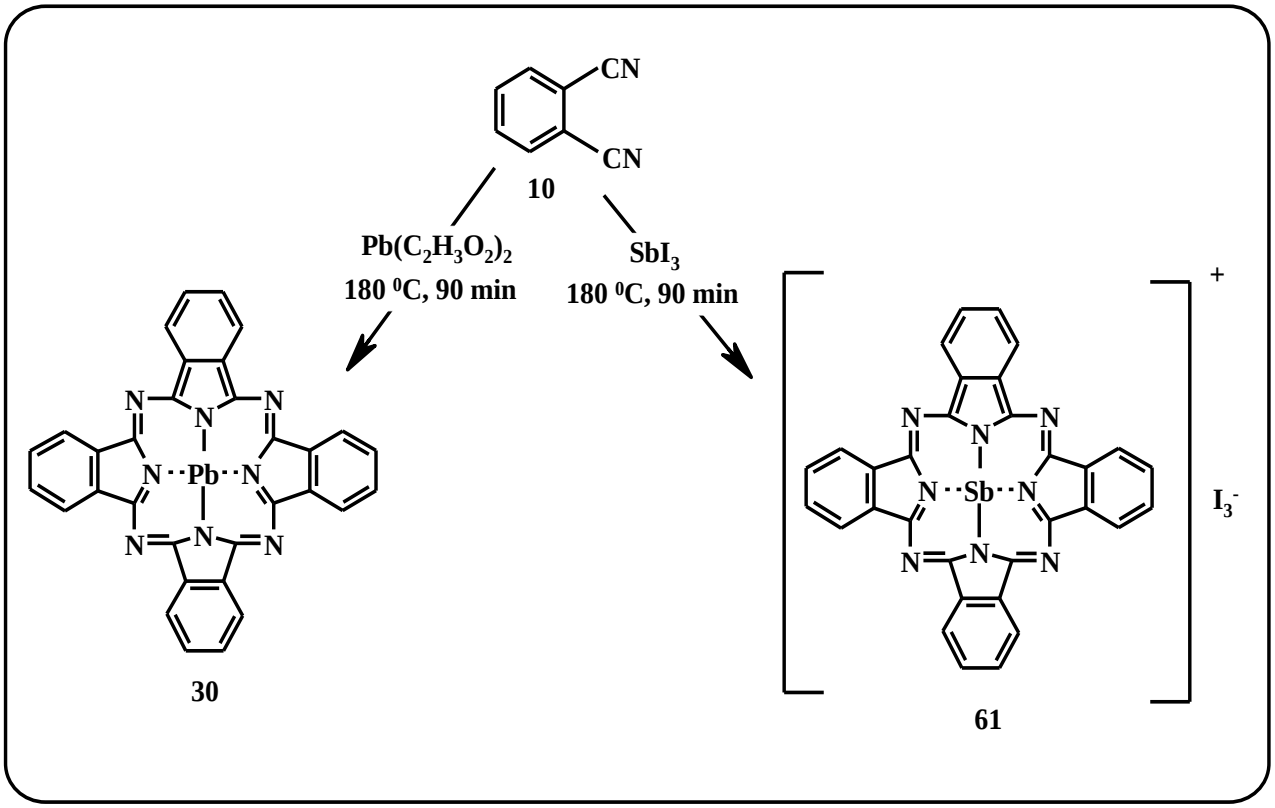

Scheme 3.1: Synthetic route for PbPc (30) and [Sb(III)Pc]$^{+}$I$_3^{-}$ (61)

Scheme 3.1 gives the synthetic pathways for the unsubstituted PbPc (**30**) and [Sb(III)Pc]$^{+}$I$_3^{-}$ (**61**) complexes in this work. The syntheses and characterisation of lead (II) phthalocyanine [62] and antimony (III) phthalocyanine [86] complexes have been reported before. Pb(II)Pc (**30**) and [Sb(III)Pc]$^{+}$I$_3^{-}$ (**61**) were obtained by cyclotetramerization of phthalonitrile (**10**) in the presence of Pb acetate or SbI_3, respectively, for 90 minutes at 180 °C. The experiment for PbPc complex (**30**) was performed under a blanket of nitrogen as Pb acetate is moisture sensitive. Purification

of these complexes was achieved by washing the precipitate with glacial acetic acid, methanol, ethanol and acetone, respectively, and then, finally, Soxhlet extraction was also employed to obtain pure products.

The IR spectra showed peaks between 700-1000 cm^{-1} for SbPc and PbPc, which may be attributed to non-planar deformation vibrations of the C-H bonds of Pc skeletal [76, 158, 159]. Bands around 3050 cm^{-1} are assigned to aromatic C-H stretching vibrations, 1600 and 1480 cm^{-1} to C=C benzene ring skeletal stretching vibrations [62].

The proton NMR spectra showed two doublets between 9.29- 9.32 and 8.27-8.43 ppm for complex **30** and 7.77 and 7.67 ppm for complex **61**, due to the respective equivalent peripheral and non-peripheral protons. The peaks integrated to sixteen protons in total.

Fig. 3.1 shows the ground state electronic absorption spectra of complexes **30** and **61** in DMSO. It is well documented that unsubstituted phthalocyanines lack solubility in most organic solvents; this is due to intramolecular interactions between their π-system, dissolving mostly in coordinating solvents such as pyridine. Complexes **30** and **61** thus behave as expected; they dissolve in polar, coordinating solvents such as DMSO and DMF. The complexes were monomeric as judged by the relatively sharp Q bands (Fig. 3.1), absorbing at 702 and 732 nm for **30** and **61**, respectively. The B band region of these complexes was observed around 345 nm in DMSO (Fig.3.1). For complex (**61**), the band around 370 nm may be due to triiodide ions. The absorption spectrum of PbPc (**30**) shows a band at around 470 nm, which may be attributed to C_{4V} symmetry [160].

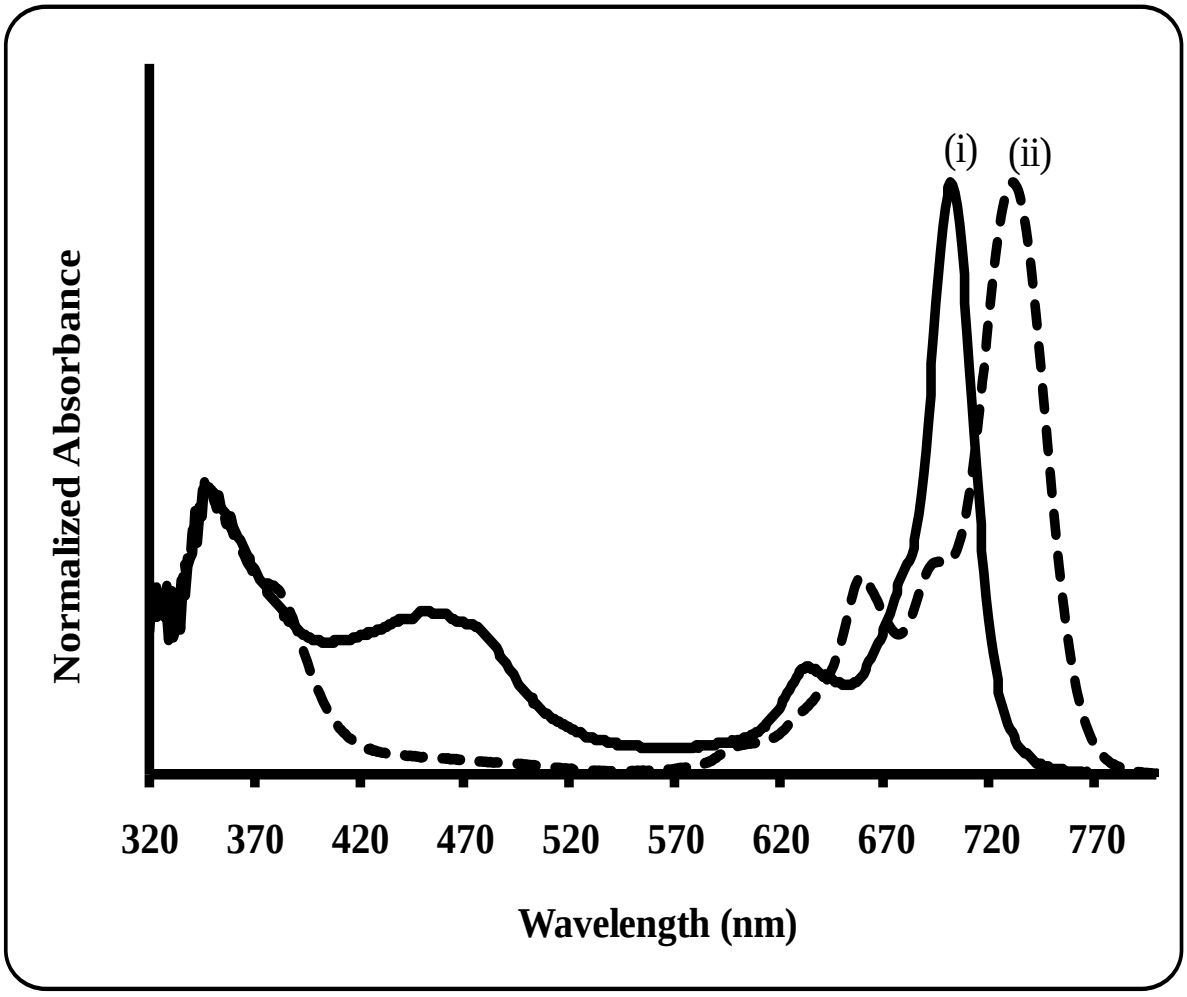

Fig. 3.1: Ground state electronic absorption spectra of (i) PbPc (30) and (ii) $[Sb(III)Pc]^{+}I_3^{-}$ (61) in DMSO. Concentration: ~ 2.0 x10^{-6} mol. dm^{-3}

3.1.2. Synthesis of phthalonitriles for substituted phthalocyanines

3.1.2.1. 3- and 4- Nitrophthalonitriles

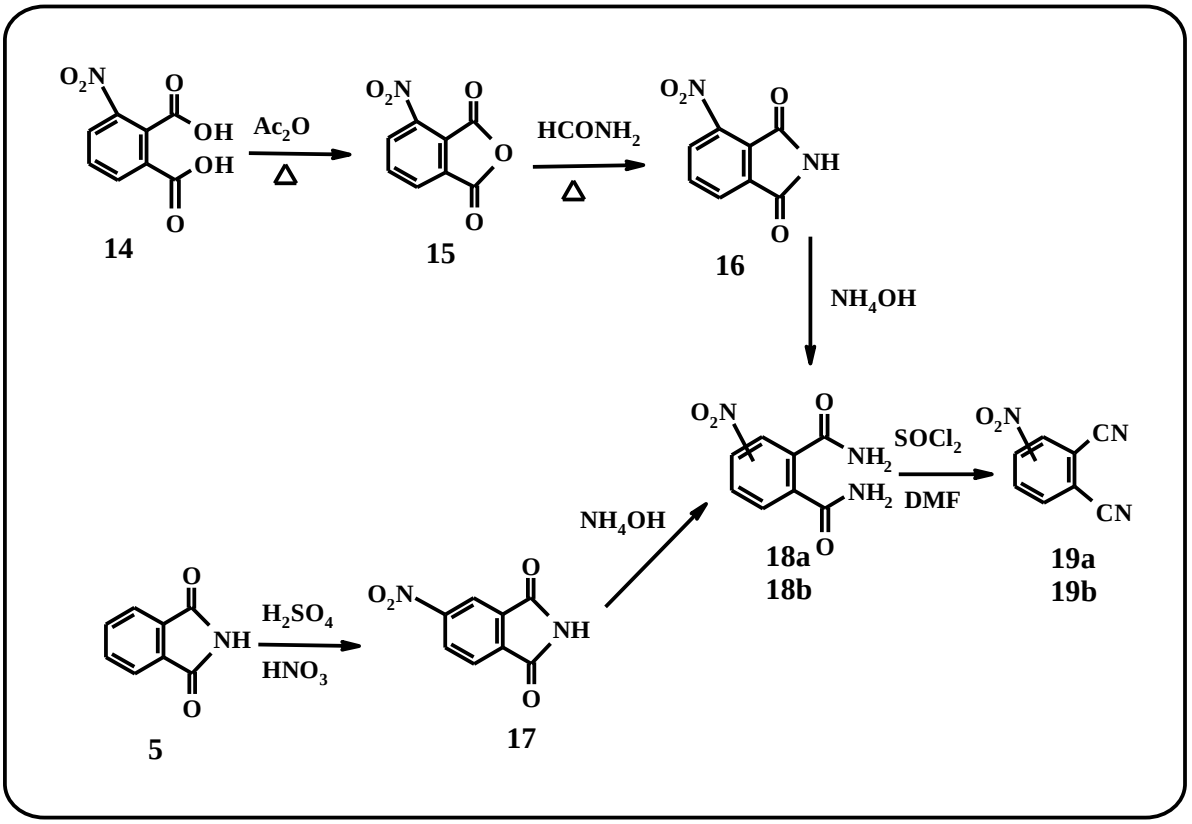

Scheme 3.2: Synthetic pathway to 3-nitrophthalonitrile (19a) and 4-nitrophthalonitrile (19b)

Scheme 3.2 depicts the synthetic pathways followed to achieve the precursors 3-nitrophthalonitrile (**19a**) and 4-nitrophthalonitrile (**19b)** for the monosubstituted phthalonitriles employed in obtaining tetrasubstituted phthalocyanines in this work.

A strategy for the preparation of the monosubstituted phthalonitriles started from the inexpensive 3-nitrophthalic acid (**14**), and phthalimide (**5**). Dehydration of 3-nitrophthalic acid (**14**) in acetic

anhydride occurred in less than an hour, and formed 3-nitrophthalic anhydride (**15**) in relatively good yields. Addition of formamide to compound **15** resulted in the formation of 3-nitrophthalimide (**16**). 4-Nitrophthalimide (**17**) may similarly be synthesised, however in this work, the compound was prepared via direct nitration (mixture of H_2SO_4 and HNO_3) of the phthalimide (**5**), Scheme 3.2. Ammonolysis of the imides (**16**, **17**) was achieved to afford the respective amides **18a**, and **18b**, followed by dehydration of these compounds in $SOCl_2$ and DMF, to give the corresponding phthalonitriles **19a**, and **19b** in good yields.

The IR spectra show the formation of phthalonitriles indicated by C≡N group vibration at 2230 cm^{-1}. The ^{1}H-NMR spectra confirmed the purity of phthalonitriles by observation of the proton peaks in their respective region, as described in the experimental section.

3.1.2.2. 4.5-dichlorophthalonitrile

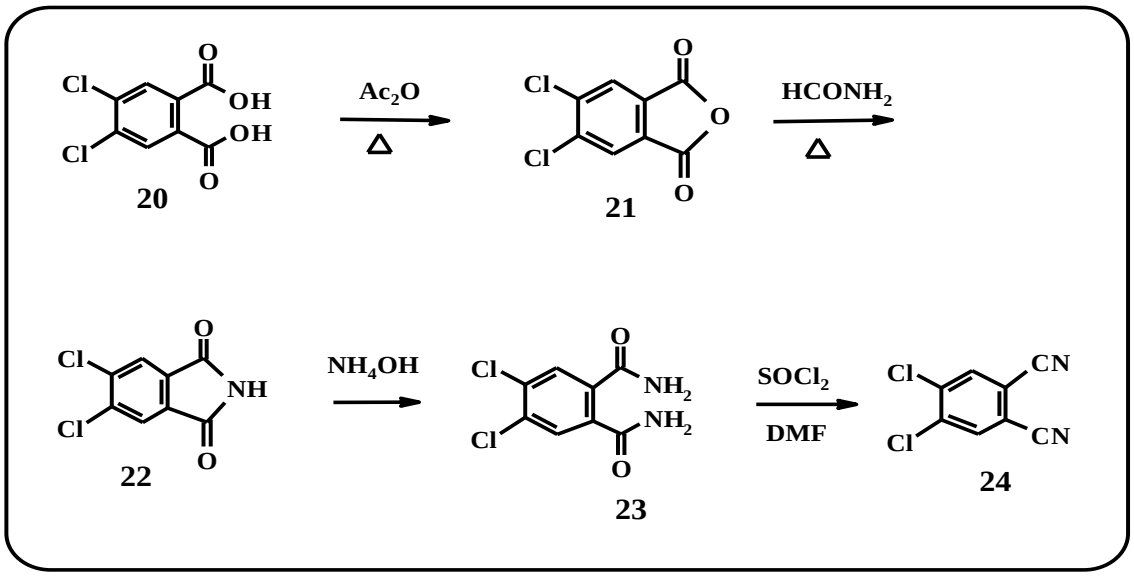

Scheme 3.3: Synthetic pathway to 4,5-dichlorophthalonitrile (24)

The synthetic procedure employed for preparation of 4,5-dichlorophthalonitrile **(24)** (Scheme 3.3) was as for 3-nitropthalonitrile (**19a**) described above, from the commercially available 4,5-dichlorophthalic acid (**20**) through the 4,5-dichlorophthalic anhydride (**21**), 4,5-dichlorophthalimide (**22**) and 4,5-dichlorophthalamide (**23**) to yield the final product (**24**). The purity of the 4,5-dichlorophthalonitrile **(24)** was shown by ^{1}H NMR. The IR spectrum was also used to confirm the presence of the characteristic C≡N stretches at 2230 cm^{-1}.

3.1.2.3. Phthalonitriles substituted with phenoxy derivatives

Scheme 3.4 (below) shows the synthetic procedure for preparation of 3-monosubstituted phthalonitrile (**25**), 4-monosubstituted phthalonitrile (**26**) and 4,5-disubstituted phthalonitrile (**28**), which were employed in obtaining tetra- and octa-substituted phthalocyanines in this work.

3-Nitrophthalonitrile (**19a**), 4-nitrophthalonitrile (**19b**) and 4,5-dichlorophthalonitrile (**24**) were employed to prepare 3-monosubstituted, 4-monosubstituted and 4,5-disubstituted phthalonitrile derivatives, respectively, through base catalysed (K_2CO_3) nucleophilic aromatic displacement.

The same reaction sequence as employed for **19a**, **19b** and **24** was used to prepare compound **25**, **26** and **28** by reacting phenol, 4-t-butylphenol or 4-benzyloxyphenol with compound **19a**, **19b** and **24**, respectively (Scheme 3.4). The reactions were carried out in DMSO at room temperature and gave yields of 57 % for compound **25a**, 42 % for **25b** and **26a**, 40 and 49 % for **25c** and **26c**, respectively, 35 % for **26b**, 63 % for **28a**, 72 % for **28b** and 57 % for **28c**.

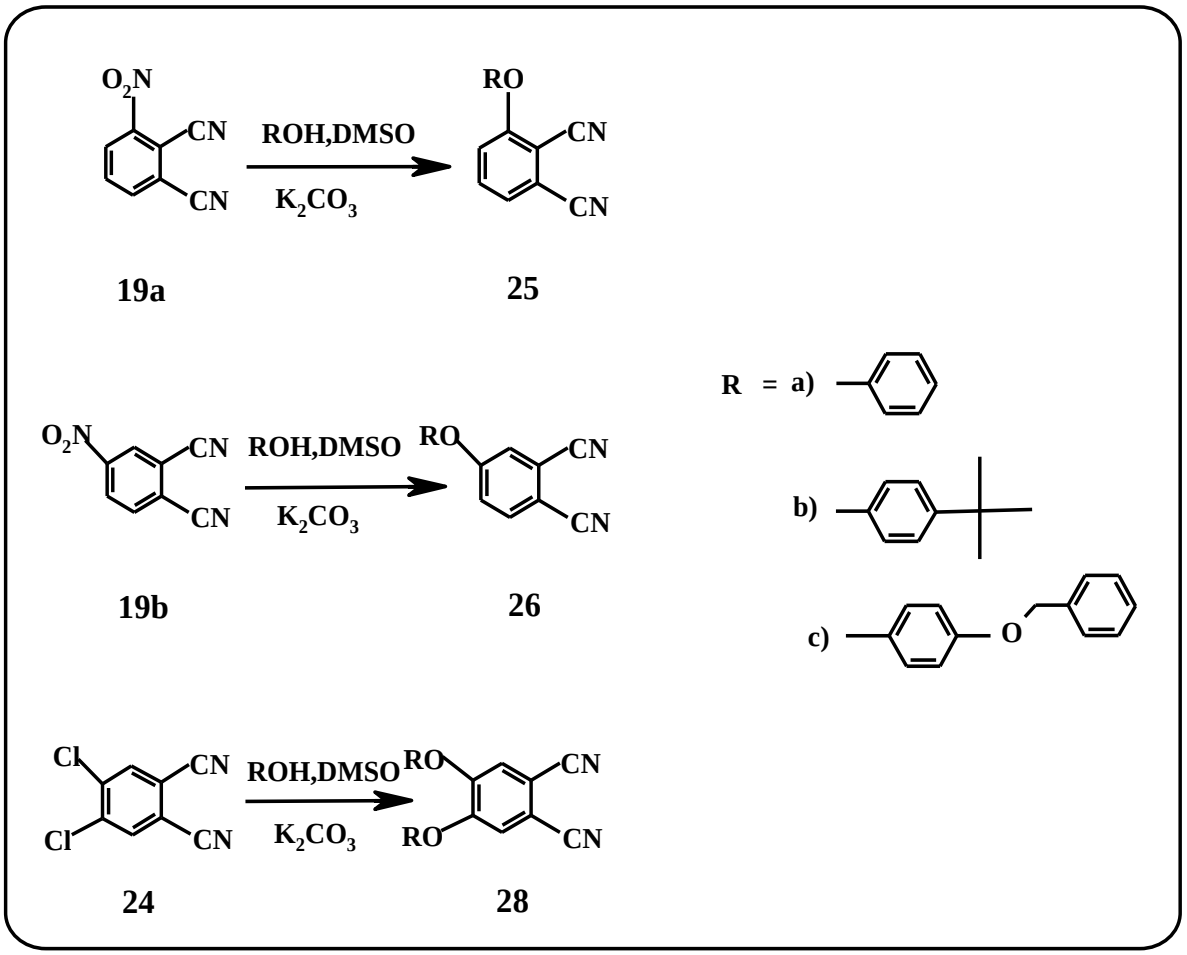

Scheme 3.4: Synthesis of 3-monosubstituted (25) and 4-monosubstituted (26) and 4,5-disubstituted phthalonitrile (28), substituted with (a) phenoxy, (b) 4-t-butylphenoxy and (c) 4-benzyloxyphenoxy groups

The characteristic C≡N, C-O-C and Ar-H IR stretches were observed at the 2224 –2253 cm^{-1}, 1201 – 1260 cm^{-1} and 2961 -2989 cm^{-1}, respectively.

The purity of the substituted phthalonitrile was confirmed by ^{1}H NMR. The appropriate resonances were observed in their respective regions, e.g. for 4-t-butyl protons were observed at around 1.19-1.35 ppm (aliphatic region) and benzyl protons were observed at around 7.00-8.50 ppm (aromatic region).

3.1.3. Substituted lead phthalocyanines

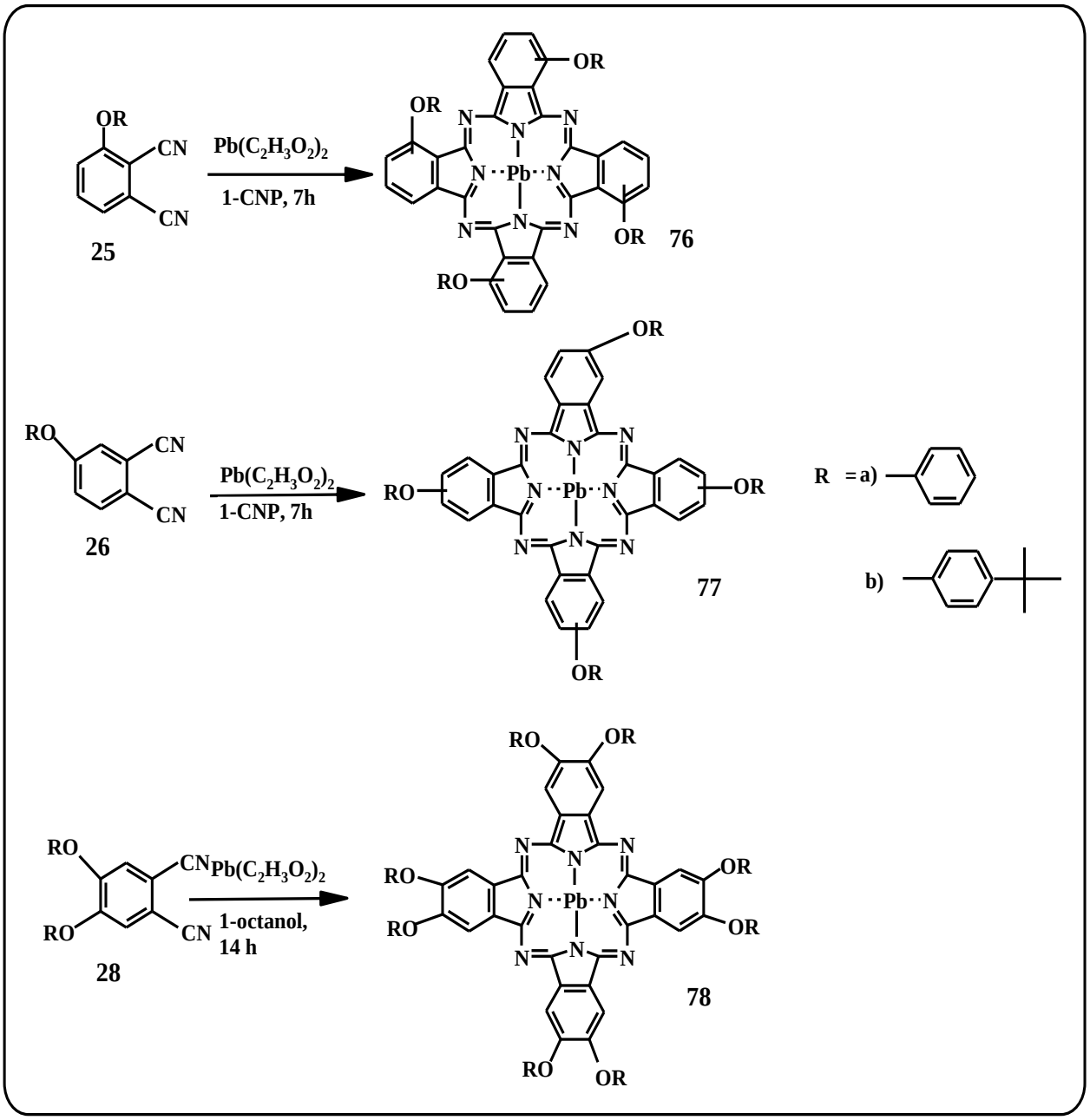

Scheme 3.5A: Synthesis of phenoxy (a) and 4-*t*-butylphenoxy (b) tetra- and octa-substituted lead phthalocyanines

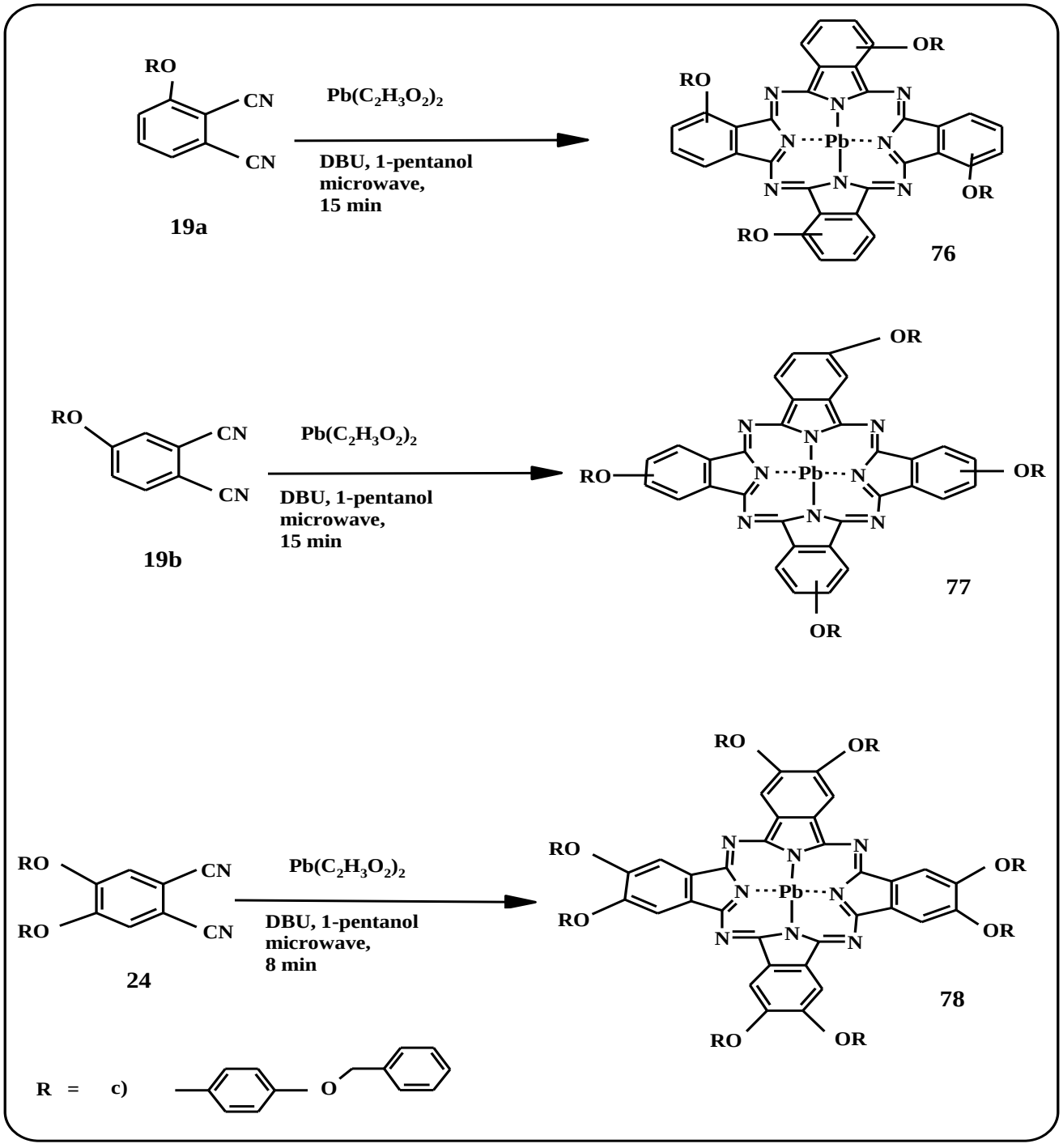

Scheme 3.5B: Synthesis of 4-benzyloxyphenoxy (c) tetra- and octa-substituted lead phthalocyanines

The substituted lead phthalocyanines used in this study were synthesized by cyclotetramerization of substituted phthalonitriles. 4-Tetra-substituted lead phthalocyanines were preparted from 4-substituted phthalonitriles, while 3-tetra-substituted lead phthalocyanines were obtained from 3-substituted analogues [161]. Octa-substituted lead phthalocyanines were synthesized from the appropriate 4,5-disubstituted phthalonitriles [51].

The syntheses of metallophthalocyanine complexes (**76**, **77** and **78**) were achieved by treatment of phthalonitrile **28** with lead acetate in 1-octanol for the octa-substituted, and **25** and **26** in 1-CNP for the tetra-substituted compounds (Scheme 3.5A).

PbPcs can be synthesized in a variety of ways by treatment of phthalonitrile with lead acetate without solvent [65-71]; or in the presence of a high boiling solvent [69-71]; or by addition of lead acetate to a solution of Li_2Pc or H_2Pc in alcohol [69,75]; or by using the microwave method [76]. In this work, the microwave method was also employed to prepare the PbPcs substituted with 4-benzyloxyphenoxy group (**76c**, **77c** and **78c**), Scheme 3.5B.

During synthesis, high boiling point solvents were used because lead is a large atom and high energy is required to insert the metal ion into the phthalocyanine ring cavity. As such, solvents such as 1-chloronaphthalene, 1-octanol and 1-pentanol were used for this purpose. Column chromatography with silica gel was employed to obtain pure product.

The PbPc derivatives were characterized by UV–Vis, IR and NMR spectroscopies, together with elemental analyses. The analyses were consistent with the predicted structures as shown in the experimental section (Chapter 2). The elemental analyses for complexes **76a**, **76c**, **78a**, **78b** and

78c gave excellent percentage carbon values that were very close to calculated values. For the rest of the complexes (**76b**, **77a**, **77b** and **77c**), the elemental analysis values were within 2% of the expected values. It has been reported before that for large Pc molecules, elemental analyses often give unsatisfactory results [162]. However, the purity of the complexes was also established by NMR, which gave excellent results (see below).

The sharp peak for the C≡N vibrations in the IR spectra of the phthalonitriles **25a**, **25b**, **25c**, **26a**, **26b**, **26c**, **28a**, **28b** and **28c** at ~2233, 2230, 2237, 2233, 2231, 2236, 2237, 2232 and 2224 cm^{-1}, respectively, disappeared after conversion into lead phthalocyanines. All PbPc derivatives showed vibration peaks between 700 and 1000 cm^{-1} which may be assigned to the phthalocyanine skeletal vibrations with C_{4v} symmetry [76, 158, 159]. The characteristic vibrations corresponding to ether groups (C–O–C) at ca. 1200–1260 cm^{-1}, C=C at ca. 1500-1600 cm^{-1} and aliphatic C-H stretching at ca. 2900–3000 cm^{-1} were observed for the PbPc derivatives.

The ^{1}H NMR spectra of the diamagnetic lead derivatives in $CDCl_3$ or DMSO-d_6 were found to be pure with all the substituent and Pc ring protons observed in their respective regions. Tetra-substituted PbPcs (**76** and **77**) show complex patterns due to the presence of mixed isomers. For complex **76a**, ^{1}H NMR spectra gave multiplets between 8.60–9.06 ppm for three sets of phthalocyanine ring protons, integrating for a total of 12 protons. The phenyl protons were observed as multiplets between 7.78–8.01 ppm integrating to 20 protons. Compound **76b** gave multiplets between 8.40–9.06, 7.73–8.00 and 1.27–1.32 ppm integrating to 12 protons for the Pc ring, 16 for the phenyl protons and 36 for the methyl protons (*t*-Bu), respectively. For compound **76c**, the CH_2 protons were observed at 5.42 ppm, integrating for 8 protons, while the

resonanances belonging to the aromatic protons were observed between 7.43-7.68 ppm as multiplets, integrating for a total of 48 protons.

The ^{1}H NMR spectra of **77a**, **77b** and **77c** show similar spectral features to that of **76a**, **76b** and **76c**, respectively. Compound **77a** showed multiplets between 8.26–8.78 ppm, integrating to 12 protons for the Pc ring, while peaks attributed to the phenyl rings in the region between 7.73–7.97 ppm integrated to 20 protons. The ^{1}H NMR spectrum of **77b** showed a multiplet at 8.43–9.01 ppm intergrated to 12 Pc ring protons, a multiplet at 7.52–7.55 ppm accounting for 16 phenyl protons and a singlet integrating for 36 methyl protons were observed at 1.33 ppm. For complex **77c**, the CH_2 protons were observed at 5.20 ppm integrated to 8 protons, while aromatic protons observed between 7.22-7.58 ppm integrating to a total of 48 protons. The presence of isomers for tetra-substituted complexes as well as phthalocyanine aggregation at the concentrations used for the NMR measurements generally leads to broadening of the aromatic signals [54] but the data reported in this work was reasonably well resolved .

The ^{1}H NMR spectra for the octa-substituted complex **78** shows a singlet integrating for 8 Pc ring protons at 8.50 ppm (**78a**) and at 8.91 ppm (**78b**). Phenyl protons were observed as multiplets between 7.23–7.44 ppm (**78a**) integrating to 40H, while signals between 7.13–7.43 ppm (**78b**) represented 32 protons. Complex **78b** also showed a singlet at 1.38 ppm for 72 methyl protons. With respect to complex **78c**, the CH_2 protons were observed at 5.09-5.26 ppm and integrated to 16 protons, while the resonanances belonging to aromatic protons were observed as broad peaks between 7.22-7.56 ppm, integrating to a total of 80 protons as expected.

UV/Vis spectra of the PbPc complexes synthesized (**76**, **77** and **78**) showed characteristic absorptions in the Q- and B-band regions, Figs. 3.2A-C. The peaks obtained in the Q-band

region in the range 706–742 nm in five different solvents (Table 3.1) are responsible for the observed green colour of the complexes. The spectra showed monomeric behaviour, evidenced by a single (narrow) Q-band, typical of unaggregated phthalocyanine complexes in DMSO [38, 163]. The B band region was observed around 300–400 nm in DMSO (Figs. 3.2A-C) and was broad due to the superimposition of the B_1 and B_2 bands. Symmetry of PbPc is C_4v and is red-shifted (702 in DMSO) compared to GaPc (680 nm in DMSO) [164].

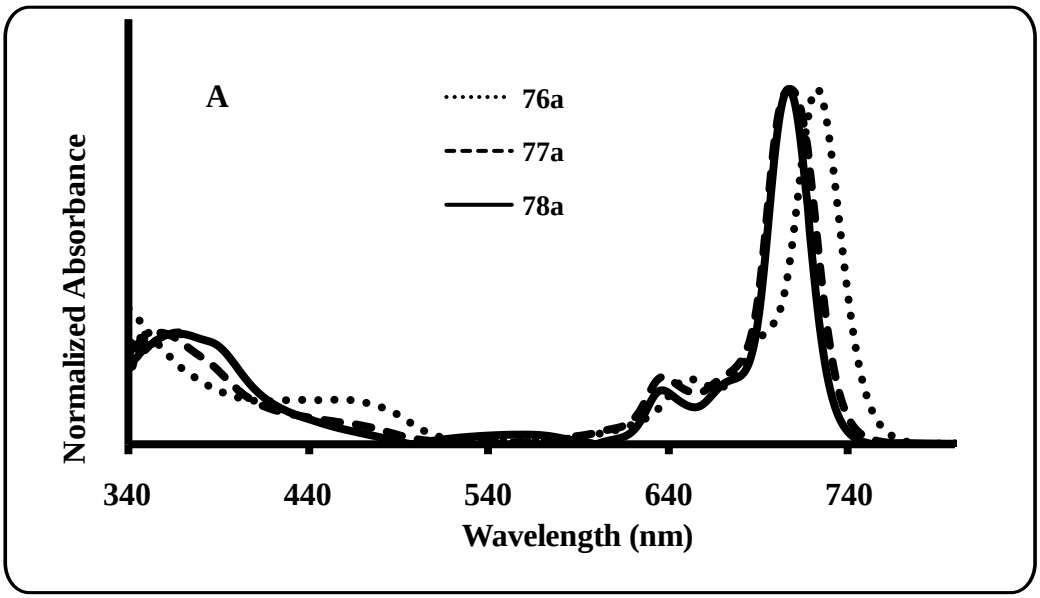

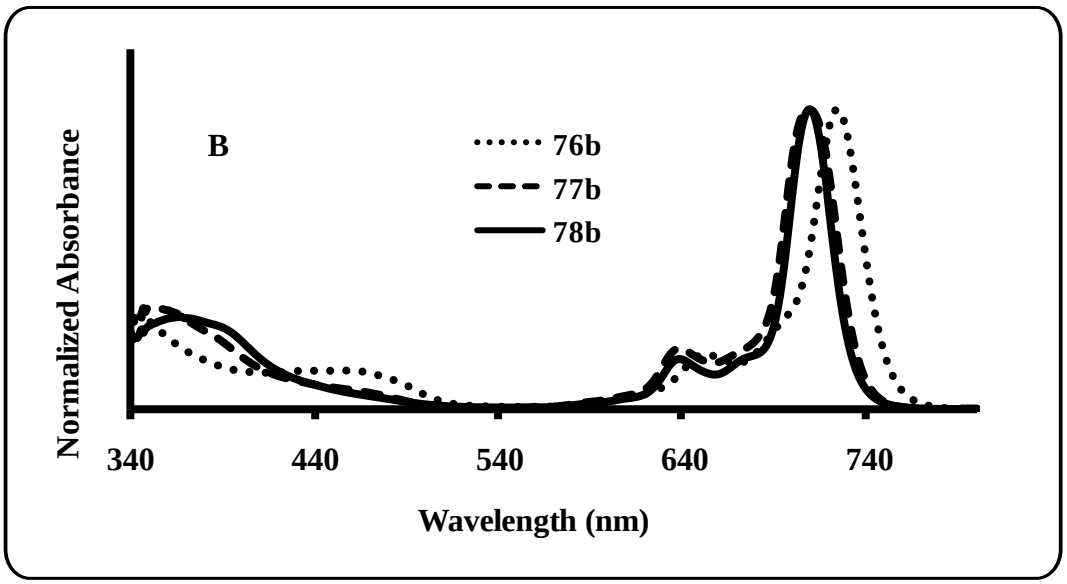

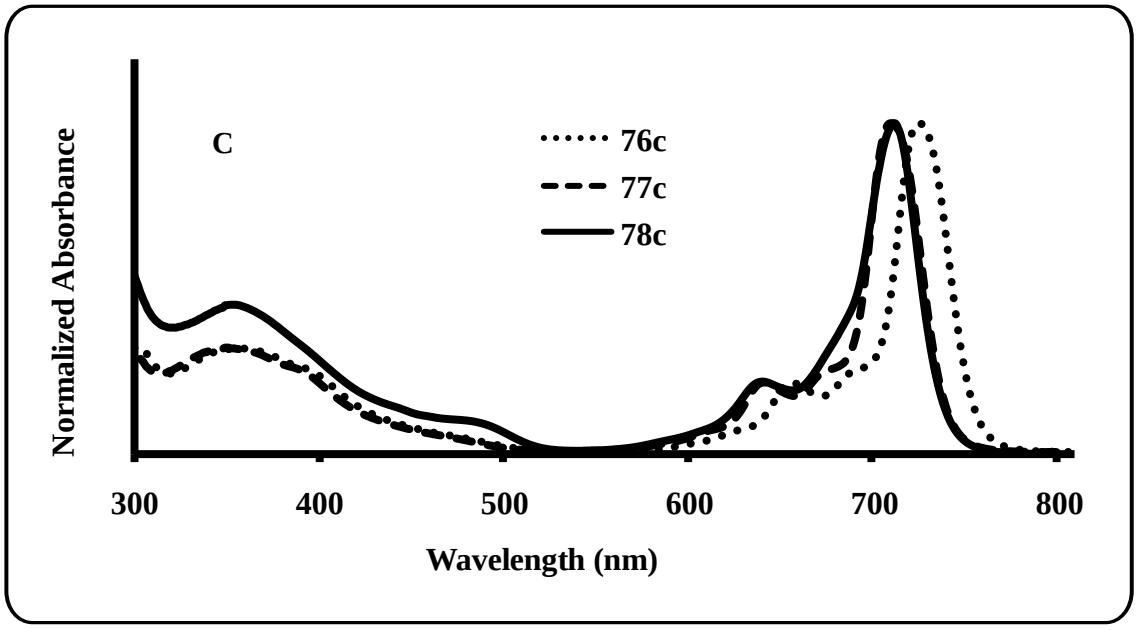

Fig. 3.2: UV–Vis spectra for tetra- and octa-substituted lead phthalocyanines A) phenoxy B) 4-t-butylphenoxy and C) 4-benzyloxyphenoxy. Solvent = DMSO. Concentration ~2 x 10^{-6} mol.dm^{-3}

The Q-band of the non-peripherally tetra-substituted complexes (**76**) is red-shifted when compared to the corresponding peripherally tetra- and octa-substituted complexes. The observed red spectral shift is typical of phthalocyanines with substituents at the non-peripheral positions and has been explained [31, 32, 165, 166] to be due to linear combinations of orbitals (LCAO) coefficients at the non-peripheral positions of the HOMO being greater than those at the peripheral positions. As a result, the HOMO level is destabilized to a greater extent at non-peripheral positions than at the peripheral positions. Essentially, the energy gap (ΔE) between the HOMO and LUMO becomes smaller.

The Q bands of the complexes are slightly red shifted when compared to unsubstituted PbPc (**30**), suggesting a small electron donating ability of the substituents, hence lowering HOMO-LUMO gap.

Generally, MPc complexes are insoluble in most organic solvents; however, introduction of substituents on the ring increases the solubility. All PbPc complexes exhibited excellent solubility in most organic solvents such as DMSO, DMF, $CHCl_3$, THF and toluene (Table 3.1). Table 3.1 shows that the largest red-shift observed for a Q-band was in chloroform. This observation could be partly explained by considering the refractive indices of the solvents. It is known that red-shifting of absorption spectra is a function of the solvent's refractive index [34].

Table 3.1: Q-band spectral data of all PbPc complexes (**30**, **76**-**78**) in various solvents

MPc	Solvent	λ_Q/nm (log ε)	MPc	Solvent	λ_Q/nm (log ε)
30	DMSO	702 (4.98)	**77b**	DMSO	709 (5.00)
	DMF	700 (4.96)		DMF	707 (4.99)
	Toluene	[a]		Toluene	716 (5.01)
	$CHCl_3$	[a]		$CHCl_3$	722 (4.98)
	THF	[a]		THF	709 (4.97)
76a	DMSO	723 (5.33)	**77c**	DMSO	709 (4.98)
	DMF	722 (5.25)		DMF	707 (4.97)
	Toluene	732 (5.31)		Toluene	718 (4.99)
	$CHCl_3$	740 (5.28)		$CHCl_3$	723 (5.00)
	THF	724(5.13)		THF	708 (5.01)
76b	DMSO	724 (5.22)	**78a**	DMSO	707 (5.18)
	DMF	724 (5.21)		DMF	706 (5.16)
	Toluene	734 (5.18)		Toluene	716 (5.09)
	$CHCl_3$	742 (5.23)		$CHCl_3$	720 (5.07)
	THF	726 (5.17)		THF	709 (5.12)
76c	DMSO	725 (5.01)	**78b**	DMSO	709 (4.94)
	DMF	724 (5.03)		DMF	707 (4.95)
	Toluene	736 (5.01)		Toluene	717 (5.01)
	$CHCl_3$	742 (4.99)		$CHCl_3$	723 (4.99)
	THF	728 (4.98)		THF	711 (5.02)
77a	DMSO	708 (4.95)	**78c**	DMSO	712 (5.01)
	DMF	706 (4.98)		DMF	710 (4.99)
	Toluene	715 (4.99)		Toluene	720 (5.04)

77a	$CHCl_3$	721 (4.97)	**77c**	$CHCl_3$	725 (5.02)
	THF	708 (4.99)		THF	709 (4.96)

[a]**30** insoluble in THF, $CHCl_3$ and toluene

Aggregation behaviour of PbPc complexes (76-78)

Phthalocyanines readily aggregate in solution and as such the formation of aggregates was explored in this work by recording the spectra with increasing the concentration for the PbPc complexes. Fig. 3.3 shows the concentration dependence of complex **78a**, in DMSO. As the concentration was increased, the intensity of the Q-band also increased and there was no red (or blue) shifting of bands due to aggregated species for the complex. The Beer–Lambert's law was obeyed for all phenoxy (**a**) and 4-*t*-butylphenoxy (**b**) compounds for concentration less than 1 x 10^{-5} mol.dm^{-3} in chloroform, DMF, DMSO, THF and toluene. Aggregation has also been found to be dependent on the nature of the solvent.

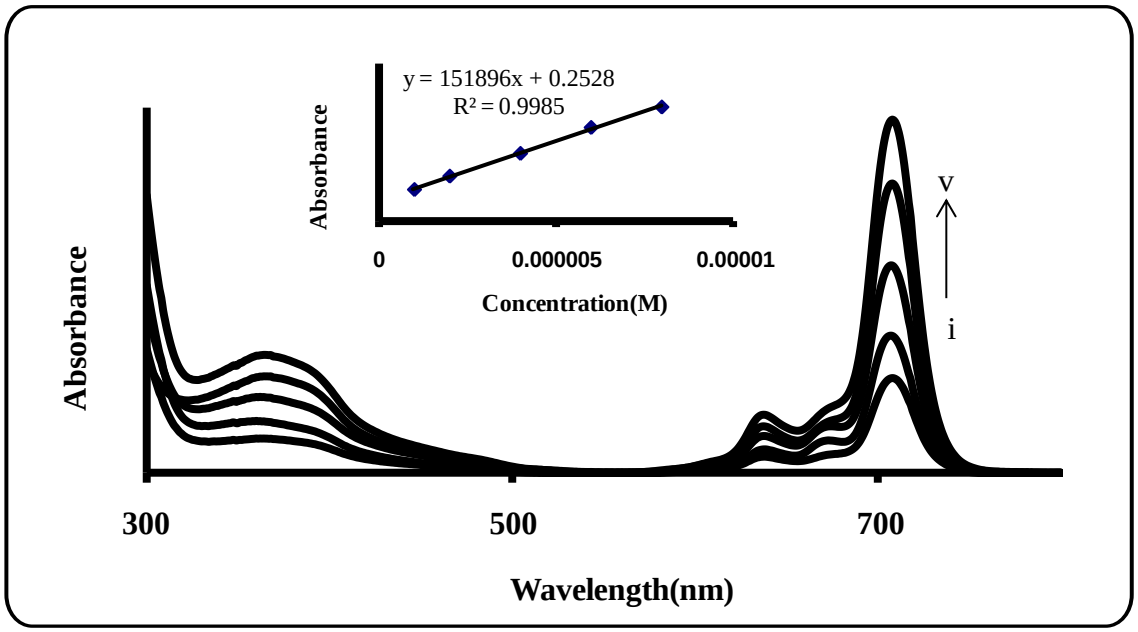

Fig. 3.3: Absorption spectra of compound 78a in DMSO at different concentrations: (i) 8 x 10^{-6}, (ii) 6 x 10^{-6}, (iii) 4 x 10^{-6}, (iv) 2 x 10^{-6}, (v) 1 x 10^{-6} mol.dm^{-3}

The aggregation behaviour of PbPc complexes were investigated in different solvents (DMSO, DMF, Toluene, THF and $CHCl_3$) (Fig. 3.4), and no new bands were observed in any of the solvents for the phenoxy (**a**) and 4-*t*-butylphenoxy (**b**) PbPc complexes (e.g. Fig. 3.4A for complex **77a**). PbPc complexes substituted with 4-benzyloxyphenoxy group show some broadening in the Q band area, with new bands appearing in the 650 nm region, suggesting aggregation [167], for complex **78c** (Fig. 3.4B). 4-Benzyloxyphenoxy is known to prevent aggregation since it is bulky substituent. However, it has been observed [168] previously that some Pc substituted with 4-benzylophenoxy aggregate in solution.

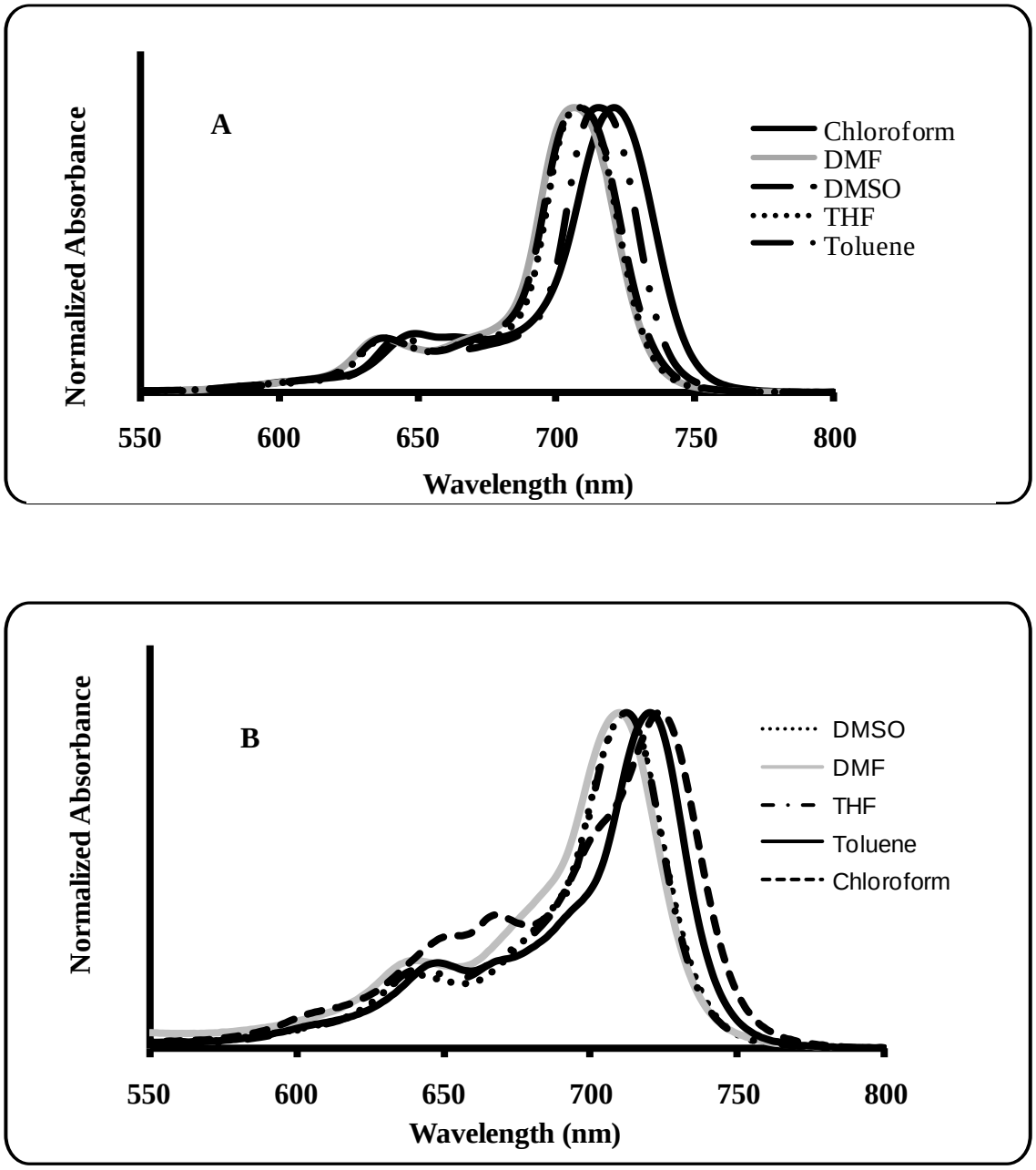

Fig. 3.4: Absorption spectra of A) complex 77a and B) 78c in different solvents. Concentrations ~2 × 10^{-6} mol.dm^{-3}

3.1.4. Substituted antimony phthalocyanines

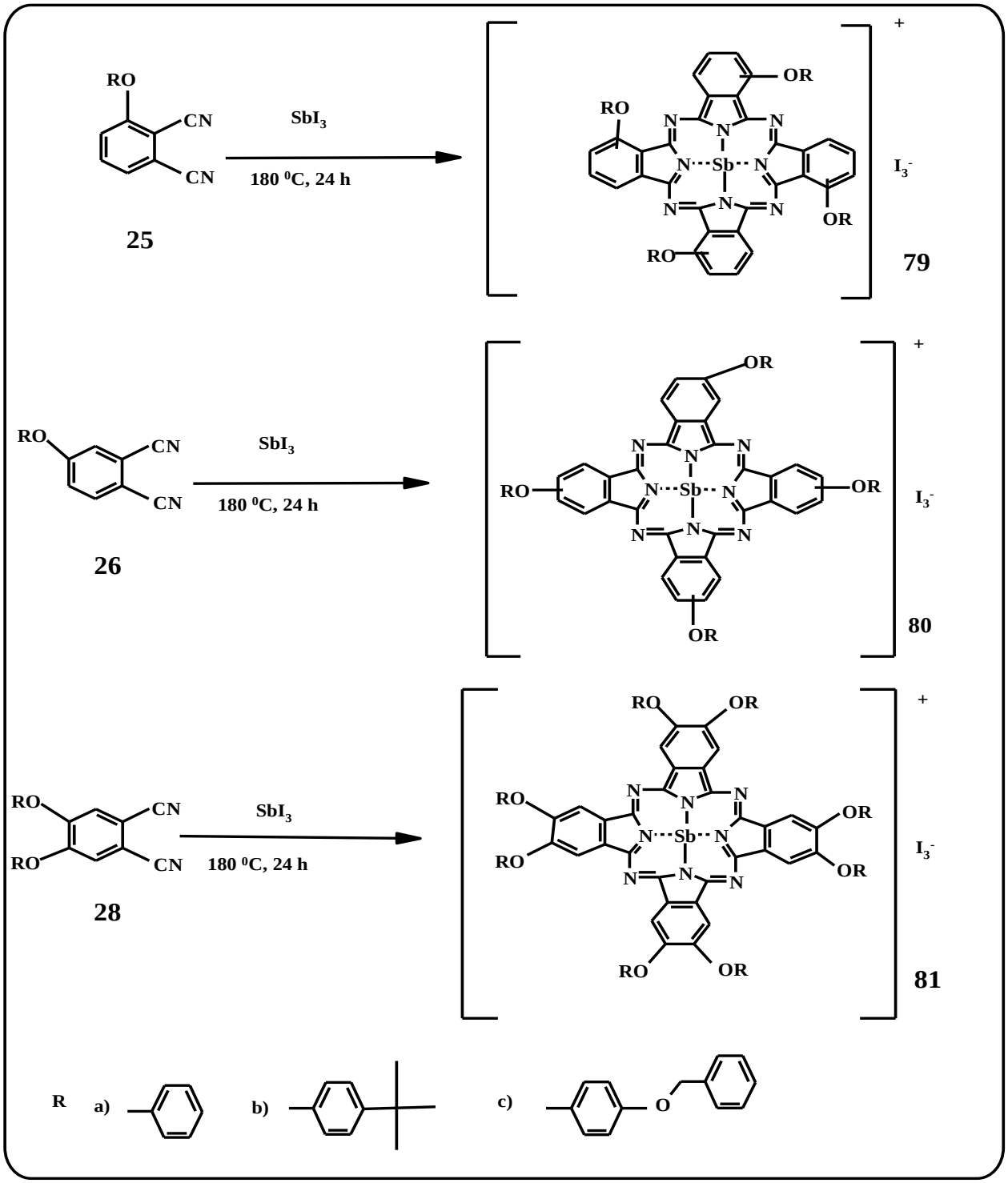

Scheme 3.6: Synthesis of phenoxy (a), 4-*t*-butylphenoxy (b) and 4-benzyloxyphenoxy (c) tetra- and octa-substituted antimony phthalocyanines

Scheme 3.6 gives the synthetic pathways for the SbPc complexes. The syntheses of substituted antimony phthalocyanine complexes (**79**, **80** and **81**) were achieved using a dry synthesis method, by treatment of appropriate substituted phthalonitriles with antimony triodide at 180 °C for 24 hours. Soxhlet extraction was subsequently employed to obtain the pure products.

The SbPc derivatives were characterized by UV/Vis, IR and NMR spectroscopies and elemental analyses. The analyses of the SbPc complexes show behaviour similarly observed for the PbPc complexes above. The elemental analyses results obtained for complexes **79a**, **79b**, **80a**, **80b**, **81a** and **81b** gave results that were close to the calculated values, while **79c**, **80c** and **81c**, analyses values were within 2% of the expected values.

The IR spectra confirmed formation of SbPc complexes (Fig. 3.5) by the disappearance of the sharp peak associated with C≡N vibrations of phthalonitriles. Other vibrational peaks for the SbPc compounds were observed in the same regions as with the PbPc complexes such as C-O-C, C=C, Ar-H, and the usual phthalocyanine skeletal vibrations between 700-1000 cm^{-1} for Pc with large central metal atoms [76, 158, 159].

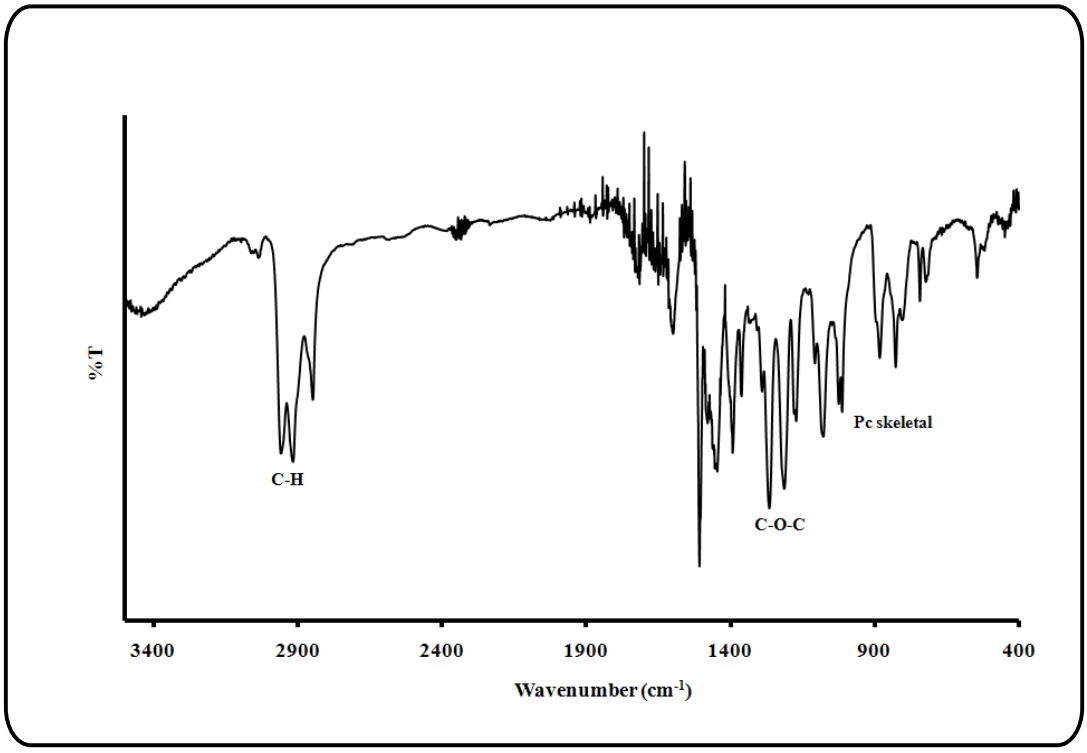

Fig. 3.5: IR spectrum of complex 80b

The antimony phthalocyanines were found to be pure by ^{1}H NMR where the substituents and ring protons were observed in their expected, respective regions. The phenoxy substituted complex **79a** showed the resonances belonging to the ring protons as a multiplet at 8.78-9.19 ppm and a multiplet between 7.45- 7.88 ppm, integrating for 12 and 20 protons, respectively. Complex **80a** showed the resonances belonging to the ring protons as a multiplet in the region 8.52-8.69 ppm, and a multiplet between 7.35- 7.76 ppm, integrating for 12 and 20 protons, respectively. Complex **81a** (Fig. 3.6) showed the resonances belonging to ring protons as a singlet at 8.75 ppm, and a multiplet between 7.35- 7.76 ppm, integrating for 8 and 40 protons, respectively.

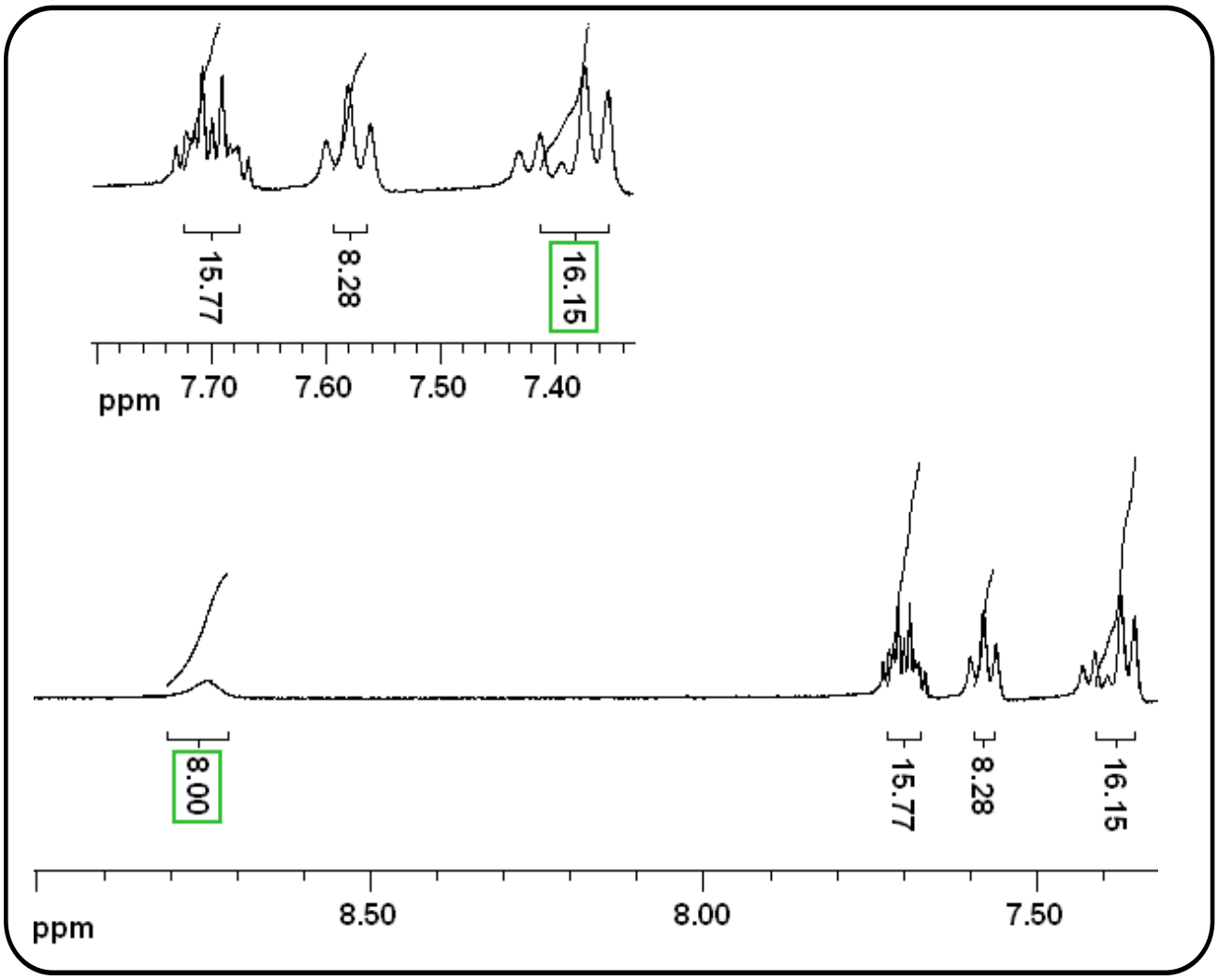

Fig. 3.6: ^{1}H NMR spectrum of complex 81a in DMSO

The ^{1}H NMR for 4-t-butylphenoxy substituted, complex **79b** showed the resonances belonging to the ring protons as a multiplet at around 8.81-9.20 ppm, a multiplet at about 7.34-7.61 ppm for aromatic protons and a multiplet between 1.21-1.34 ppm, integrating for 12, 16 and 36 protons, respectively. Complex **80b** showed ring protons as a multiplet at approximately 8.31-8.80 ppm, a multiplet at around 7.14-7.51 ppm for aromatic protons and a multiplet between 1.13-1.36 ppm for CH_3 protons (aliphatic), integrating for 12, 16 and 36 protons, respectively. Complex **81b**

showed ring protons as a singlet at 8.70 ppm and a multiplet between 7.01 and 7.40 ppm corresponding to the aromatic protons, integrating for 8 and 32 protons each, respectively, giving a total of 40 protons as expected. The methyl protons appear as multiplets between 1.1 and 1.4 ppm and integrate for 72 protons.

For 4-benzyloxyphenoxy substituted, compounds **79c** and **80c**, the CH_2 protons were observed at 5.20 and 5.09 ppm, respectively, integrating for 8 protons, while resonanances belonging to the aromatic protons were observed to be between 7.53-7.78 and 7.41-7.61 ppm, respectively, for **79c** and **80c**, as multiplets integrating for a total of 48 protons. The methylene protons of complex **81c** were observed at 4.98-5.16 ppm and integrated for 16 protons, while the aromatic protons were observed as broad peaks between 7.38-7.68 ppm, integrating for a total of 80 protons expected.

The ground state electronic absorption spectra of the SbPc complexes show relatively sharp Q band, typical of unaggregated MPc complexes, as has been reported before for other antimony derivatives [86-99], Fig. 3.7. It has been reported that the spectra of SbPc complexes are slightly broadened compared to other MPc complexes [91]. Sb(III) is larger than the equilibrium cavity size of the ring and cannot be accommodated without ring expansion, thus the metal ion has been reported [169] to protrude out of the cavity, forming a domed shape. Under this circumstances, the symmetry of these complexes drops from D_{4h} to C_{4v} (from square planar geometry to square pyramidal) [169] as was the case with PbPc derivatives. This symmetry lowering allows some hitherto forbidden transitions, and consequently, spectral splitting and/ or broadening are observed (Fig. 3.7). The Q bands were observed in the range 734-776 nm for all solvents studied, Table 3.2. As reported previously [91], the triiodide ion does not contribute to the Q band

absorption, but contributes to absorption near 360 nm in Fig. 3.7. Thus the B band spectra will be affected by absorption from the triiodide ions. A large red shift has been reported in aromatic solvents [167], hence the red shift of the SbPc derivatives in toluene is not surprising.

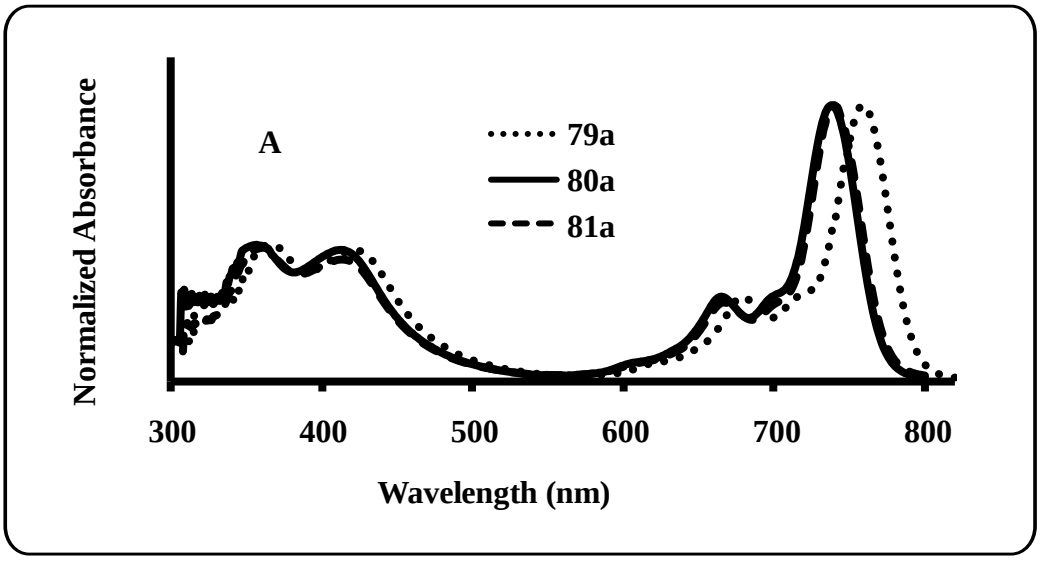

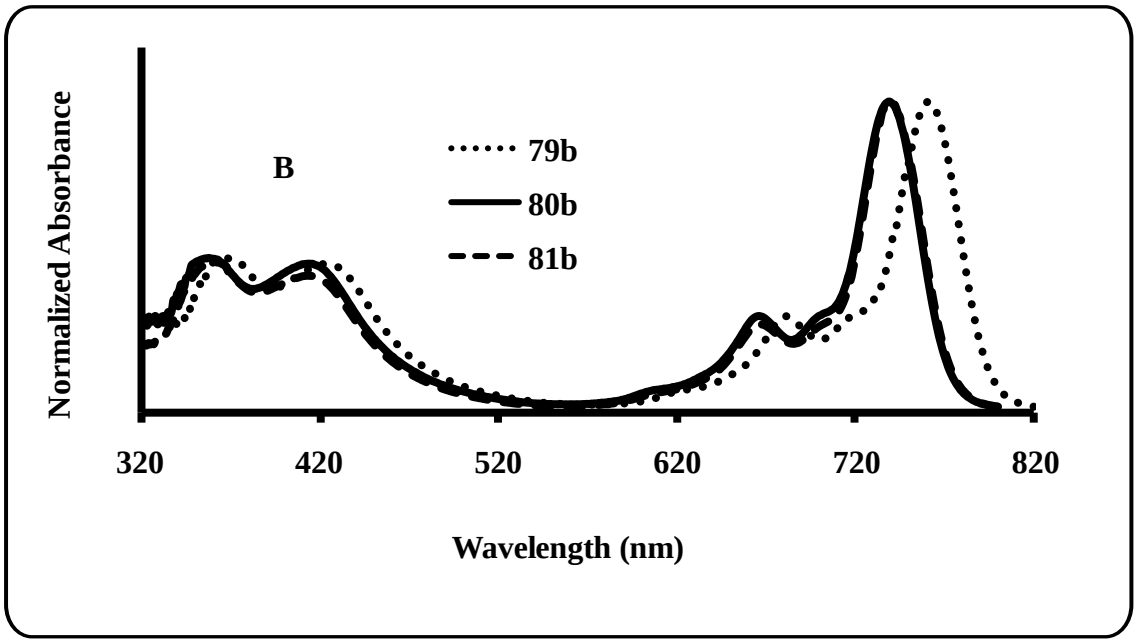

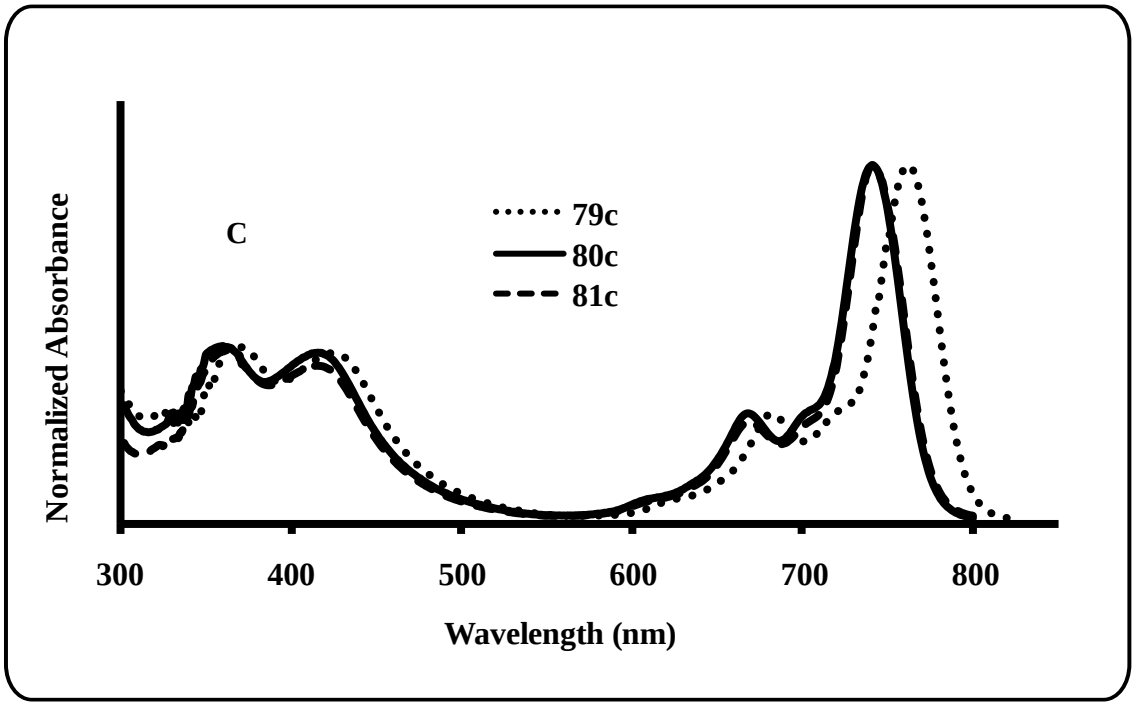

Fig. 3.7: UV–Vis spectra for tetra- and octa-substituted antimony Phthalocyanines with A) phenoxy, B) 4-t-butylphenoxy and C) 4-benzyloxyphenoxy. Solvent = DMSO. Concentration ~4 x 10^{-6} mol.dm^{-3}

Table 3.2: Q-band spectral data for all SbPc complexes (**61**, **79-81**) in DMSO, DMF and toluene

MPc	Solvent	λ_Q/nm (log ε)	MPc	Solvent	λ_Q/nm (log ε)
61	DMSO	732 (4.99)	**80b**	DMSO	739 (5.01)
	DMF	728 (4.98)		DMF	735 (4.99)
	Toluene	[a]		Toluene	753 (4.98)
79a	DMSO	759 (5.01)	**80c**	DMSO	741 (4.97)
	DMF	757 (5.00)		DMF	739 (4.96)
	Toluene	775 (5.03)		Toluene	754 (4.99)
79b	DMSO	761 (4.99)	**81a**	DMSO	740 (5.03)
	DMF	760 (5.02)		DMF	735 (5.04)
	Toluene	776 (4.98)		Toluene	758 (5.01)
79c	DMSO	762 (5.03)	**81b**	DMSO	740 (5.02)
	DMF	761 (5.00)		DMF	735 (5.03)
	Toluene	776 (4.99)		Toluene	753 (4.96)
80a	DMSO	738 (5.02)	**81c**	DMSO	742 (5.01)
	DMF	734 (5.03)		DMF	739 (4.99)
	Toluene	752 (5.04)		Toluene	758 (4.97)

[a] **61** insoluble in toluene

Aggregation behaviour of SbPc complexes (79-81)

At the concentrations employed in Fig. 3.8 for complex **81a** (2×10^{-5} to 3×10^{-6} M in DMSO), the intensity of the Q-bands increased with increasing concentration and no evidence of aggregated species was observed, hence comfirming lack of aggregation.

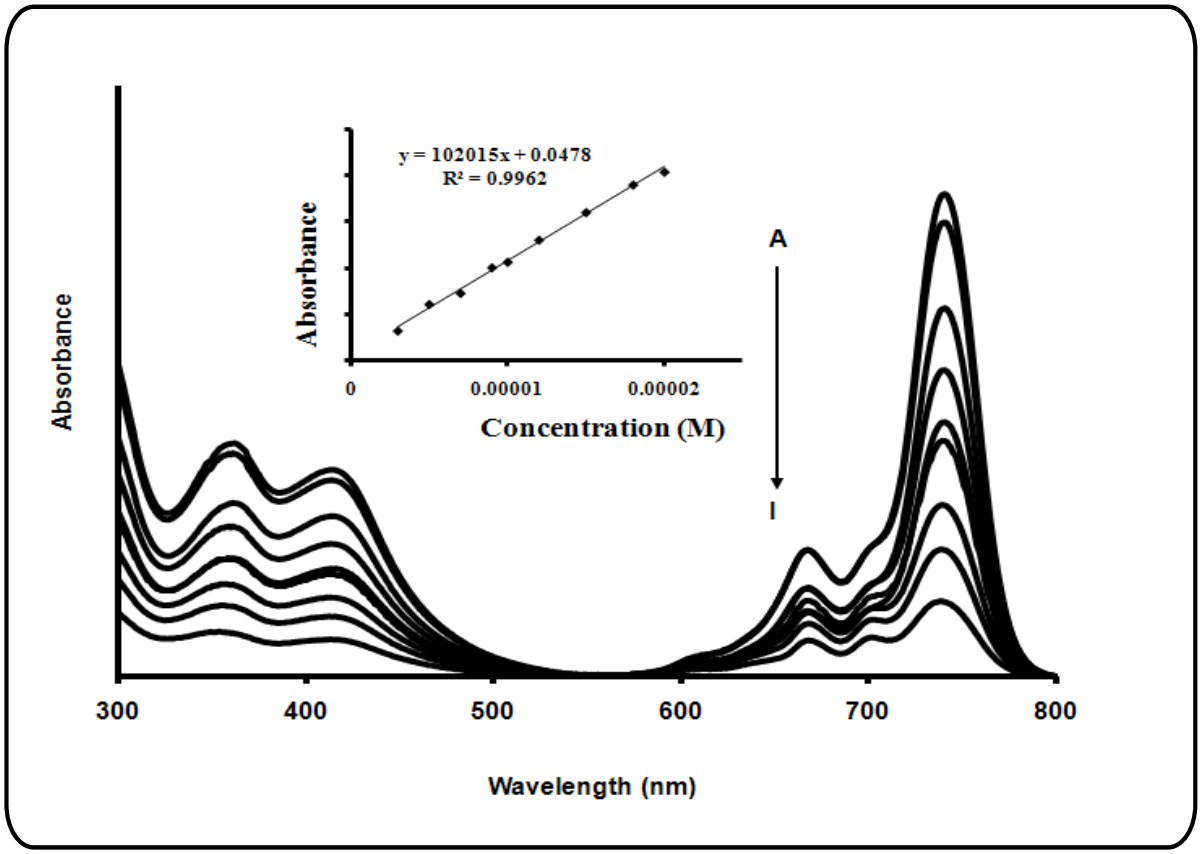

Fig. 3.8: Absorption spectra of compound 81a in DMSO at different concentrations: (A) 2 x 10^{-5}, (B) 1.8 x10^{-5}, (C) 1.5 x10^{-5}, (D) 1.2 x10^{-5}, (E) 1 x10^{-5}, (F) 9 x10^{-6}, (G) 7 x10^{-6}, (H) 5 x10^{-6}, (I) 3 x10^{-6} mol.dm^{-3}

Fig. 3.9 shows absorption spectra of complex **81b** in DMSO, DMF and toluene, and even though some SbPc complexes are known to demetallate in donor solvents such as DMF and THF [98], there was no evidence of demetalation for SbPc complexes **79**, **80** and **81** in these solvents. Additionally, there was no red (or blue) shifting observed due to aggregated species.

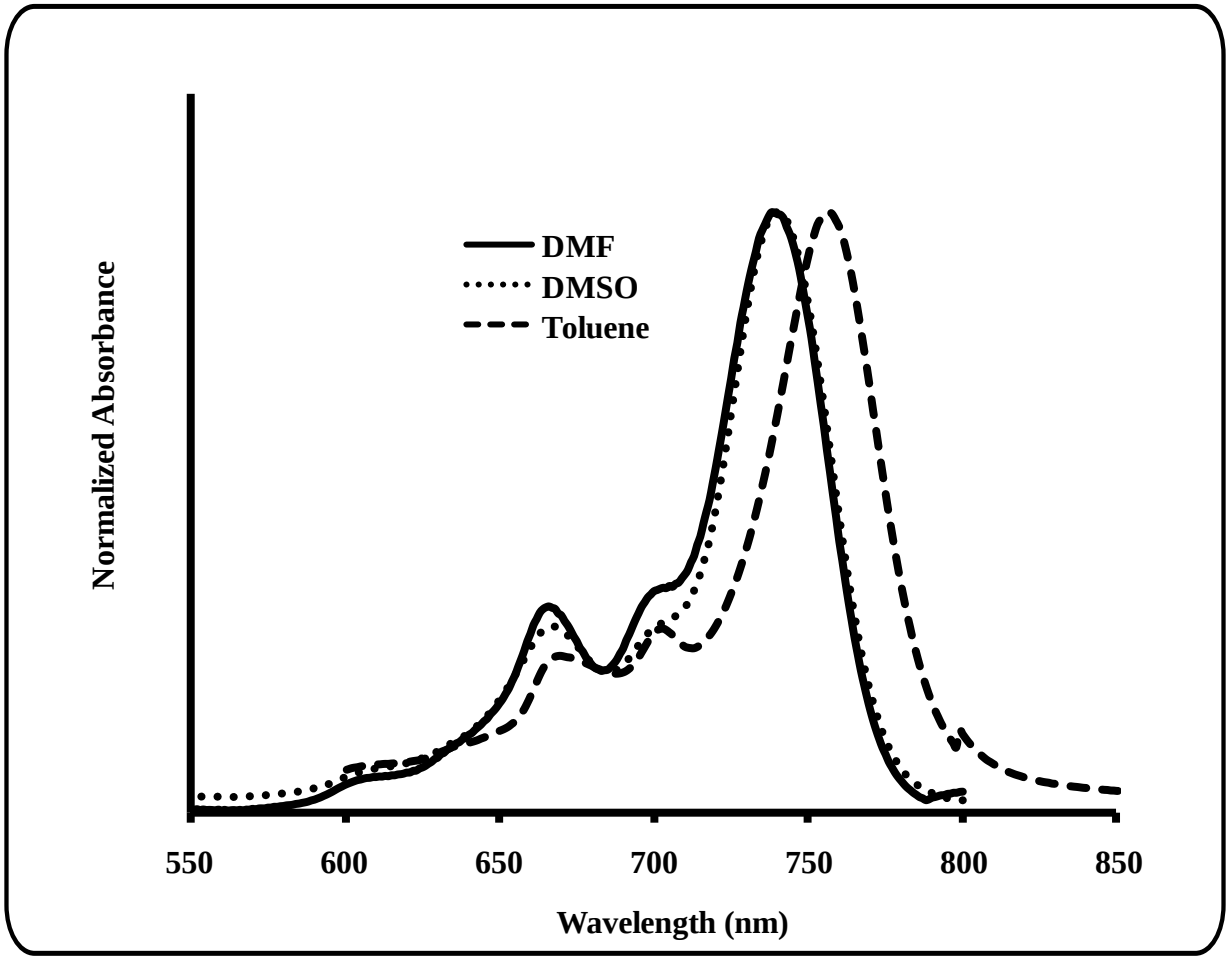

Fig. 3.9: Absorption spectra of complex 81b in DMF, DMSO and Toluene (~4x 10^{-6} mol.dm^{-3})

Oxidation of $Sb^{III}Pc$ to $Sb^{V}Pc$ derivatives

Since $Sb^{III}Pc$ derivatives themselves do not fluoresce (discussed below), complexes **61**, **79**, **80** and **81** were oxidized to $Sb^{V}Pc$ in order to study their fluorescence behaviour. The oxidized antimony complexes have been prepared through oxidative addition process using H_2O_2 as the oxidant [87]. It was found that antimony (III) phthalocyanine complexes can be readily

converted to the corresponding antimony (V) derivatives through oxidative addition process [87]. Even though H_2O_2 is a readily available oxidant, it is known that clean spectra are generally not obtained for the resulting $Sb^{V}Pc$ [88], and thus for this work, an organic oxidant tert-butylhydroperoxide (TBHP) was employed instead. The oxidation of $Sb^{III}Pc$ derivatives is known to proceed more cleanly if organic peroxides such as tert-butyl perbenzoate are employed as oxidants [88].

After addition of TBHP to $Sb^{III}Pc$ complexes (**61**, **79**, **80** and **81**), the Q-bands were blue-shifted, indicative of oxidized $Sb^{III}Pc$ derivatives, Figs. 3.10a and b, with Q-bands were observed at 710, 735 and 731 nm in DMSO for the oxidized forms of complexes **61**, **81a** and **81b**, respectively. Sb(V) is smaller than Sb(III) (ionic radii are 0.62 Å and 0.89 Å respectively), and is also more electronegative. The smaller size and higher electronegativity results in an increase in the conjugation of the Pc's HOMO orbital with the metal $5p_z$ orbital [170], resulting in a lower charge density and energy of the Pc's HOMO orbital. This accounts for the observed blue-shifting of spectral band positions (Figs. 3.10).

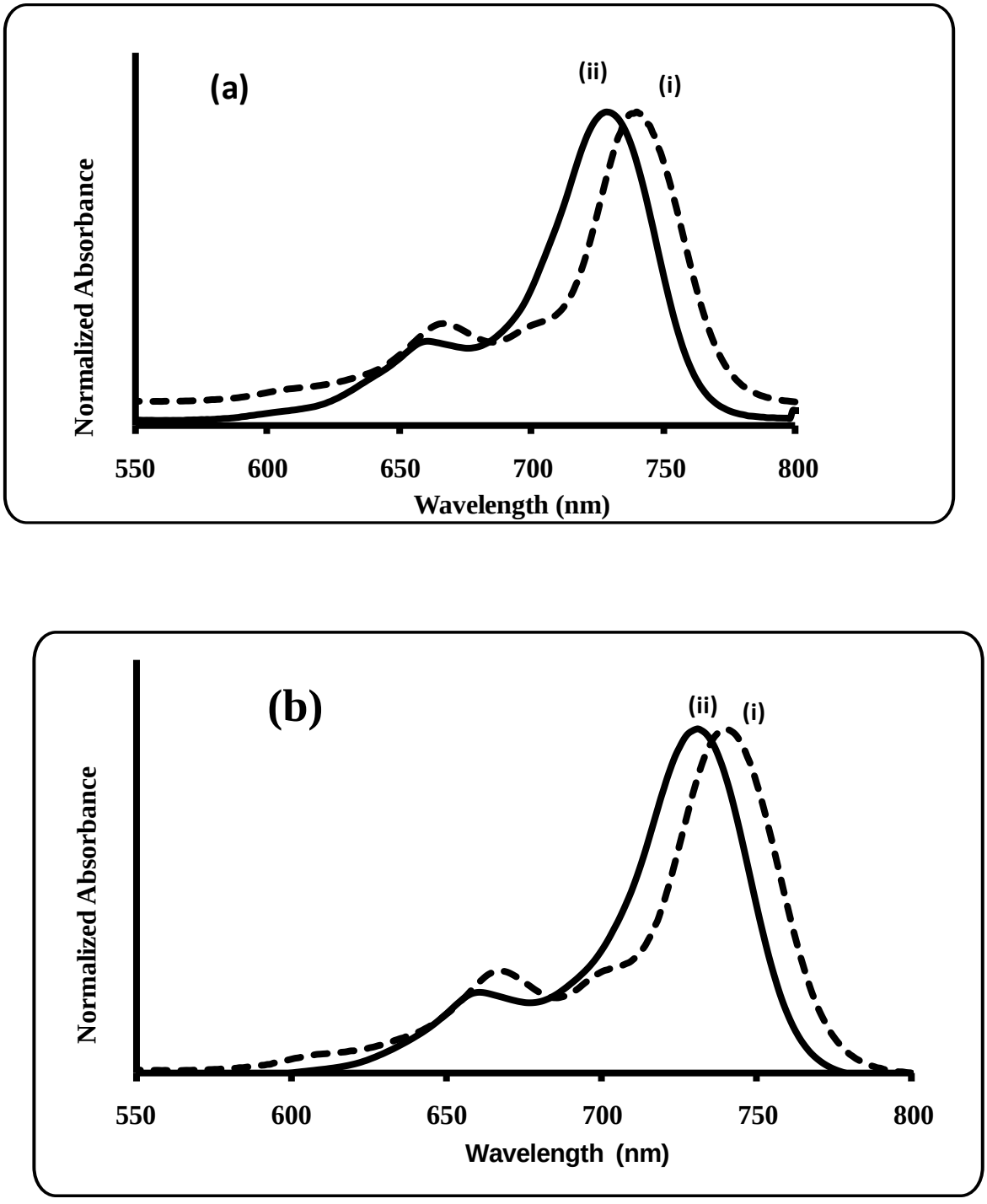

Fig. 3.10: Absorption spectra before (i) and after (ii) oxidation of (A) complex 80a and (B) complex 81b using TBHP in DMSO as an oxidant. Concentration - 1 x 10^{-5} mol.dm^{-3}

3.2. PHOTOPHYSICAL PROPERTIES

3.2.1. Photophysical properties of PbPc complexes

3.2.1.1. Fluorescence spectra and quantum yields

The values of Φ_F are widely known to be influenced by the factors such as temperature, molecular structure, solvent parameters (polarity, viscosity and refractive index), and the presence of heavy atoms in the solvent and in the molecule itself.

Figs. 3.11 and 3.12 show the absorption, fluorescence emission and excitation spectra for the complexes in various solvents. No emission was observed to the red of the Q-band of the absorption spectra. The excitation spectra for the PbPcs were different to the absorption and emission spectra in all solvents as shown in Figs. 3.11 and 3.12. The excitation spectrum shown in Fig. 3.11a shows demetallation of **76b** in toluene upon excitation (as an example of all complexes in toluene), as judged by the blue shifted and split Q band. The excitation spectrum in Fig. 3.11a was similar to the absorption spectra of the corresponding demetallated H_2Pc derivatives, confirming demetallation upon excitation. The occurrence of demetallation is due to a heavy size of Pb atom, since the metal seats outside of the ring, it has a tendency to be lost upon excitation, resulting in demetallated spectra. Metal free Pcs are known to fluoresce with only one main peak in non-aqueous media, which has been assigned as the 0–0 transition of the fluorescence [171]. Complete splitting of the Q band was observed for all complexes in THF, toluene and chloroform. There was broadening in DMSO (Fig. 3.11b) and partial splitting in DMF (Fig. 3.11c) of the Q band in the excitation spectra of **76b**. Both DMSO and DMF are basic solvents. It has been documented that in strongly basic solvents, the inner pyrrole hydrogens are

acidic enough to dissociate and Pc^{-2} species becomes symmetrical and thus will possess an unsplit Q band [165]. This is observed as a partially split Q band in DMF (Fig. 3.11c) and a broadened Q band in DMSO (Fig. 3.11b) for **76b**. The broading and splitting in excitation spectra was also observed for complexes **76a** and **76c** in DMF and DMSO. The lack of split Q band in DMSO is more clear in the fluorescence excitation spectra for **77** and **78** in DMSO (e.g. Fig. 3.11d for **78a**), which exhibited a single band upon excitation. Emission for all complexes was attributed to demetallated species, as evidenced by the red shift observed for emission when compared to the excitation spectra and not the absorption spectra. As stated above, for **76a-c** in DMSO, there was broadening of the excitation spectra without showing complete splitting. Thus, the more basic solvents such as DMSO and DMF resulted in a single or broadened excitation spectrum, whereas the less basic solvents (THF, chloroform and toluene) resulted in complete splitting of the Q band in the excitation spectra due to demetallation.

The extent of splitting in the Q band also depends on the nature of the complex when considering the same solvent, Fig. 3.12. For example, the excitation spectrum of **76a** is broadened but not split in DMF (Fig. 3.12a), while in the same solvent the Q band in excitation spectrum of **78a** is split. Thus, the extent of deprotonation of the ring by the basic solvent depends on the nature of substituents.

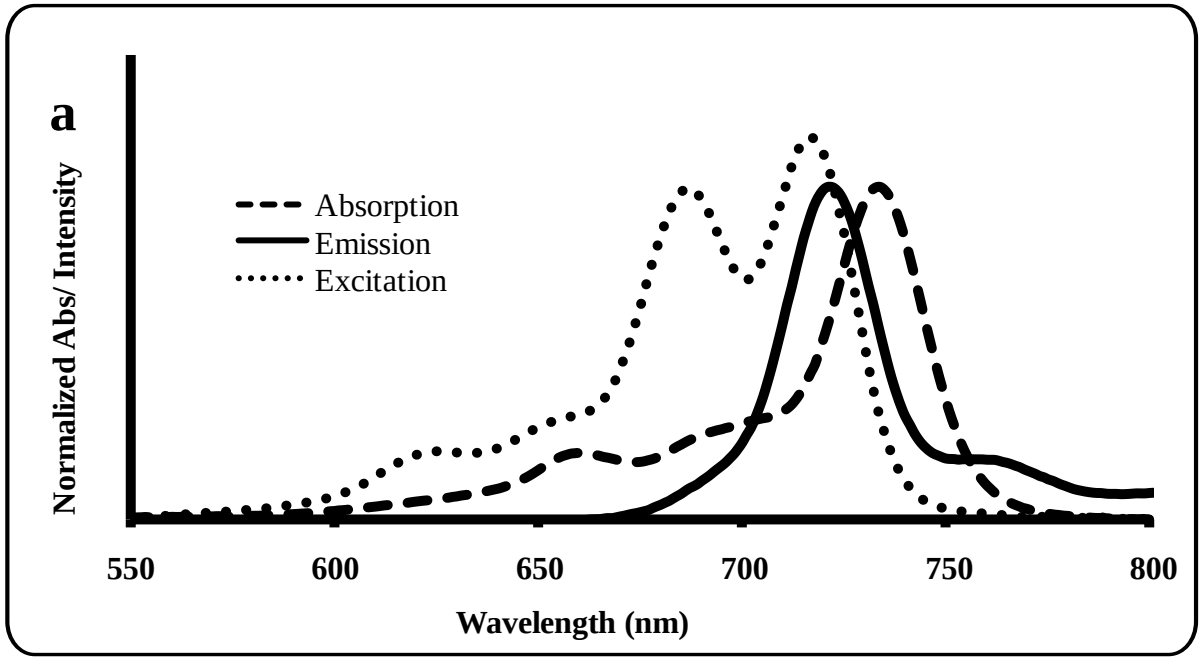
a
Normalized Abs/ Intensity
Absorption
Emission
Excitation
550
600
650
700
750
800
Wavelength (nm)

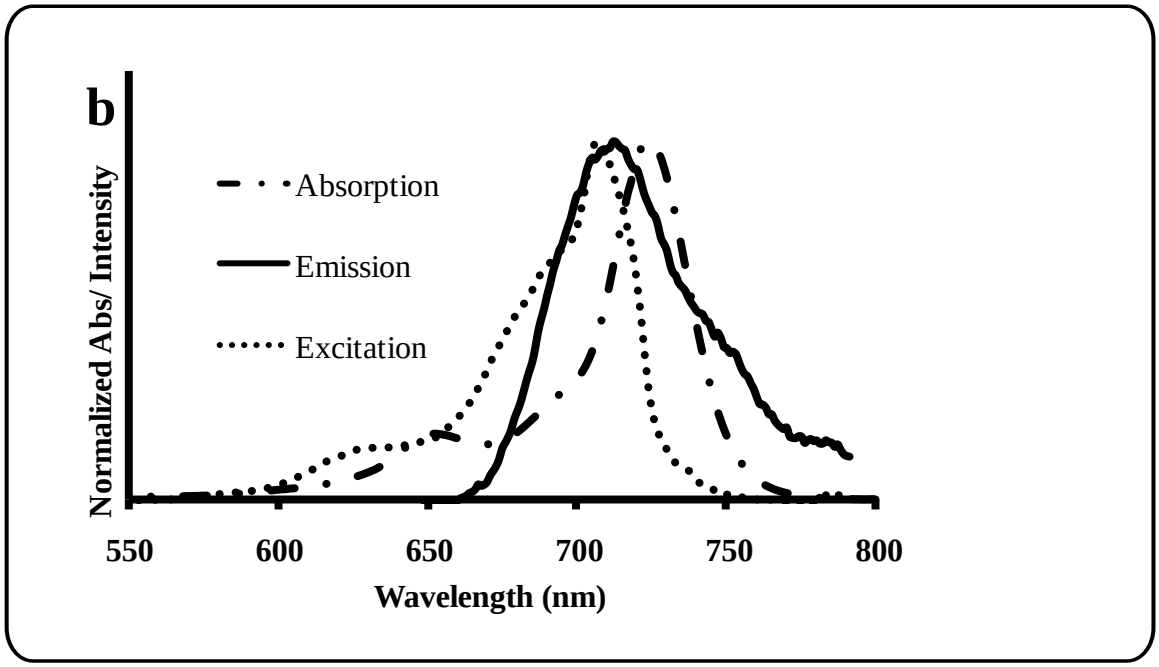
b
Normalized Abs/ Intensity
Absorption
Emission
Excitation
550
600
650
700
750
800
Wavelength (nm)

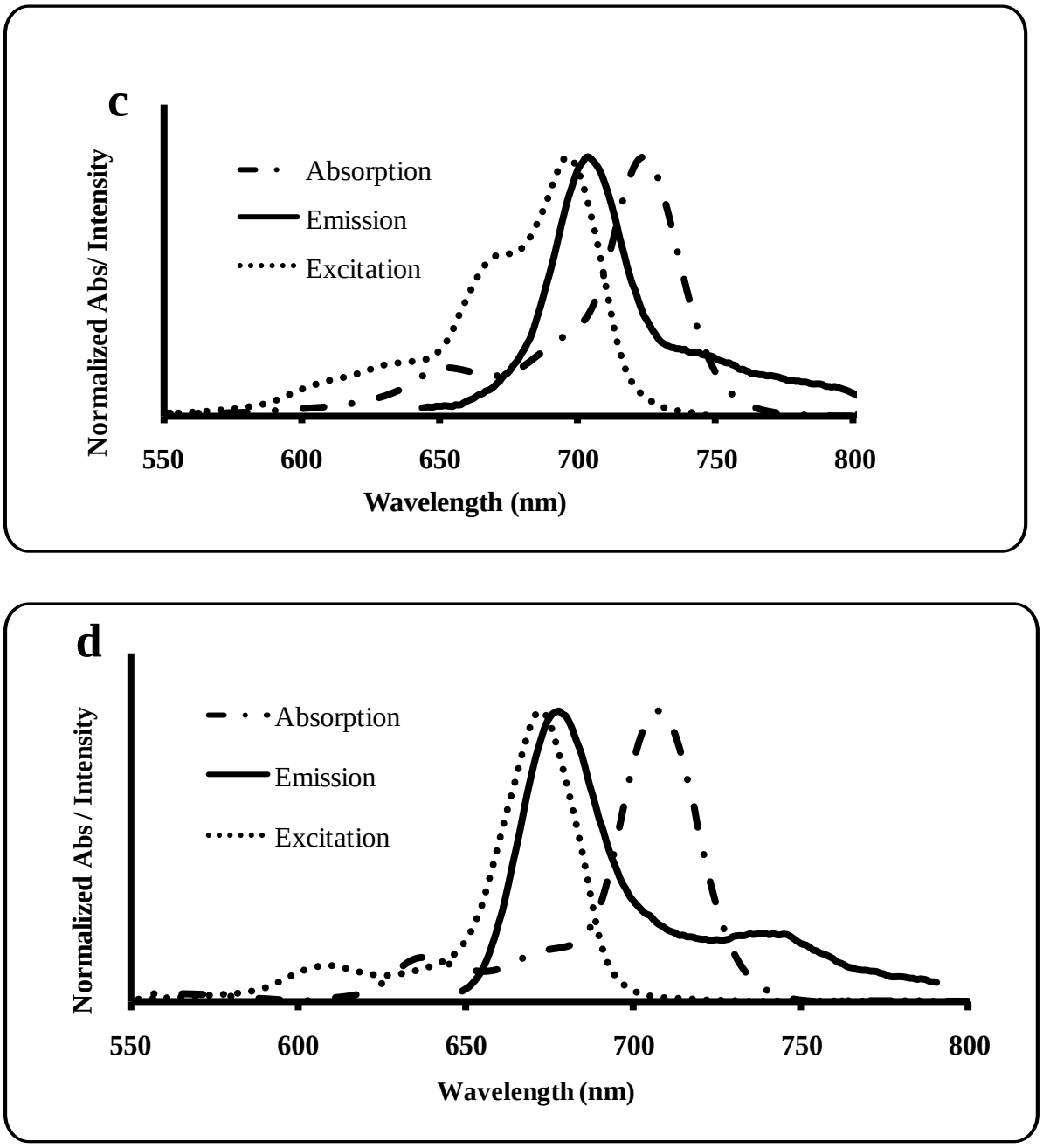

Fig. 3.11: Absorption, emission and excitation spectra of (a) compound 76b in tolune, (b) 76b in DMSO, (c) 76b in DMF and (d) 78a in DMSO. Concentration ~1 x 10^{-6} mol.dm^{-3}

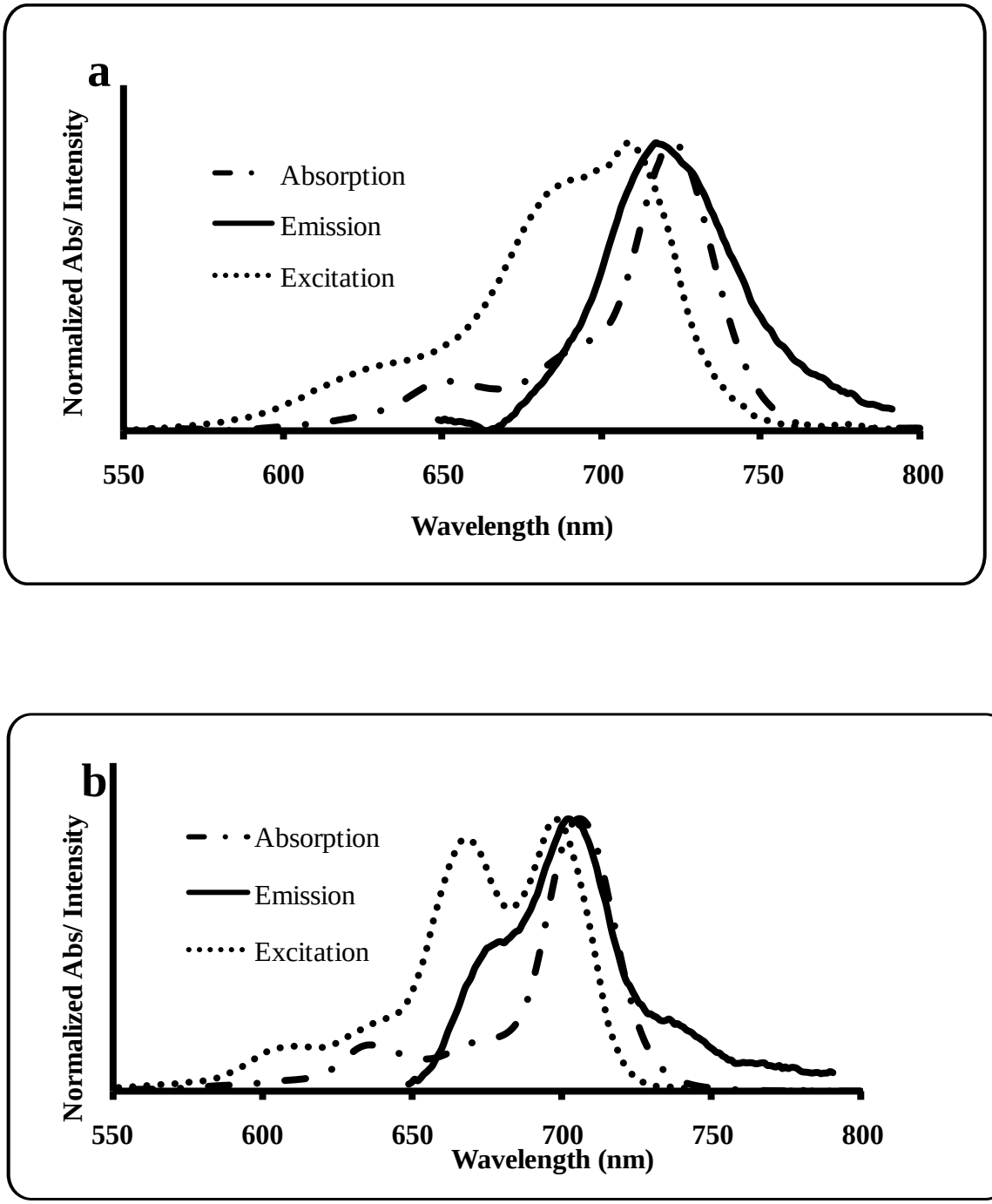

Fig. 3.12: Absorption, emission and excitation spectra of (a) compound 76a in DMF and (b) 78a in DMF. Concentration ~1 x 10^{-6} mol.dm^{-3}

The fluorescence quantum yield (Φ_F) values for the PbPc complexes (Table 3.3) were found to be less than 0.1, less than the values typically detained for MPc complexes (e.g. ZnPc in DMSO, Φ_F = 0.2 [108]). The Φ_F values are thought to be very small due to the presence of a heavy atom (Pb) in solution, which enhances intersystem crossing to populate the triplet state, consequently reducing the number of fluorescing molecules. Relatively higher Φ_F values were observed in $CHCl_3$ compared to the rest of the solvents. This contradicts the heavy atom effect of the chlorines in chloroform, which should encourage intersystem crossing resulting in lower fluorescence quantum yield values. The fact that the PbPc complexes become demetallated upon excitation suggests that the reported Φ_F values are for the fully or partially demetallated complexes. However the effects of Pb, in terms of the heavy atom effect, will still influence the values since the Pb atom is still in solution.

Table 3.3: Spectral, photophysical parameters of PbPc derivatives in various solvents

Solvent	MPc	λ_{max}			Φ_F	Φ_T	Φ_{IC}	τ_T(μs)
		Q_{abs} (nm)	Q_{ems} (nm)	Q_{exc} (nm)				
DMSO	[a]**30**	703	688	678	0.02	0.70	0.28	30
	76a	723	709	704	<0.01	0.78	0.21	40
	76b	724	712	702	<0.01	0.80	0.20	30
	76c	725	710	703	<0.01	0.84	0.15	40
	77a	708	678	675	<0.01	0.76	0.24	20
	77b	709	681	676	<0.01	0.72	0.28	30
	77c	710	706	699	<0.01	0.82	0.17	40
	78a	707	678	672	0.01	0.76	0.23	20
	78b	709	678	673	<0.01	0.88	0.11	50
	78c	712	706	700	<0.01	0.84	0.15	50
DMF	[a]**30**	702	687	677	0.03	0.68	0.29	9
	76a	722	717	708	0.03	0.72	0.25	10
	76b	724	704	696	0.02	0.82	0.17	9
	76c	724	708	699	0.01	0.83	0.16	10
	77a	706	706	700,669	<0.01	0.75	0.25	9
	77b	707	706	700,669	<0.01	0.78	0.21	9
	77c	707	705	702,672	<0.01	0.80	0.19	5
	78a	706	703	699,668	<0.01	0.78	0.22	5
	78b	707	706	700,669	<0.01	0.74	0.26	5
	78c	710	704	701,671	<0.01	0.83	0.16	6
Toluene	**76a**	732	720	715,685	0.01	0.82	0.17	8
	76b	734	721	717,687	0.05	0.70	0.25	7

	76c	736	723	720,695	0.04	0.84	0.12	8
	77a	715	706	701,667	0.02	0.77	0.21	8
	77b	716	706	701,667	0.04	0.78	0.18	9
	77c	718	707	702,673	0.03	0.83	0.14	6
	78a	716	704	698,667	0.01	0.85	0.14	7
	78b	717	706	702,669	<0.01	0.74	0.26	6
	78c	720	708	703,674	0.01	0.86	0.13	7
[b]THF	**76a**	724	720	713,685	0.02			10
	76b	726	723	715,687	0.03			10
	76c	728	721	717,691	0.02			9
	77a	708	703	697,665	<0.01			6
	77b	709	704	698,665	0.03			6
	77c	708	702	698,671	0.02			4
	78a	709	702	697,665	0.01			10
	78b	711	704	698,667	<0.01			9
	78c	709	702	699,671	0.02			8
[b]$CHCl_3$	**76a**	740	723	717,688	0.05			7
	76b	742	726	720,692	0.08			10
	76c	742	727	721,693	0.06			10
	77a	721	707	701,668	0.04			10
	77b	722	708	702,668	0.07			10
	77c	723	710	702,671	0.07			5
	78a	720	706	700,667	0.07			6
	78b	723	707	702,670	0.03			6
	78c	725	710	703,672	0.05			5

[a] **30** insoluble in toluene, THF and $CHCl_3$.[b] Values of Φ_T and Φ_{ISC} not determined due to lack of standards

3.2.1.2. Triplet quantum yields (Φ_T) and lifetimes (τ_T) of PbPc complexes

Both the triplet quantum yields and lifetimes were determined by laser flash photolysis. Transient spectra (Fig. 3.13) in DMSO showed a single Q band but at a different Q band wavelength from that observed for absorption, thus confirming the changes in the molecule following excitation. As discussed above the molecules demetallate upon excitation, but show a single Q band in basic solvents like DMSO. Fig. 3.14 shows a typical triplet decay curve for compound **78a** in DMSO.

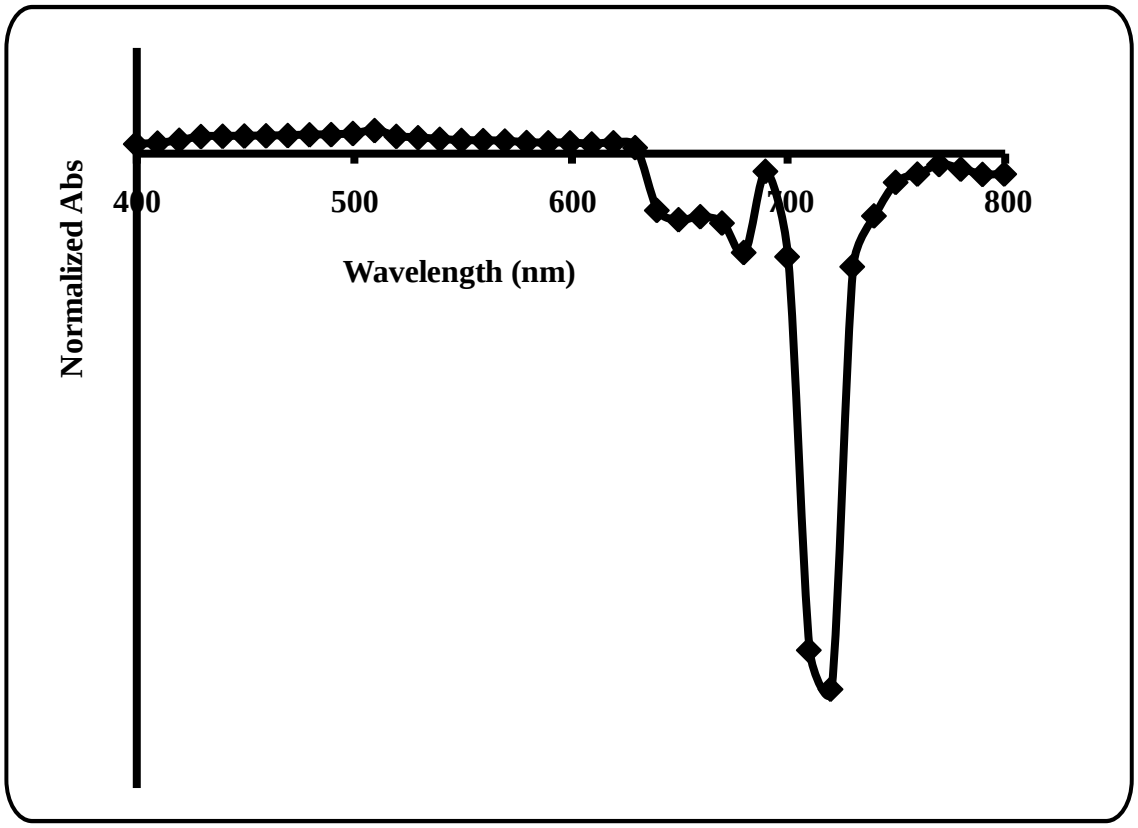

Fig. 3.13: Transient absorption spectrum for 78a in DMSO

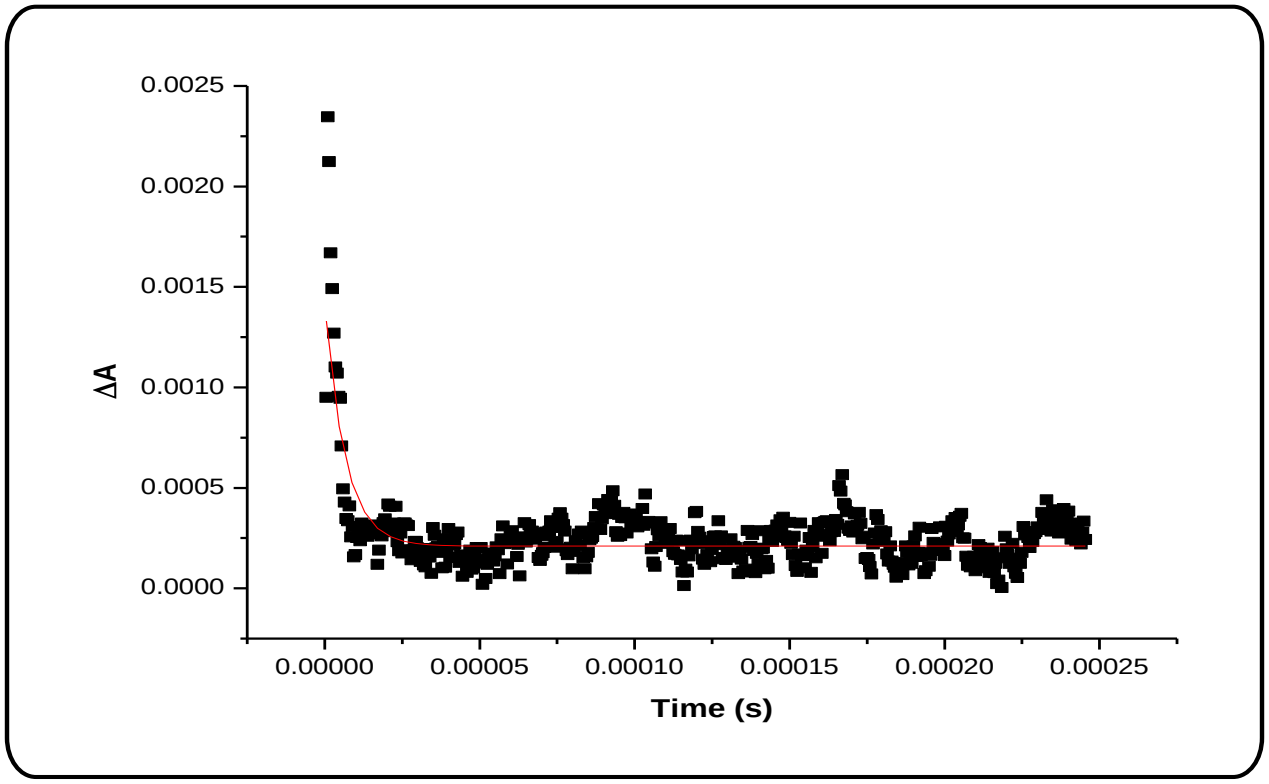

Fig. 3.14: Triplet decay curve for 78a in DMF. Excitation wavelength (λ_{exc}) = 510 nm.

Since intersystem crossing and fluorescence are two competing deactivating processes for the excited singlet state, the values for a particular species are expected to be complementary. Table 3.3 shows high Φ_T values (0.70–0.88) in DMSO, DMF and toluene, corresponding to low Φ_F values observed of these complexes. The Φ_T values are high due to the presence of lead. The Φ_T values in $CHCl_3$ and THF could not be determined due to the lack of readily available standard Φ_T values in these solvents. The Φ_T values (Table 3.3) do not change much with a change in substituents, showing that the effect of the phenoxy, *tert*-butylphenoxy and 4-benzyloxyphenoxy substituents on triplet quantum yield was minimal, and the Φ_T values range from 0.72 to 0.88 in DMSO, 0.72 to 0.83 in DMF and 0.70 to 0.86 in toluene. Thus, the nature of the solvent also has

an insignificant effect on the Φ_T values. Again the Φ_T values are for the partially or totally demetallated species, since demetallation occurs on excitation, but the Pb is still present in solution.

The triplet curve in Fig. 3.14 obeyed second order kinetics, which is typical of MPc complexes at high concentrations ($>1 \times 10^{-5}$ M) [172] due to triplet-triplet recombination. The concentration employed in this work was in this range, thus triplet–triplet recombination is expected.

The triplet lifetime (τ_T) values were found to be low for PbPc complexes compared to ZnPc or AlPc derivatives [83, 173], but are similar to the corresponding InPc derivatives [174], which also contain a heavy metal, even though the InPc derivatives were not demetallated upon excitation. The τ_T values in DMSO were much longer than those observed in DMF, chloroform, THF and toluene, which may be attributed to the higher viscosity of DMSO, as previously reported [164, 175]. Diffusion-like movement that enhance non-radiation deactivation of the excited state are impeded in viscous solvents, resulting in longer excited state lifetimes. The values in DMSO ranged from 20 to 50 μs for PbPc complexes. The triplet lifetimes were very low in the low viscocity solvents DMF, chloroform, THF and toluene, and were found to be less than or equal to 10 μs. Quantum yields of internal conversion (Φ_{IC}) were calculated according to Eq. 1.4. Table 3.3 shows that the values of Φ_{IC} were all quite similar.

3.2.1.3. Nonlinear optical parameters of PbPc complexes

The nonlinear optical parameters were calculated for PbPc complexes (**61**, **76-78**) in DMSO. The absorption cross sections (Fig. 3.15) were calculated and gave k (σ_{ex}/σ_g) > 1, Table 3.5. As

mentioned previously, a good optical limiter should have a *k* ratio of more than one. The value of *k* showed that the complexes are good optical limiters. The higher the value of *k*, the better the limiting power, and as such the octa-substituted PbPcs (**78**) were found to be better optical limiters than their corresponding tetrasubstituted PbPc derivatives (**76** and **77**).

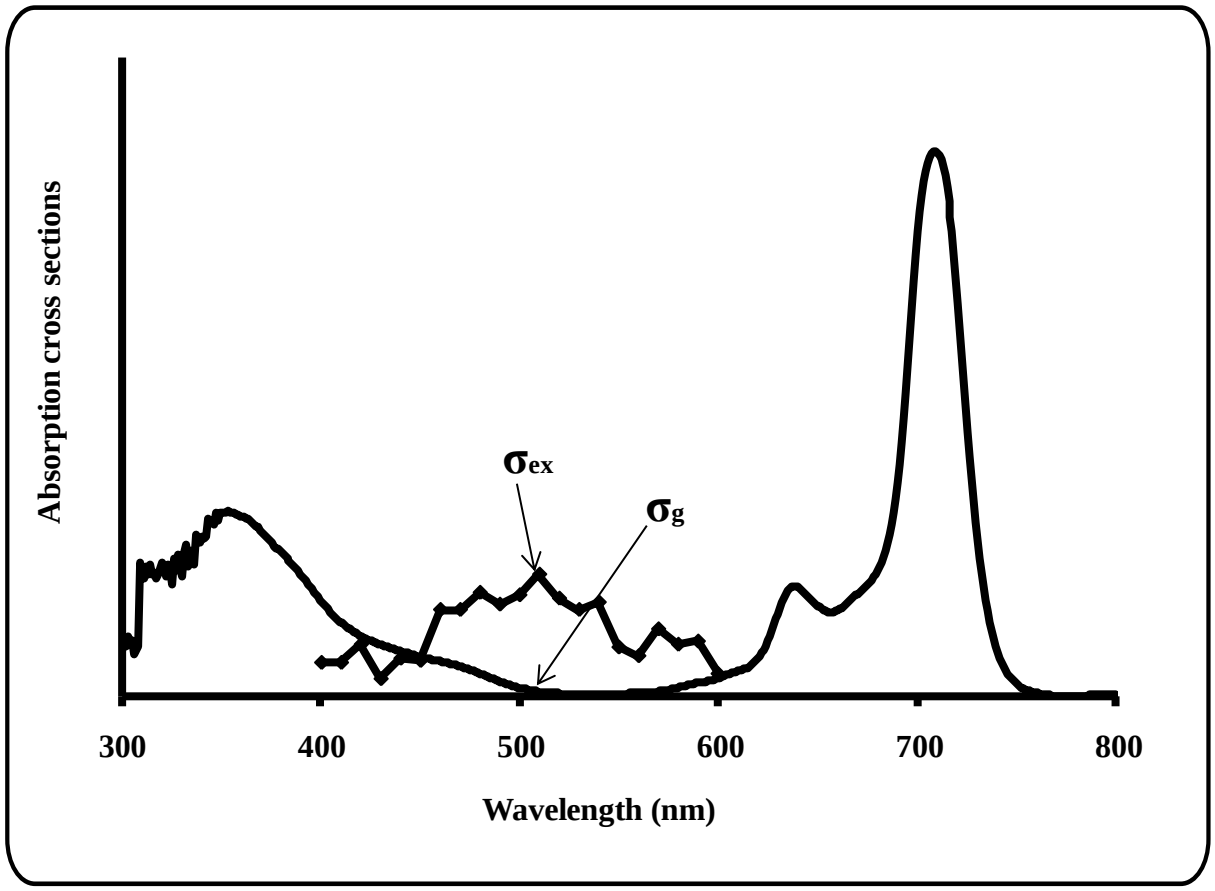

Fig. 3.15: Absorption cross sections for the ground (a) and excited triplet (b) state for compound 77b in DMSO (~ 1 x 10^{-6} mol.md^{-3})

Table 3.4: Nonlinear optical parameters of PbPc derivatives in DMSO

MPc in DMSO	τ_T (μs)	Im[$\chi^{(3)}$] (esu)	γ (esu)	(k) σ_{ex}/σ_g	I_{lim} (W.cm^{-2})
30	30	2.4×10^{-12}	0.6×10^{-34}	21	6.8
76a	40	4.2×10^{-12}	1.8×10^{-34}	26	4.1
76b	30	4.3×10^{-12}	1.5×10^{-34}	28	4.2
76c	40	5.1×10^{-12}	2.3×10^{-34}	27	3.5
77a	20	6.3×10^{-12}	1.6×10^{-34}	27	3.1
77b	30	3.3×10^{-12}	0.9×10^{-34}	23	6.6
77c	40	5.3×10^{-12}	1.3×10^{-34}	26	3.9
78a	20	4.8×10^{-12}	2.8×10^{-34}	35	2.1
78b	50	4.2×10^{-12}	2.2×10^{-34}	26	3.8
78c	50	5.6×10^{-12}	2.9×10^{-34}	33	2.3

The limiting threshold intensity (I_{lim}) values (Table 3.4) were found to be small, compared to those reported in the literature for GaPcs and InPcs [175]. An optical limiter should possess a low threshold limit value in order to be reliable in terms of protection of optical elements. The value of 10^2 W/cm^2 is generally taken as the standard minimum intensity value using the human eye as the reference light-sensing element [119]. The I_{lim} values obtained in Table 3.4 showed

that PbPc derivatives are good optical limiters. The smaller the liming intensity (I_{lim}), the better optical limiter.

Table 3.4 also shows the values obtained for third order susceptibility ($I_m[\chi^{(3)}]$) and second hyperpolarizability (γ) parameters for PbPc complexes. For a good optical limiter, $I_m[\chi^{(3)}]$ should fall within the 10^{-15} to 10^{-9} esu range while γ is within the 10^{-34} and 10^{-29} esu range [77, 176-179]. The third order susceptibility ($I_m[\chi^{(3)}]$) values were within the above range, but were lower than the values obtained for InPc and GaPc [175]. This is most likely due to the heavy atom effect as it has been reported that the value of $I_m[\chi^{(3)}]$ decreased in MPcs with increasing atomic number of a metal ion [119], hence the small values obtained for PbPc are not surprising. Except for complexes **77a**, the $Im[\chi^{(3)}]$ values for octasubstituted PbPcs were larger than the tetrasubstituted PbPc derivatives (e.g. compare **77b** with **78b** and **77c** with **78c**). The second hyperpolarizability (γ) values were well within the range of the values reported in the literature for Ga and InPc derivatives [175].

3.2.2. Photophysical properties of SbPc complexes

3.2.2.1. Fluorescence spectra and quantum yields

It is known that low valent main group porphyrin and phthalocyanine complexes (such as $Sb^{III}Pc$ derivatives) do not show emission around the Q-band wavelengths [91]. The $[Sb^{III}Pc]^+I_3^-$ (**61**, **79-81**), complexes were oxidized to the corresponding $[X_2Sb^{V}Pc]^+I_3$ (where X represents monoanionic axial ligands containing oxygen donors OR) complexes using TBHP.

Fig. 3.16 shows the absorption and fluorescence spectra of the oxidized complex **61** and **81b** in DMSO. Similar spectra were observed for the rest of SbPb complexes **(79-81)**. The observed emission spectra are red-shifted when compared to their corresponding excitation and absorption spectra. The fluorescence excitation spectral maxima agree very well with absorption maxima of the compounds, Table 3.5, suggesting that there are no differences in the nuclear configuration of the ground and excited states, Fig. 3.16. The fluorescence emission peaks were observed at 716 nm, 741 nm and 736 nm for the oxidized compounds **61**, **81a** and **81b** (in DMSO), respectively. Table 3.5 lists all the observed emission peaks for all oxidized SbPc complexes.

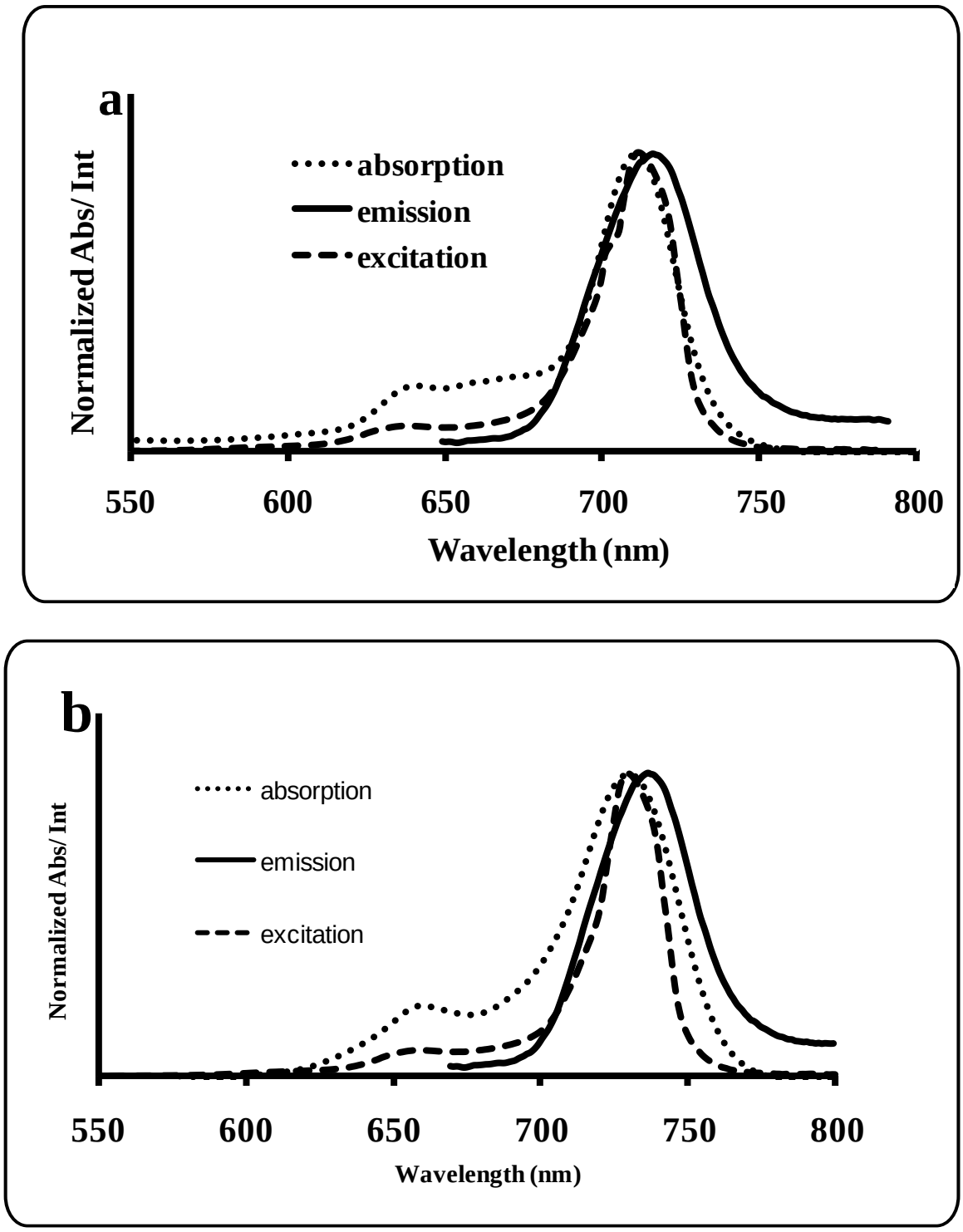

Fig. 3.16: Absorption, emission and excitation spectra of oxidized a) compound 61 and b) compound 81b in DMSO using TBHP as oxidant (~ 8 x 10^{-6} M)

Table 3.5: Spectral, photophysical parameters of $Sb^{V}Pc$ derivatives in DMSO, DMF and toluene

MPc	**Solvent**	**λ_{max} (nm)**			**Φ_F**	**Φ_T**	**Φ_{IC}**	**τ_T(μs)**
		Q_{abs} (nm)	**Q_{ems} (nm)**	**Q_{exc} (nm)**				
[a]Oxidized **61**	DMSO	710	716	711	<0.01	0.71	0.28	70
	DMF	706	710	705	<0.01	0.72	0.27	8
Oxidized **79a**	DMSO	745	753	746	<0.01	0.75	0.24	40
	DMF	742	749	740	<0.01	0.77	0.22	8
	Toluene	760	769	759	<0.01	0.76	0.23	8
Oxidized **79b**	DMSO	747	756	747	<0.01	0.77	0.22	40
	DMF	746	754	745	<0.01	0.79	0.20	8
	Toluene	763	770	761	<0.01	0.78	0.21	9
Oxidized **79c**	DMSO	747	756	748	<0.01	0.78	0.21	40
	DMF	747	755	748	<0.01	0.77	0.22	8
	Toluene	762	769	761	<0.01	0.76	0.23	9
Oxidized **80a**	DMSO	729	735	730	<0.01	0.73	0.26	40
	DMF	727	734	727	<0.01	0.75	0.24	8
	Toluene	743	748	741	<0.01	0.74	0.25	8
Oxidized **80b**	DMSO	728	734	728	<0.01	0.75	0.24	40
	DMF	727	733	728	<0.01	0.72	0.27	8
	Toluene	740	746	738	<0.01	0.74	0.25	9
Oxidized **80c**	DMSO	727	733	725	<0.01	0.76	0.23	50
	DMF	725	732	723	<0.01	0.76	0.23	9
	Toluene	738	744	737	<0.01	0.75	0.24	10
Oxidized **81a**	DMSO	735	741	736	<0.01	0.74	0.25	60

	DMF	728	733	727	<0.01	0.74	0.25	9
	Toluene	743	750	742	<0.01	0.73	0.26	10
Oxidized **81b**	DMSO	731	736	730	<0.01	0.76	0.23	50
	DMF	730	734	729	<0.01	0.77	0.22	8
	Toluene	742	748	740	<0.01	0.78	0.21	9
Oxidized **81c**	DMSO	730	735	729	<0.01	0.77	0.22	60
	DMF	729	735	729	<0.01	0.78	0.21	9
	Toluene	741	750	740	<0.01	0.76	0.23	10

[a] **61**- is insoluble in toluene.

The Φ_F values listed in Table 3.5 for the oxidized complexes **61**, **79**-**81** are very low as reported previously (Φ_F < 0.01) for Sb(V)Pc complexes [88]. The Φ_F yields were similar to the values obtained for the PbPc complexes and are therefore relatively low when compared to MPc in general [108], due to heavy atom effect (antimony ion).

3.2.2.2. Triplet quantum yields (Φ_T) and lifetimes (τ_T) of SbPc complexes

Fig. 3.17 shows representative triplet decay curves for the $Sb^{III}Pc$ derivatives, which is similar to their oxidized counterparts ($Sb^{V}Pc$) and also to the PbPc complexes discussed previously. Fig. 3.17 shows the triplet decay curve for the complex **81a** obeying second order kinetics.

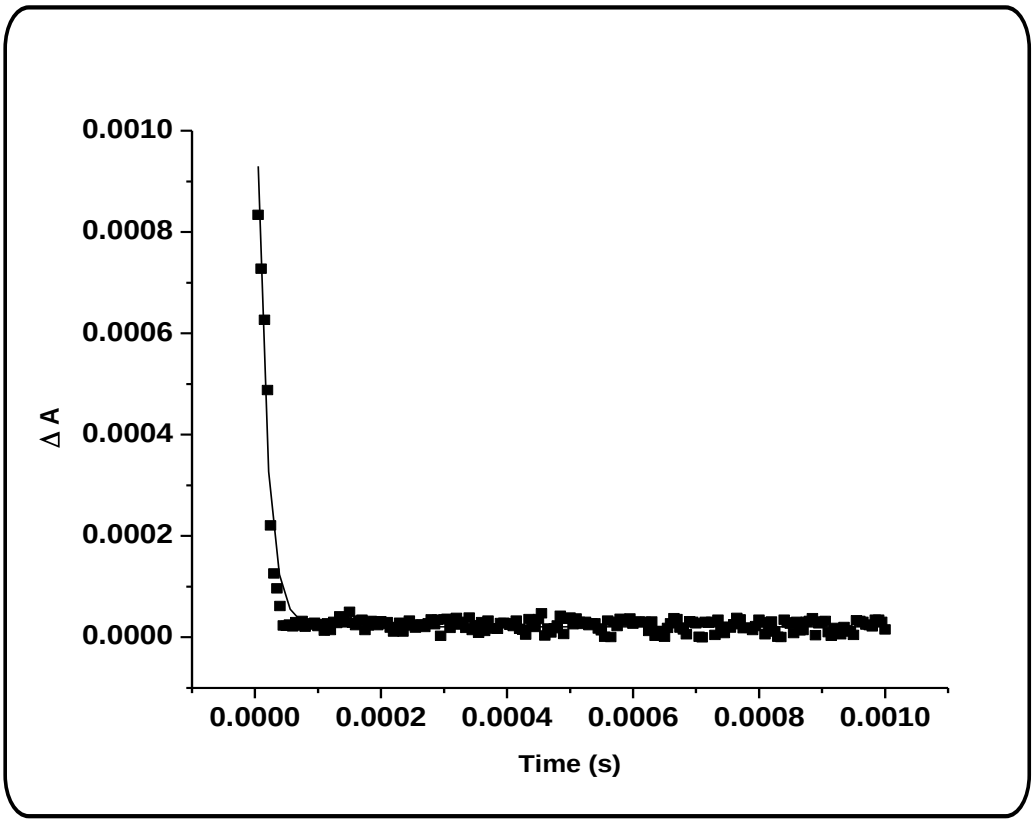

Fig. 3.17. Triplet decay curve of complex 81a in DMSO. Excitation wavelength = 510 nm.

Tables 3.5 and 3.6 give the triplet state parameters, Φ_T and τ_T. Table 3.6 shows high Φ_T values (0.75–0.82, for complexes **61**, **79-81**) in DMSO, DMF and toluene, due to the presence of antimony. It seems that the introduction of substituents onto the ring had only a small effect on the Φ_T, the values increased from 0.75 for complex **61**, and 0.82 for **79c** in DMSO. The Φ_T values (0.71–0.78) for the oxidized $Sb^{V}Pc$ complexes (Table 3.5) were slightly lower than that for the $Sb^{III}Pc$ complexes (Table 3.6). The values are in general high due to the heavy atom effect of Sb.

The triplet lifetime (τ_T) values were found to be low for SbPc complexes when compared to ZnPc or AlPc [173] derivatives, but are similar to PbPc complexes and to the corresponding InPc [174, 175] derivatives. The τ_T values in DMSO (Table 3.6) ranged from 20 to 30 μs for $Sb^{III}Pc$ complexes while in DMF and toluene the τ_T values were less than 10 μs. τ_T values are lower in DMF than in DMSO because of the greater absorption by DMF (than DMSO) in the region of the complexes' triplet energy [108]. The τ_T values for the oxidized $Sb^{V}Pc$ complexes were longer than for their $Sb^{III}Pc$ counter parts.

Quantum yields of internal conversion (Φ_{IC}) for the oxidized complexes ($Sb^{V}Pc$) (Table 3.5) shows that the values of Φ_{IC} were similar to each other and also to PbPc complexes, while Φ_{IC} for $Sb^{III}Pc$ complexes were not determined due to inability of the $Sb^{III}Pc$ complexes to fluoresce.

Table 3.6: Spectral, photophysical parameters of $Sb^{III}Pc$ derivatives in different solvents.

MPc	Solvent	λ_Q/nm	Φ_T	τ_T(μs)	MPc	Solvent	λ_Q/nm	Φ_T	τ_T(μs)
[a]**61**	DMSO	730	0.75	30	**80b**	DMSO	739	0.78	20
	DMF	728	0.76	7		DMF	735	0.80	6
	Toluene					Toluene	753	0.82	5
79a	DMSO	759	0.80	20	**80c**	DMSO	741	0.76	30
	DMF	757	0.79	6		DMF	739	0.78	4
	Toluene	775	0.78	5		Toluene	754	0.77	6
79b	DMSO	761	0.81	30	**81a**	DMSO	740	0.79	20
	DMF	760	0.80	7		DMF	735	0.78	5
	Toluene	776	0.82	8		Toluene	758	0.77	7
79c	DMSO	762	0.82	20	**81b**	DMSO	740	0.80	30
	DMF	761	0.81	6		DMF	735	0.82	5
	Toluene	776	0.80	5		Toluene	753	0.78	6
80a	DMSO	738	0.77	20	**81c**	DMSO	742	0.78	30
	DMF	734	0.79	4		DMF	739	0.80	7
	Toluene	752	0.78	8		Toluene	758	0.79	5

[a] **61** insoluble in toluene

3.3. PHOTODEGRADATION/BLEACHING QUANTUM YIELD

Photodegradation or photobleaching quantum yields (Φ_{Pd}) calculations are used to determine the photostability of MPc molecules and is identified by a decrease in the intensity of the absorption spectra without the appearance of new peaks. Photodegradation is a function of the nature of the substituents attached to the phthalocyanine ring, the solvent and the central metal. The photochemical stability of MPc complexes in the presence of light plays a vital role in their functionality and therefore it is important to determine the photostability of PbPc and SbPc complexes when exposed to light and to determine any possible pathways of degradation. The photodegradation studies were done, using the experimental set-up described in Chapter 2.

SbPc derivatives have been shown to photodegrade without transformation to other visible absorbing species [98]. The spectral changes observed during photobleaching were similar for all the PbPc and SbPc complexes during irradiation. The collapse of the Q-band in the absorption spectra without any distortion of shape confirms clean photodegradation not associated with photo-transformation (e.g. Fig. 3.18 for complex **81a** in DMSO).

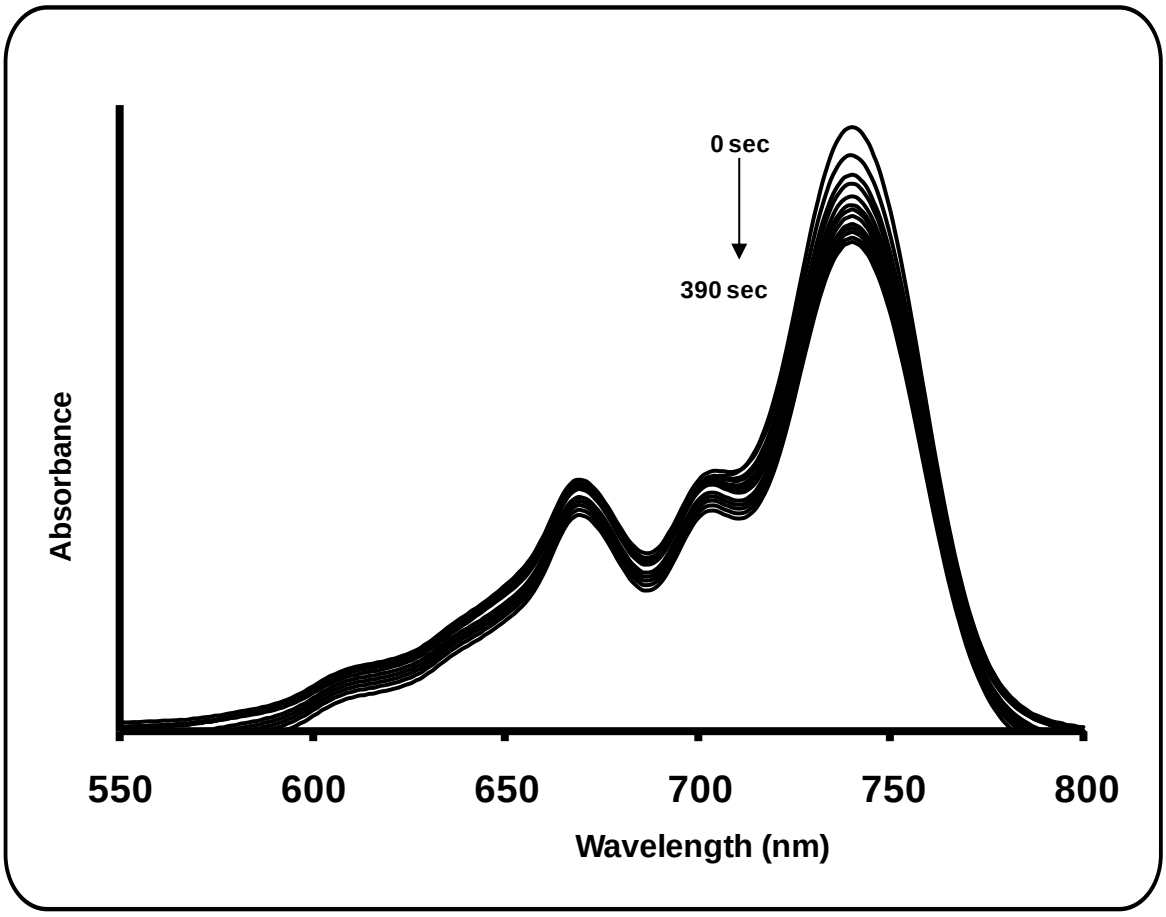

Fig. 3.18: Photobleaching of complex 81a in DMSO

Table 3.7 and 3.8 list Φ_{Pd} values for PbPc and SbPc complexes, respectively. All the complexes showed similar stability as compared to InPc and GaPc [174, 175, 180], with Φ_{Pd} values of the order of 10^{-5}. Φ_{Pd} values for all PbPc and SbPc complexes (excluding complex **81a** (0.61×10^{-5}) and oxidized complex **81b** (3.22×10^{-5}) in DMF) are lower in DMSO and DMF than in non-coordinating solvents such as toluene and chloroform (Table 3.7 and 3.8), which implies that these complexes are more photostable in coordinating solvents than in non-coordinating solvents.

This observation could be explained in terms of singlet oxygen interaction with the MPc central metal to form a complex (for non-coordinating solvents) [149].

Table 3.7: Photodegradation of PbPc derivatives in various solvents

MPc	Solvent	Φ_{Pd} (x 10^{-5})	MPc	Solvent	Φ_{Pd} (x 10^{-5})
[a]**30**	DMSO	0.51	**77b**	DMSO	0.73
	DMF	0.49		DMF	0.76
	Toluene			Toluene	1.34
	$CHCl_3$			$CHCl_3$	1.03
	THF			THF	1.16
76a	DMSO	0.76	**77c**	DMSO	0.75
	DMF	0.82		DMF	0.81
	Toluene	0.99		Toluene	1.37
	$CHCl_3$	1.32		$CHCl_3$	0.98
	THF	1.21		THF	1.13
76b	DMSO	0.78	**78a**	DMSO	0.81
	DMF	0.68		DMF	0.76
	Toluene	1.14		Toluene	0.99
	$CHCl_3$	0.94		$CHCl_3$	1.04
	THF	0.89		THF	0.92
76c	DMSO	0.86	**78b**	DMSO	0.92
	DMF	0.78		DMF	0.88
	Toluene	1.45		Toluene	1.57
	$CHCl_3$	1.56		$CHCl_3$	1.63
	THF	1.38		THF	1.08

77a	DMSO	0.66	**78c**	DMSO	0.93
	DMF	0.74		DMF	0.91
	Toluene	1.33		Toluene	1.43
	$CHCl_3$	0.95		$CHCl_3$	1.07
	THF	1.02		THF	1.11

[a] **30** insoluble in toluene, THF and $CHCl_3$.

Table 3.8a: Photodegradation of $Sb^{III}Pc$ complexes in DMSO, DMF and toluene

MPc	Solvent	Φ_{Pd} ($x\ 10^{-5}$)	MPc	Solvent	Φ_{Pd} ($x\ 10^{-5}$)	MPc	Solvent	Φ_{Pd} ($x\ 10^{-5}$)
[a]**61**	DMSO	0.31	**80a**	DMSO	0.51	**81a**	DMSO	0.42
	DMF	0.52		DMF	0.44		DMF	0.61
79a	DMSO	0.46		Toluene	0.88		Toluene	0.57
	DMF	0.42	**80b**	DMSO	0.47	**81b**	DMSO	0.48
	Toluene	0.67		DMF	0.41		DMF	0.53
79b	DMSO	0.37		Toluene	0.75		Toluene	0.81
	DMF	0.45	**80c**	DMSO	0.45	**81c**	DMSO	0.51
	Toluene	0.72		DMF	0.52		DMF	0.62
79c	DMSO	0.54		Toluene	0.62		Toluene	0.78
	DMF	0.61						
	Toluene	0.98						

[a]**61** insoluble in toluene.

Table 3.8b: Photodegradation of $Sb^{V}Pc$ complexes in DMSO, DMF and toluene

MPc	Solvent	Φ_{Pd} ($x\ 10^{-5}$)	MPc	Solvent	Φ_{Pd} ($x\ 10^{-5}$)	MPc	Solvent	Φ_{Pd} ($x\ 10^{-5}$)
(**[a]61**)	DMSO	1.23	**(80a)**	DMSO	1.78	**(81a)**	DMSO	1.51
	DMF	2.42		DMF	2.52		DMF	2.23
(79a)	DMSO	1.61		Toluene	3.48		Toluene	3.42
	DMF	2.11	**(80b)**	DMSO	2.07	**(81b)**	DMSO	2.01
	Toluene	3.12		DMF	3.01		DMF	3.22
(79b)	DMSO	1.59		Toluene	4.34		Toluene	2.42
	DMF	2.73	**(80c)**	DMSO	2.05	**(81c)**	DMSO	1.94
	Toluene	3.42		DMF	2.98		DMF	3.13
(79c)	DMSO	1.55		Toluene	3.77		Toluene	3.62
	DMF	1.77						
	Toluene	2.99						

[a]**61** insoluble in toluene. **( )** = Oxidized complex ($Sb^{V}Pc$)

4. CONCLUSIONS

In conclusion, this work reports on the synthesis of new nonperipherally and peripherally (phenoxy, 4-*t*-butylphenoxy and 4-benzyloxyphenoxy) tetra-substituted and peripherally octa-substituted lead and antimony phthalocyanine complexes. Spectroscopic methods were employed to characterize the complexes as well as elemental analysis which confirmed the purity of the complexes. A significant increase in the solubility of the complexes was observed by the introduction of substituents, which resulted in a red-shift of the Q-band, which was more obvious for Pcs with substituents at the non-peripheral position. The synthesised complexes were further studied to determine their photophysical properties. The fluorescence spectra of PbPc complexes were different to the absorption spectra due to the loss of symmetry incurred as a result of demetallation upon excitation. For the oxidized $[Sb^{V}Pc]^{+}I_3^{-}$ complexes, the excitation spectra were the same as absorption spectra and both are mirror images of the emission spectra. The low fluorescence quantum yields, high triplet quantum yields and low triplet lifetimes observed were as a result of heavy atoms (antimony and lead ions). The optical limiting threshold intensity (I_{lim}) values for the PbPc derivatives confirm that they are good optical limiters. The I_{lim} values obtained were far less than of 10^2 Wcm^{-2}, which is generally taken as the standard value for the minimum intensity using the human eye as the reference light sensing element. The photodegradation stuidies of these PbPc and SbPc complexes showed that they are stable in the presence of light.

5. REFERENCES

[1] A. Braun, J. Tcherniac, *Ber. Dtsch. Chem. Ges.* 40 (1907) 2709.

[2] H. de Diesbach, E. von der Weid, *Helv. Chim. Acta,* 10 (1927) 886.

[3] A.G. Dandridge, H.A.E. Drescher, J. Thomas, *Dyes British Patent,* 322 (1929)169.

[4] R. P. Linstead, *Br. Ass. Adv. Sci. Rep*. (1933) 465.

[5] R. P. Linstead, J. *Chem. Soc.* (1934)1016.

[6] J. M. Robertson, *J. Chem. Soc.* (1935) 615.

[7] C.C. Leznoff, A.B.P. Lever, Editors, *Phthalocyanines: Properties and Applications* vol. 1-4, VCH Publishers, New York (1989-1993).

[8] R. Bonnett, *Chemical aspects of photodynamic therapy*, Gordon and Breach Science Publishers, Germany, 2000.

[9] Y. Chen, D. Dini, M. Hanack, M. Fujitsuka, O. Ito, *Chem. Commun*. (2004) 340.

[10] H.I. Beltrán, R. Esquivel, A. Sosa-Sánchez. *Inorg. Chem*. 43 (2004) 3555.

[11] E.A. Ough, M.J. Stillman, *Inorg. Chem*. 33 (1994) 573.

[12] I. Chambrier, M.J. Cook , P.T. Wood. *Chem. Commun.* (2000) 2133.

[13] M. Casstevens, M. Samok, J. Pfleger, N. Prasad, *J. Chem. Phys.* 92 (1990) 2019.

[14] J. F. Van der Pol, E. Neeleman, J. W. Zwikker, R. J. M. Nolte, W. Drenth, J. Aerts, R. Visser, S. J. Picken, *Liq. Cryst*. 6 (1989) 577.

[15] H. Schultz, H. Lehmann, M. Rein, M. Hanack, *Struct. Bond.* (Berlin). 74 (1991) 41.

[16] J. Kuder, *J. Imag. Sci.* 32 (1988) 51.

[17] M. Riou, C. Clarisse, *J. Electroanal. Chem*. 249 (1988) 181.

[18] T. J. Marks, *Science,* 227 (1985) 881.

[19] R. A. Collins, K. A. Mohammed, J. *Phys. D: Appl. Phys.* 21 (1988) 154.

[20] E. Lukyanets, *J. Porphyr. Phthalocya.* 3 (1999) 424.

[21] T. J. Klofta, J. Danziger, P. Lee, J. Pankow, K. W. Nebesny, N. R. Armstrong, *J. Phys. Chem*. 91 (1987) 5646.

[22] S. Takano, T. Enokida, A. Kakuta, Y. Mori, *Chem. Lett*. (1984) 2037.

[23] B. Henderson, T. Dougherty, *Photochem. Photobiol.* 55 (1992) 145.

[24] T. Nyokong, Z. Gasyna, M. J. Stillman, *Inorg. Chem*. 26 (1987) 548.

[25] M. Gouterman, in The Porphyrins, (Ed. D. Dolphin), *Part A. Physical Chemistry,* Academic Press, New York, (1978).

[26] A. J. McHugh, M. Gouterman, C. Weiss, *Theoret. Chim. Acta,* 24 (1987) 246.

[27] A. M. Schaffer, M. Gouterman, E. R. Davidson, *Theoret. Chim. Acta,* 30 (1973) 9.

[28] F. R. Fan, L. R. Faulkner, *J. Am. Chem. Soc.* 101 (1979) 4779.

[29] M. Hanack, M. Lang, *Adv. Mater.* 6 (1994**)** 819.

[30] J.V. Bakboord, M.J. Cook, E. Hamuryudan, *J. Porphyr. Phthalocya.* 4 (2000) 510.

[31] A.B.P. Lever, S.R. Pickens, P.C. Minor, S. Cicoccia, B.S. Ramamswamy, K. Magnell, *J. Am. Chem. Soc.* 103 (1981) 6800.

[32] M. A. Diaz Garcia, I. Ledoux, J.A. Duro, T. Tores, F. Agullo-Lopez, J. Zyss, *J. Phys. Chem.* 98 (1994) 8761.

[33] W. Eberhardt, M. Hanack, *Synthesis* (1997) 95.

[34] A. Ogunsipe, D. Maree, T. Nyokong, *J. Mol. Struct*. 650 (2003) 131.

[35] N. Kobayashi, A.B.P. Lever, *J. Am. Chem. Soc.* 109 (1987) 7433.

[36] A.R. Monahan, J.A. Brado, A.F. DeLuca, *J. Phys. Chem*. 76 (1972) 1994.

[37] R. D. George, A. W. Snow, J. S. Shirk, W. R. Barger, *J. Porphyr. Phthalocya.* 2 **(**1998) 1.

[38] M. J. Stilman, T. Nyokong, *in Phthalocyanines: Properties and Applications* (Eds. C. C. Leznoff, A. B. P. Lever, VCH, New York, (1989).

[39] A. Ogunsipe, T. Nyokong, *J. Photochem. Photobiol. A: Chem*. 173 (2005) 211.

[40] E.S. Emerson, M.A. Conlin, A.E. Rosenoff, K.S. Norland, H. Rodriguez, D. Chin, G.R. Bird, *J. Phys. Chem*. 71 (1967) 2396.

[41] E. Coates, *J. Soc. Dyers. Col.* 85 (1969) 355.

[42] M. Kasha, *Radiat. Res.* 20 (1960) 55.

[43] H. Enkelkamp, R.J.M. Nolte, *J. Porphyr. Phthalocya.* 4 (2000) 454.

[44] M. Hanack, H. Heckmann, R. Polley, *in Methoden der Organischen Chemie* (Houben–Weyl), vol. E9d; 4th ed.; Thieme Verlag :Stuttgart (1997).

[45] P. Yiru, H. Fenghua, L. Zhipeng, C. Naisheng, H. Jinling, *Inorg. Chem. Commun.* **7 (**2004) 967.

[46] V. Csokai, G. Parlagh, A. Grofesik, M. Kubonyi, I. Bitter, *Synth. Commun.* 33 (2003) 1615.

[47] R.D. George, A.W. Snow, *J. Heterocyclic Chem.* 32 (1995) 495.

[48] J.G. Young, W. Onyebuagu, *J. Org. Chem.* 55 (1990) 2155.

[49] G. Schmid, M. Sommerauer, M. Hanack, *Angew. Chem. Int. Ed. Engl.* 32 (1993) 1422.

[50] G. Schmid, M. Sommerauer, M. Geyer, M. Hanack, *in Phthalocyanines: Properties* (Eds. C. C. Leznoff, A. B. P. Lever), VCH, New York, vol 4 (1996) 1.

[51] D. Wöhrle, M. Eskes, K. Shigehara, A. Yamada, *Synthesis* (1993) 194.

[52] A. Cicek, J.T. Guthrie, *Dyes Pigm.* 5 (1984) 225.

[53] K. I. Ozoemena, T. Nyokong, *Inorg. Chem. Commun.* 6 (2003) 1192.

[54] S. Gaspard, P. Maillard, *Tetrahedron* 43 (1987) 1083.

[55] P. Tau, T. Nyokong, *Dalton Trans.* (2006) 4482.

[56] S. Kera, H. Fukagawa, T. Kataoka, S. Hosoumi, H. Yamane, N. Ueno, *Phys. Rev.* B 75 (2007) 121305.

[57] K. Ukei, *Acta Crystallogr.* 29 B (1973) 2290.

[58] K. Ukei, *J. Phys. Soc. Jpn.* 40 (1976) 140.

[59] Y. Iyechika, K. Yakushi, I. Ikemoto, H. Kurado, *Acta Crystallogr.* B 38 (1982) 776.

[60] F. Przyborowski, C. Hamann, *Cryst. Res. Technol.* 17 (1982) 1041.

[61] T.L. Bluhm, H.J. Wagner, R.O. Loutfy, *J. Mater. Sci. Lett.* 2 (1983) 85.

[62] W. J. Kroenke, M.E. Kenney, *Inorg. Chem.* 3 (1964) 251.

[63] P.M. Burnham, M.J. Cook, L.A. Gerrard, M.J. Heeney, D.L. Hughes, *Chem. Commun.* (2003) 2064.

[64] C. Piechocki, J.C. Boulou, J. Simon, *Mol. Cryst. Liq. Cryst.* 149 (1987) 115.

[65] A.W. Snow, N.L. Jarvis, *J. Am. Chem. Soc.* 106 (1984) 4706.

[66] W.T. Ford, L. Sumner, W. Zhu, Y.H. Chang, P.-J. Um, K.H. Choi, P.A. Heiney, N.C. Maliszewskyj, *New J. Chem.* 18 (1994) 495.

[67] C. Piechocki, J. Simon, A. Skoulios, D. Gullion, P. Weber, *J. Am. Chem. Soc.* 104 (1982) 5245.

[68] J. Simon, C. Sirlin, *Pur. Appl. Chem.* 61 (1989) 1625

[69] Y. Bian, L. Li, J. Dou, D.Y. Y Cheng, R. Li, C. Ma, D.K.P. Ng, N. Kobayashi, J. Jiang, *Inorg. Chem.* 43 (2004) 7539.

[70] H. A. Dinçer, H. Çerlek, A. Gül, M. B. Koçak, *Main Group Chem.* 4 (2005) 209.

[71] A. Koca, H. A. Dinçer, H. Çerlek, A. Gül, M. B. Koçak, *Electrochim. Acta* 52(2006) 1199.

[72] T. M. M. Kumar, B. N. Achar, *J. Organomet. Chem.* 691 (2006) 331.

[73] M. Hanack, A. Beck, H. Lehmann, *Synthesis* 8 (1987) 703.

[74] Y. Machida, Y. Saito, A. Taomoto, K. Nichogi, K. Waragai, S. Asakawa, *Jap. J. Appl. Phys.* 28 (1989) 297.

[75] Z. Bıyıklıoğlu, I. Acar, H. Kantekin, *Inorg. Chem. Commun.* 11 (2008) 630.

[76] Z. Bıyıklıoğlu, H. Kantekin, M. Özil, *J. Organomet. Chem.* 692 (2007) 2436.

[77] A. Auger, W. J. Blau, P.M. Burnham, I. Chambrier, M. J. Cook, B, Isare, F. Nekelson, S. M. O'Flaherty, *J. Mater. Chem.* 13 (2003) 1042.

[78] E. M. Maya, A. W. Snow, J. S. Shirk, R. G. S. Pong, S. R. Flom and G. L. Roberts, *J. Mater. Chem.* 13 (2003) 1603.

[79] Y. Zhang, X. Zhang, Z. Liu, Y. Bian, J. Jiang, *J. Phys. Chem. A* 109 (2005) 6363.

[80] X. Cai,Y. Zhang, X. Zhang, J. Jiang, *J. Mol. Struc. THEOCHEM* 801 (2006) 71.

[81] H. A. Dinçer, M. K. Şener, A. Koca, A. Gül, M. B. Koçak, *Electrochim. Acta* 53 (2008) 3459.

[82] H. A. Dinçer, E. Gonca, A. Gül, *Dyes Pigm.* 79 (2008) 166.

[83] S. Foley, G. Jones, R. Liuzzi, D.J. McGarvey, M.H. Perry, T.G. Truscott, *J. Chem. Soc. Perkin Trans.* 2 (1997) 1725.

[84] T. V. Basova, A. G. Gürek, D. Atilla, A. K. Hassan, V. Ahsen, *Polyhedron* 26 (2007) 5045.

[85] P. A. Barrett, D. A. Frye, R. P. Linstead, *J. Chem. Soc.* (1938) 1157.

[86] R. Kubiak, J. Janczak, M. Razik, *Inorg. Chim. Acta* 293 (1999) 155.

[87] G. Knör, *Inorg. Chem.* 35 (1995) 7916.

[88] H. Isago, K. Miura, Y. Oyama, *J. Inorg. Biochem.* 102 (2008) 380.

[89] Y. Kagaya, H. Isago, *Bull. Chem. Soc. Jpn.* 70 (1997) 2179.

[90] Y. Kagaya, H. Isago, *Chem. Lett.* (1994) 1957.

[91] H. Isago, *Chem. Commun.* (2003) 1864.

[92] H. Isago, Y. Kagaya, *Chem. Lett.* 35 (2006) 8.

[93] R. Kubiak, M.Razik, *Acta Cryst. C* 54 (1998) 483.

[94] H. Isago, *J. Porphyr. Phthalocya.* 8 (2004) 408.

[95] H. Isago, Y. Kagaya, *Bull. Chem. Soc. Jpn.* 67 (1994) 383.

[96] H. Isago, Y. Kagaya, *Bull. Chem. Soc. Jpn.* 67 (1994) 3212.

[97] H. Isago, Y. Kagaya, S.-I. Nakajima, *Chem. Lett.* 32 (2003) 112.

[98] H. Isago, K. Miura, M. Kanesato, *J. Photochem. Photobiol. A: Chem.* 197 (2008) 313.

[99] Md.H. Zahir, Y. Kagaya, H. Isago, T. Furubayashi, *Inorg. Chim. Acta* 357 (2004) 2755.

[100] P. Suppan, *Chemistry and Light, Royal Society*, Cambridge, 1st ed. (1994).

[101] G. J. Perpétuo, J. Janczak, *Acta Cryst. C* 61 (2005) m 2003.

[102] A. Gilbert, J. Baggott, *Essentials of molecular photochemistry*, library of congress, USA, (1995).

[103] R. A. Mayers, *Encyclopedia of analytical chemistry: Applications, Theory, and instrumentation* 2000, Vol. 12, John Wiley & Sons Ltd, UK.

[104] J.R. Lakowicz, *Principles of Fluorescence Spectroscopy*, Kluwer Academic/ Plenum Publishers, New York, (1999).

[105] J.R. Lakowicz, *Anal. Biochem*. 298 (2001) 1.

[106] S. Fery-Forgues, D. Lavabre, J. *Chem*. *Ed*. 76 (1999) 1260.

[107] J. Fu, X.Y. Li, D.K.P. Ng, C. Wu, *Langmuir* 18 (2002) 3843.

[108] A. Ogunsipe, J. Y. Chen, T. Nyokong, *New*. *J. Chem*. 28 (2004) 822.

[109] S. Dhami, A. J. de Mello, G. Rumbles, S. M. Bishop, D. Philips, A. Beeby, *Photochem*. *Photobiol.* 61 (1995) 341.

[110] D.R. Lide, *CRC Handbook of Chemistry and Physics*, Boca Raton, CRC Press, Florida, 84th ed. 2003.

[111] D.A. Fernandez, J. Awruch, L. Dicelio, *Photochem*. *Photobiol.* 63 (1996) 784.

[112] A. Ferencz, D. Neher, M. Schulze, G. Wegner, L. Viaene, F.C. de Schryver,

Chem. *Phys. Lett*. 245 (1995) 23.

[113] A.P. de Silva, H.Q.N. Gunaratne, T. Gunnlaugsson, A.J.M. Huxley, C.P. McCoy, J.T. Rademacher, T.E. Rice, *Chem*. *Rev*. 97 (1997) 1515.

[114] B. Bhattacharya, A. Samanta, *Chem*. *Phys. Lett*. 442 (2007) 316.

[115] P. Kubát, J.Mosinger, *J. Photochem*. *Photobiol. A: Chem*. 96 (1996) 93.

[116] T. H. Tran-Thi, C. Desforge, C. Thiec, S. Gaspard. *J. Phys. Chem*. 93 (1989) 1226.

[117] C. Schweitzer, R. Schmidt, *Chem. Rev*. 103 (2003) 1685.

[118] N. Bloembergen, *Nonlinear Optics*, Benjamin, New York, (1965).

[119] D. Dini, M. Hanack, *The Porphyrin Handbook: Physical Properties of Phthalocyanine-Based Materials*, (Eds. K.M. Kadish, K.M. Smith, R. Guilard) vol 17, (2003), 22, Academic press, USA.

[120] T. H. Mainman, *Nature*, 187 (1960) 493.

[121] V. B. Nakagawara, K. J. Wood, R. W. Montgomery, *Optometry*. 79 (2008) 518.

[122] M. D. Harris, A. E. Lincoln, P. J. Amoroso, B. Stuck, D. Sliney, *Aviation, Space, and Environmental Medicine*. 74 (2003) 947.

[123] M. M. Michaelisa A. Forbes W. Klopper, H. Bencherif, S. Jolivet, R. Moorgawa, E. McKenzie, G. Turner, *South African Journal of Science*. 102 (2006) 296.

[124] Y. R. Shen, *The Principles of Nonlinear Optics*. Wiley, New York, (1984).

[125] B. Shechy, L. F. Di Mauro, *Annual Review of Physical Chemistry*. 47 (1996) 463.

[126] M. Hanack, T. Schneider, M. Barthel, J.S. Shirk, S.R. Flom, R.G.S. Pong, *Coord. Chem. Rev*. 219–221 (2001) 235.

[127] D. Dini, M. Hanack, M. Meneghetti, *J. Phys. Chem. B*. 109 (2005) 12691.

[128] J. L. Bredas, C. Adant, P. Tacks, A. Persoons, *Chem. Rev*. 94 (1994) 243.

[129] F. Gires, IEEE *J. Quantum Electronics QE*. 2 (1966) 624.

[130] J. W. Perry, *in Nonlinear Optics of Organic Molecules and Polymers*, (Eds. H. S. Nalwa, S. Miyata), CRC press, Boca Raton, FL, (1997) 813.

[131] M. Hanack, D. Dini, M. Barthel, S. Vargin, *The Chemical Records.* 2 (2002) 129.

[132] D. Dini, M. J. F. Calvete, M. Hanack, W. Chen, W. Ji, *ARKIVOC* (2006) 77.

[133] D. Dini, M. Barthel, T. Schneider, M. Ottmar, S. Verma, M. Hanack, *Solid State Ionics*. 165 (2003) 289.

[134] L.W. Tutt, T.F. Boggess. *Prog. Quant. Elec.* 17 (1993)299.

[135] Y. Chen, M. Hanack, Y. Araki, O. Ito, *Chem. Soc. Rev*. 34 (2005) 517.

[136] D. Dini, M. Barthel, M. Hanack, Eur. *J. Org. Chem*. (2001) 3759.

[137] E.R. Menzel, K.E. Rieckhoff, E.M. Voigt, *J. Chem. Phys.* 58 (1973) 5726.

[138] J. S. Shirk, R. G. S. Pong, S. R. Flom, F. J. Bartoli. M. E. Boyle, A. W. Snow, *Pure Appl. Opt*. 5 (1996) 701.

[139] Q. Yang, T. Chen, J. Si, T. Lin, X. Hou, G. Qian, J. Guo, *Optics Commun.* 281 (2008) 831.

[140] H. Zhan, W. Chen, M. Wang, *Mater. Lett*. 59 (2005) 1395.

[141]. W. Sun, C.C. Byeon, M.M. Mckerns, G.M. Gray, D. Wang, C.M. Lawson, *SPIE* 3472 (1998) 127.

[142] P. Buck, A. Dogariu, D.J. Hagan and E.W. Van Stryland, *SPIE* 2853 (1996) 12.

[143] W. Spiller, H. Kliesch, D. Wöhrle, S. Hackbarth, B. Röder, G. Schnurpfeil, *J. Porphyr. Phthalocya.* 2 (1998) 145.

[144] R. Bonnett, B.D. Djelal, P.A. Hamilton, G. Martinez, F. Wierrani, *J. Photochem. Photobiol. B: Biol*, 53 (1999) 136.

[145] G. Schnurpfeil, A. Sobbi, W. Spiller, H. Kliesch, D. Wöhrle, *J. Porphyr. Phthalocya*. 1 (1997) 159.

[146] A.K. Sobbi, D. Wöhrle, D. Schlettwein, *J. Chem. Soc. Perkin Trans.* 2, (1993)481.

[147] S. Maree, T. Nyokong, *J. Porphyr. Phthalocya.* 5 (2001) 5782.

[148] M. D. Maree, N. Kuznetsova, T. Nyokong, *J. Photochem. Photobiol. A: Chem.* 140 (2001) 117.

[149] R. Sota, G. Dyrda, *Inorg. Chem,* 42 (2003) 5743.

[150] J. D. Spikes, *Photochem. Photobiol.* 55 (1992) 797.

[151] D. Dini, M. Calvete, S. Vargin, M. Hanack, A. Eriksson, C. Lopes, *J. Porphyr. Phthalocya.* 10 (2006) 1165.

[152] Z. Zhao, A. Ogunsipe, D. Maree, T. Nyokong, *J. Porphyr. Phthalocya.* 9 (2005) 186.

[153] M. Idowu, T. Nyokong, *J. Photochem. Photobiol A: Chem* 188 (2007) 200.

[154] W. Chidawanyika, A. Ogunsipe, T. Nyokong, *New. J. Chem.* 31 (2007) 337.

[155] J. Kossanyi, O. Chahraoui, *Int. J. Photoenerg*. 2 (2000) 9.

[156] S.M. Bishop, A. Beeby, A.W. Parker, M.S.C. Foley, D. Phillips, *J. Photochem. Photobiol. A: Chem*. 90 (1995) 29.

[157] B.H. Nicolet, J.A. Bender, *Org. Synth. Coll.*, 1 (1941) 410.

[158] M.M. El-Nahass, K.F. Abd-El-Rahman, A.A.A. Darwish, *Mater. Chem. Phys.* 92 (2005) 185.

[159] A. Ahmad, R. A Collins, *J. Phys. D: Appl. Phys*. 24 (1991) 1894.

[160] L. Edwards, M. Gouterman, *J. Mol. Spectry.* 33 (1970) 292.

[161] C.C. Leznoff, in: C.C. Leznoff, A.B.P. Lever (Eds.), *Phthalocyanines, Properties and Applications*, vol. 1, VCH Publishers, New York, 1989 (Chapter 1).

[162] S. M. Marcuccio, P.I. Svirskaya, S. Greenberg, A.B.P. Lever, *Can. J. Chem*. 63 (1985) 3057.

[163] M. Idowu, T. Nyokong, *J. Photochem. Photobiol A: Chem* 197 (2008) 273.

[164] V. Chauke, A. Ogunsipe, M. Durmuş, T. Nyokong, *Polyhedron* 26 (2007) 2663.

[165] J. Mark, M.J. Stillman, *J. Am. Chem. Soc.* 116 (1994) 1292.

[166] M. Konami, M. Hatano, A. Tajiri, *Chem. Phys. Lett*. 166 (1990) 605.

[167]. A. Ogunsipe, T. Nyokong, *J. Mol. Struct.* 689 (2004) 89.

[168] M. Durmuş, T. Nyokong, *Spect. chim. Acta A.* 69 (2008) 1170.

[169] D. R. Tackley, G. Dent, W. E. Smith, *Phys.Chem. Chem. Phys.* 3 (2001) 1419.

[170] J.A. Shelnutt, *J. Am. Chem. Soc.* 105 (1983) 774.

[171] W. Freyer, S. Mueller, K. Teuchner, *J. Photochem. Photobiol. A: Chem.* 163 (2004) 231.

[172] M. G. Debacker, O. Deleplanque, B. Van Vlierberge, F. X. Sauvage, *Laser Chem*. 8 (1988) 1.

[173] T. Nyokong, *Coord. Chem. Rev*. 251 (2007) 1707.

[174] M. Durmuş, T. Nyokong, *Tetrahedron* 63 (2007) 1385.

[175] V. Chauke, M. Durmuş, T. Nyokong, *J. Photochem. Photobiol. A: Chem.* 192 (2007) 179.

[176] Y. Liu, S.M. O'Flaherty, Y. Chen, Y. Araki, J. Bai, J. Doyle, W.J. Blau, O. Ito, *Dyes Pigm*. 75 (2007) 88.

[177] E.M. García-Frutos, S.M. O'Flaherty, S.V. Hold, G. de la Torre, S. Maier, P. Vázquez, W. Blau, T. Torres, *Synth. Met*. 137 (2003) 1479.

[178] E.M. García-Frutos, S.M. O'Flaherty, E. M .Maya, G. de la Torre, W. Blau, P. Vázquez, T. Torres, *J. Mater. Chem*. 13 (2003) 749.

[179] S.M. O'Flaherty, S.V. Hold, M.J. Cook, T. Torres, Y. Chen, M. Hanack, W.J. Blau, *Adv. Mater.* 15 (2003) 19.

[180] M. Durmuş, T. Nyokong, *Polyhedron* 26 (2007) 3323.